UNIVERSITY OF CALIFORNIA

Santa Barbara

The Effects of pCO_2 on Bacterioplankton-Mediated Carbon Cycling

A dissertation submitted in partial satisfaction of the

requirements for the degree of Doctor of Philosophy

in Marine Science

by

Anna Katherine James

Committee in charge:

Professor Craig A. Carlson, Chair

Professor Mark A. Brzezinski

Dr. Uta Passow, Researcher

Professor Debora Iglesias-Rodriguez

December 2017

The dissertation of Anna Katherine James is approved.

Debora Iglesias-Rodriguez

Mark A. Brzezinski

Uta Passow

Craig A. Carlson, Committee Chair

December 2017

ACKNOWLEDGEMENTS

I would like to thank my committee for the invaluable guidance and mentorship provided over the course of my PhD degree. I would also like to thank the graduate students, post-docs, and technicians in the Carlson Laboratory, without whose laboratory assistance and methodological guidance these projects would not have been possible. Finally, my deepest gratitude goes to my closest friends, family, and partner, for their continued support, and endless enthusiasm for the adventures that continue to keep me sane.

VITA OF ANNA KATHERINE JAMES

December 2017

EDUCATION

PhD Graduate Student, September 2011 to Current
Interdepartmental Graduate Program in Marine Science, UC Santa Barbara

GRAD 210: College and University Teaching; From Theory to Practice, Spring 2017
Graduate Division, UC Santa Barbara

Microbial Oceanography: Genomes to Biomes, May to July 2013
Center for Microbial Oceanography: Research and Education, UH

Microbial Oceanography: The Biogeochemistry, Ecology, and Genomics of Oceanic Microbial Ecosystems, June to July 2012
Bermuda Institute for Ocean Sciences, Bermuda

Bachelor of the Arts with an Emphasis in Aquatic Biology, June 2009
College of Creative Studies, UC Santa Barbara

TEACHING EXPERIENCE

Instructor of Record, Introduction to Marine Science (INT 91)
Summer 2016, UC Santa Barbara

Lead Teaching Assistant, EEMB 142B, Processes in Oceans Part B
Winter 2011 to 2015, 2017, UC Santa Barbara

Lead Teaching Assistant, EEMB 142C, Processes in Oceans Part C
Spring 2014, UC Santa Barbara

MENTORING EXPERIENCE

Mentor to Undergraduate Students
January 2012 to 2017, UC Santa Barbara

Mentor in the Women in STEM Mentorship Program
March to June 2016, UC Santa Barbara

COMMITTEES

Member of the Beyond Research Collective Planning Committee
Fall 2016 to Spring 2017, UC Santa Barbara

Graduate Student Representative for the Marine Organic Geochemistry Hiring Committee
Spring 2017, UC Santa Barbara

Member of Graduate Student Advisory Committee
Spring 2014 to 2016, UC Santa Barbara

Member of Refugio Oil Spill Response Committee
May 2015 to 2016, UC Santa Barbara

Member of UNOLS Cruise Planning Committee
January 2014 to July 2014, UC Santa Barbara

RESEARCH EXPERIENCE

Graduate student researcher for MCR-LTER research cruise
July 2014, South Pacific

Technician for two UCSB oceanographic cruises
May 2009 and May 2010, Santa Barbara Channel

Technician for CLIVAR repeat hydrography research vessel
December 2009 to February 2010, South Pacific to Chile

Parasitological research assistant
October to November 2009, Palmyra Research Station

Extensive Undergraduate Research Experience
Carlson laboratory, December 2008 to June 2009, UC Santa Barbara
Schmitt-Holbrook Laboratory, December 2006 to June 2009, UC Santa Barbara
Research Assistant, June 2008 to August 2008, Gump Research Station, Moorea, FP
PISCO Research Diver, June 2007 to August 2007

AWARDS & CERTIFICATES

Expected Recipient of Certificate in College and University Teaching
Portfolio Submitted September 2017, UC Santa Barbara

Recipient of the Charles A. Storke Fellowship
July 2016, UC Santa Barbara

Worster Fellow
May 2014 to May 2015, UC Santa Barbara

Nominated for the Excellence in Teaching Award
Spring 2013, UC Santa Barbara

PUBLICATIONS & PRESENTATIONS

Publications

James AK, Kelly LW, Nelson CE, Carlson CA. Elevated pCO_2 alters bacterial community composition and metabolic potential. In progress.

James AK, Carlson CA, Passow U, Brzezinski M. (2017). Increasing pCO_2 enhances bacterioplankton removal of organic carbon. PLoS One. doi: 10.1371/journal.pone.0173145.

Please see Research Gate for a full list: researchgate.net/profile/Anna_James3

Presentations

Invited presentation for Ocean Sciences Meeting in Portland, Oregon (2018): Elevated pCO_2 alters bacterial community composition and metabolic potential.

Poster presentation at Aquatic Science in Honolulu, Hawaii (2017): Comparing bacterial metagenomes across pCO2 levels.

Oral presentation at Moorea Coral Reef, Long Term Ecological Research All Scientists Meeting, UCSB (2016): Update on the biological, biogeochemical, and physical dynamics from the Kilo Moana cruise – a work in progress.

Oral presentation at Ocean Sciences in New Orleans, USA (2016): Elevated pCO_2 reduces the role of dissolved organic carbon in vertical export.

Oral presentation at Ocean Sciences in Granada, Spain (2015); Elevated pCO_2 increases respiration of dissolved organic carbon by natural bacterioplankton.

ABSTRACT

The Effects of pCO_2 on Bacterioplankton-Mediated Carbon Cycling

by

Anna Katherine James

The concentration of atmospheric carbon dioxide (CO_2) is increasing at extraordinary rates (e.g. Le Quéré et al. 2016). Effectively mitigating the impacts of increasing atmospheric CO_2 on climate change, the ocean has absorbed roughly 30 % of the anthropogenic CO_2 produced since the Industrial Revolution (e.g. Doney et al. 2009). However, increased levels of CO_2 in the surface ocean may have lasting implications for marine biogeochemical cycles (e.g. Riebesell et al. 2013). In addition to gradual increases in concentrations of CO_2 in the surface ocean through rising atmospheric CO_2, mixing of deep water upwards leads to the injection of elevated partial pressures of CO_2 (pCO_2) into the surface ocean, exposing some areas of the surface ocean to transient pulses of elevated pCO_2 equivalent to those projected for the year 2100 (Feely et al. 2008, Hofmann et al. 2011). This broad range of exposure to elevated pCO_2, from ephemeral pulses to gradual increases, highlights the necessity to understand the impacts of pCO_2 on marine biogeochemical processes on a variety of timescales.

Heterotrophic bacterioplankton play a key role in the biogeochemical cycling of carbon in the ocean through the consumption and remineralization of dissolved organic carbon (DOC). The physical mixing of DOC that accumulates in the surface ocean into the mesopelagic represents ~ 20 % of global annual organic carbon export (Hansell and Carlson 2015), making DOC export an important pathway in the biological carbon pump. Export of DOC to ocean depths removes this carbon from interaction with the atmosphere on a variety of timescales. Processes that remove or reduce the accumulation of DOC in the surface ocean can decrease the amount of DOC available for export and ultimately lessen the effectiveness of DOC export as a sink of carbon in the ocean. As the primary consumers of DOC, heterotrophic bacterioplankton can reduce the amount and rate of DOC accumulation in the surface ocean. Thus, factors that affect the ability of bacterioplankton to consume DOC can affect DOC accumulation and have implications for DOC export potential.

In Chapter I, I present results from seawater culture experiments that were designed to assess the effects of pCO_2 on bacterioplankton consumption of DOC. Results from these experiments provide evidence that short-term exposure to elevated pCO_2 can enhance the rate of removal of photosynthetically-derived surface DOC by natural bacterioplankton communities. To evaluate potential physiological and metabolic mechanisms responsible for these enhanced rates of DOC removal by marine bacterioplankton, I present results from a metagenomic analysis in Chapter II. These results suggest that elevated pCO_2 can alter the taxonomic composition and metabolic potential of natural bacterioplankton communities. Collectively, Chapters I and II contribute to a growing understanding of the effects of elevated pCO_2 on bacterioplankton-mediated carbon cycling in the surface ocean. Chapter

III provides the first high-resolution evaluation of key physical and biogeochemical variables controlling carbon dynamics in the oligotrophic waters surrounding the islands of Moorea and Tahiti, French Polynesia, providing the context needed to predict how short-term increases in pCO_2 may alter carbon-cycling in oligotrophic gyre ecosystems.

References

Doney, S.C., Fabry, V.J., Feely, R.A., and Kleypas, J.A. (2009). Ocean Acidification: The Other CO_2 Problem. Annual Review of Marine Science 1, 169–192.

Feely, R.A., Doney, S.C., and Cooley, S.R. (2009). Ocean acidification: Present conditions and future changes in a high-CO_2 world. Oceanography 22, 36–47.

Hansell D.A. and Carlson, C.A. (2015). Biogeochemistry of marine dissolved organic matter (Amsterdam; Boston: Academic Press).

Hofmann, G.E., Smith, J.E., Johnson, K.S., Send, U., Levin, L.A., Micheli, F., Paytan, A., Price, N.N., Peterson, B., Takeshita, Y., et al. (2011). High-Frequency Dynamics of Ocean pH: A Multi-Ecosystem Comparison. PLoS ONE 6, e28983.

Le Quéré, C., Andrew, R.M., Canadell, J.G., Sitch, S., Korsbakken, J.I., Peters, G.P., Manning, A.C., Boden, T.A., Tans, P.P., Houghton, R.A., et al. (2016). Global Carbon Budget 2016. Earth System Science Data 8, 605–649.

Riebesell, U., Gattuso, J.-P., Thingstad, T.F., and Middelburg, J.J. (2013). Preface "Arctic ocean acidification: pelagic ecosystem and biogeochemical responses during a mesocosm study." Biogeosciences *10*, 5619–5626.

TABLE OF CONTENTS

I. Introduction

Concentrations of atmospheric carbon dioxide (CO_2) are higher than those observed in the past 800,000 years (Lüthi et al. 2008). Since the industrial revolution in the mid 1800's, industrial and agricultural activities have led to a 40 % increase in atmospheric concentrations of CO_2 from approximately 280 parts per million (ppm) to over 400 ppm today (Le Quéré et al. 2016). In addition, the rate of increase in atmospheric concentrations of CO_2 over the past 250 years is remarkable – estimated at 0.5 % yr^{-1}, this rate is 100-times faster than any fluctuation experienced in the previous 650,000 years (Royal Society 2005). The Global Carbon Budget Project estimates that during the 2006 – 2015 decade, 91 % of human-produced (anthropogenic) CO_2 emissions were attributable to the burning of fossil fuels (34.1 Pg CO_2 yr^{-1}); the remaining 9 % to land-use changes (3.5 Pg CO_2 yr^{-1}). During this period, approximately 44 % of annual total anthropogenic CO_2 emissions remained in the atmosphere (16.4 Pg CO_2 yr^{-1}), while approximately 26 % (9.7 Pg CO_2 yr^{-1}), and 31 % (11.6 Pg CO_2 yr^{-1}) entered the oceanic and terrestrial biospheres.

The equilibration of atmospheric CO_2 with the surface ocean is fairly rapid and leads to annual increases in surface ocean concentrations of CO_2 in proportion to atmospheric increases (Sabine et al. 2004, Feely et al. 2009, Doney et al. 2009, Sabine and Tanhua 2010). As a result, the oceans have absorbed nearly one third of the anthropogenic CO_2 produced since the Industrial Revolution (Sabine et al. 2004). Thus, oceanic uptake of CO_2 effectively mitigates the effects of anthropogenic CO_2 on global climate change (Doney et al. 2009). However, increased levels of CO_2 in the surface ocean induces chemical reactions that

reduce seawater pH in a process referred to as "ocean acidification" (Caldeira and Wickett 2003), which may have lasting implications for marine organisms and biogeochemical cycling (e.g. Broecker and Clarke 2001, Orr et al. 2005, Doney et al. 2009, Feely et al. 2009).

As CO_2 from the atmosphere is dissolved in surface seawater, it rapidly combines with water to form carbonic acid (H_2CO_3). Subsequent dissociation through the loss of hydrogen ions converts carbonic acid to bicarbonate (HCO_3^-) ions, which can dissociate further via acid-base reactions to carbonate ions (CO_3^{2-}), through the following reactions:

$$CO_2(aqueous) + H_2O \leftrightarrow H_2CO_3 \leftrightarrow H^+ + HCO_3^- \leftrightarrow 2H^+ + CO_3^{2-}.$$

Collectively, aqueous CO_2, H_2CO_3, HCO_3^-, and CO_3^2 ions make-up dissolved inorganic carbon (DIC) in the ocean, and changes in the concentrations of one constituent will alter the relative contribution of the others. For surface seawater with pH around 8.1, approximately 90 % of the inorganic carbon is bicarbonate ion, 9 % is carbonate ion, and only 1 % is dissolved CO_2 (Doney et al. 2009). The addition of CO_2 to seawater increases aqueous CO_2, HCO_3^-, and H^+ ion concentrations, and decreases CO_3^{2-} ion concentrations. As a result, the addition of anthropogenic CO_2 decreases surface seawater pH ($pH = -\log [H^+]$). Projections by the Intergovernmental Panel on Climate Change (IPCC) suggest that at current CO_2 production rates, introduction of anthropogenic CO_2 to marine systems will increase the concentration of H^+, and thus the ocean's acidity, by 150 % by the end of the century (Orr et al. 2005, Feely et al. 2009). Consequently, surface seawater pH is projected to decrease from

a pre-industrial value of 8.2 to 7.8 over the same time frame (Orr et al. 2005, Feely et al. 2009).

In addition to increasing anthropogenic CO_2, convective mixing of elevated pCO_2 waters from depth into the surface ocean can expose organisms to ephemeral pulses of pH levels equivalent to those projected for the year 2100 (Feely et al. 2008, Hofmann et al. 2011). For example, seasonal convective mixing in subtropical and temperate systems in the northwestern Sargasso Sea near Bermuda brings elevated pCO_2 waters to the surface (Bates et al. 2012, Lomas et al. 2013). Furthermore, coastal upwelling off the west coast of North America can induce higher-frequency variability in pCO_2 (Feely et al. 2008) and result in strong shifts in pH on timescales of days in places like the Santa Barbara Channel (Hofmann et al. 2011). In contrast, seasonal or higher-frequency pulses of elevated pCO_2 are less likely in the more permanently stratified oligotrophic systems such as the South Pacific Subtropical Gyre. However, these surface waters are continually subject to rising atmospheric CO_2 concentrations and are expected to be impacted gradually. The broad range of pCO_2 variability from ephemeral pulses of elevated pCO_2 to decadal increases with rising atmospheric CO_2 highlight the necessity to understand the impacts of increasing pCO_2, and thus low pH, on marine biogeochemical processes on a variety of timescales.

The responses of marine eukaryotic organisms and communities to declining pH have been actively studied (e.g. Riebessell 2004, Doney et al. 2009, Beardall et al. 2009, Taucher et al. 2015). However, less emphasis has been placed on the direct effects of increasing partial pressures of CO_2 (pCO_2) and thus declining pH on marine heterotrophic bacteria and

archaea (collectively referred to as bacterioplankton; Joint et al. 2011). Heterotrophic bacterioplankton play an integral role in the marine carbon cycle through the consumption of dissolved organic carbon (DOC). DOC is conventionally defined as organic carbon that passes through a nominal pore-size filter of 0.7 μm (Whatman glass fiber filter; Hedges 2002). This definition encompasses a diverse array of compounds ranging from simple sugars to complex refractory molecules, the majority of which are uncharacterized because they are dilute and difficult to isolate from seawater (Borch and Kirchman 1977, Skoog and Benner 1997, Hedges 2002, Goldberg et al. 2009, Goldberg et al. 2010, Goldberg et al. 2011). As a result, bulk DOC is separated into three broadly defined pools based on its reactivity and biological availability: labile DOC is consumed on the order of hours to days, while that which persists for months to years is referred to as semi-labile DOC (Kirchman et al. 1993, Carlson and Ducklow, 1996, Hansell et al. 2012, Hansell and Carlson 2015); refractory DOC resists bacterioplankton degradation and persists in the ocean for tens to hundreds of years (Carlson et al. 1994, Carlson 2002). Collectively, the amount of carbon contained in these three pools (approximately 650 Pg C) is similar in magnitude to that present in atmospheric CO_2 (approximately 600 Pg C; Bernstein et al. 2007, Le Quére et al. 2016), suggesting that perturbations of the oceanic DOC reservoir have the potential to impact concentrations of CO_2 in the atmosphere. However, the majority of DOC is biochemically resistant (i.e. refractory DOC amounts to approximately 630 Pg C) and persists in the ocean on the timescales of centuries to millennia, suggesting that perturbations to this DOC pool have the potential to impact atmospheric CO_2 on geologic timescales. In contrast, substantially smaller pools of labile (< 1 Pg C), and semi-labile (< 10

Pg C) DOC have the potential to impact carbon cycling on much shorter time-scales (Cameron et al. 2005).

Photosynthesis is the dominant source of labile and semi-labile DOC in the ocean, with 50 – 100 % of photosynthetically-fixed carbon passing through the DOC pool (Williams 2000, Ducklow 1999, Hansell and Carlson 2015). Vertical transport of surface accumulated DOC into the ocean interior via convective mixing and subduction accounts for approximately 20 % of annual global ocean carbon export (but up to 30 – 50 % at particular sites). Thus, DOC export represents an important pathway in the biological carbon pump (the term given to the suite of biologically-mediated processes that lead to net organic carbon export from the surface ocean; Passow and Carlson 2012). Export of particulate organic carbon (~ 80 %), and active movement of carbon via vertically migrating zooplankton (< 1 %), also contribute to vertical export of organic carbon via the biological pump. Thus, factors that alter the amount of photosynthetically-derived DOC that accumulates in the surface ocean can have short-term implications for the ocean's ability to export organic carbon.

As a result of their small size and high surface-area to volume ratio (Azam et al. 1983) heterotrophic bacterioplankton are the primary consumers of photosynthetically-derived DOC (Pomeroy 1974). They are estimated to consume 50 % or more of the DOC produced in the surface ocean by photosynthesis (Azam et al. 1983, Ducklow et al. 1999). The repackaging of DOC into bacteriotplankton biomass serves as a food source to heterotrophic grazers and a potential link within the microbial food web (Azam et al. 1983). In contrast, if bacterioplankton convert consumed DOC to CO_2 through high rates of respiration, then

organic matter is remineralized and bacterioplankton serve as a sink for carbon (energy), preventing its passage to higher trophic levels (Ducklow et al. 1986). The relative amount of new bacterioplankton biomass (BB) produced per unit of DOC assimilated is reflected in the bacterioplankton growth efficiency (BGE; i.e. BGE = BB ÷ assimilated DOC). As such, BGE provides a quantitative measure of the degree to which bacterioplankton communities are functioning either as a carbon link to higher trophic levels, or as a carbon sink. Estimates of growth efficiencies of natural bacterioplankton communities exhibit large spatial as well as temporal variability, ranging from as little as 1 % up to 60 % or higher, though marine ecosystems tend to exhibit values towards the lower end of this range (del Giorgio and Cole 1998). A review of oceanic measurements of BGEs reports an open ocean mean of 15 % and a coastal mean of 27 % (del Giorgio and Cole 2000), suggesting that anywhere from 73 % to 85 % of consumed DOC is respired back to CO_2. Thus, factors that affect both the ability of bacterioplankton to consume photosynthetically-derived DOC, and the efficiency with which they convert consumed DOC to biomass (i.e. BGE), may alter the magnitude of DOC accumulation and POC production (as bacterioplankton biomass) in the surface ocean, ultimately affecting the amount of organic carbon available for export from the surface ocean via the biological pump.

There is a growing body of literature that suggests that increasing pCO_2 may impact bacterioplankton-mediated carbon cycling in the surface ocean through: Effects on bacterioplankton community composition (Krause et al. 2012, Maas et al. 2013, Siu et al. 2014, Bunse et al. 2016), increased bacterial degradation of carbohydrates through enhanced extracellular enzymatic rates of ß- glucosidase (Grossart et al. 2006, Piontek et al. 2010,

Maas et al. 2013, Piontek et al. 2013, Endres et al. 2014), and an increase in bacterioplankton abundance (Endres et al 2014, Arnosti et al. 2011). However, other studies observe negligible effects of elevated pCO_2 on bacterioplankton community composition (Sperling et al. 2013, Newbold et al. 2012, Oliver et al. 2014, Allgaier et al. 2008, Zhang et al. 2013, Roy et al. 2013), rates of extracellular ß- glucosidase (Yamada and Suzumura 2010), and bacterioplankton abundance (Grossart et al. 2006, Allgaier et al. 2008, Yamada and Suzumura 2010). A portion of these studies were conducted as mesocosm and culture experiments comprised of photoautotrophs, heterotrophic bacterioplankton, and grazers (Grossart et al. 2006, Piontek et al. 2010, Piontek et al. 2013, Endres et al. 2014, Arnosti et al. 2011, Maas et al. 2013, Sperling et al. 2013, Oliver et al. 2014, Allgaier et al. 2008, Zhang et al. 2013, Roy et al. 2013, Bunse et al. 2016), while others were conducted in the absence of phytoplankton (Siu et al. 2014, Yamada and Suzumura 2010, Krause et al. 2012). These experiments also employed various methods to alter the inorganic carbon chemistry, including chemical alteration through addition of acid (Piontek et al. 2010, Piontek et al. 2013, Yamada and Suzumura 2010, Maas et al. 2013), and aeration of seawater with CO_2 (Grossart et al. 2006, Motegi et al. 2013, Sperling et al. 2013, Newbold et al. 2012, Oliver et al. 2014, Roy et al. 2013, Zhang et al. 2013). As such, the reported variability in responses of marine bacterioplankton to elevated pCO_2 likely reflects differences in experimental design, manipulation of inorganic carbon parameters, and bacterioplankton communities resulting from various experimental sites.

Variability in the response of marine bacterioplankton to elevated pCO_2 highlights the need for studies that directly link measurements of bacterioplankton-mediated carbon cycling to

taxonomy and physiology in order to gain an understanding of the ecological function of bacteria during exposure to elevated pCO_2 in various oceanic regions. Bunse et al. (2016) conducted an elegant phytoplankton-bloom mesocosm experiment that provides insight to the physiological response of Mediterranean bacterial communities to low pH. In the presence of phytoplankton communities, Bunse et al. (2016) showed that low pH stimulated respiratory proton pumps that aid in translocating protons across the cell membrane, suggesting that bacteria upregulate respiratory proton pumps to export protons that invade the cell as a result of low external pH. Though this study offers insight to the physiological and taxonomic responses of bacteria to changes in pH, predicting how low pH will affect carbon cycling in the ocean requires measurements of organic carbon removal and bacterial growth dynamics.

In Chapters I and II, my co-authors and I present what is, to our knowledge, the first set of experiments to couple an evaluation of the direct effects elevated pCO_2 on bacterioplankton mediated-carbon cycling (Chapter I) with a mechanistic evaluation of the potential physiological implications of elevated pCO_2 on marine bacterioplankton (Chapter II). The seawater culture experiments conducted for Chapter I provide evidence to suggest that short-term exposure to elevated pCO_2 can enhance removal of photosynthetically-derived surface organic carbon by heterotrophic bacterioplankton communities. This result is consistent with results from previous mesocosm and culture studies that suggested that elevated pCO_2 conditions might lead to greater removal of organic carbon through enhanced extracellular glucosidase activity (Grossart et al. 2006, Piontek et al. 2010, Maas et al. 2013, Piontek et al. 2013, Endres et al. 2014). In addition to enhanced rates of organic carbon consumption,

estimates of the partitioning of assimilated DOC into bacterioplankton biomass versus respiration suggest that elevated pCO_2 conditions may decrease growth efficiencies. This result is in contrast to previous observations of bacterioplankton growth efficiencies in a mesocosm study, for which no effect of growth efficiencies was observed (Montegi et al. 2013); however, this may reflect trophodynamic-mediated effects of pCO_2 on DOC quality and quantity, rather than direct effects of pCO_2 on bacterioplankton growth efficiencies. Overall, results from Chapter I suggest that the cumulative effect of enhanced rates of DOC consumption and depressed growth efficiencies under elevated pCO_2 may decrease the rate at which DOC accumulates in the surface ocean, ultimately decreasing the effectiveness of DOC as a sink of carbon in the ocean via the biological pump. These results have implications for the cycling of carbon in the surface ocean, but fail to provide a mechanistic understanding of the effects of elevated pCO_2 on bacterioplankton physiology.

The use of metagenomic shotgun sequencing for Chapter II enabled the analysis of the metabolic pathways encoded by marine bacterial communities during short-term exposure to elevated pCO_2 conditions in order to identify a potential mechanistic understanding of the impacts of short term increases in pCO_2 on bacterioplankton-mediated carbon cycling. This analysis revealed that short-term increases in pCO_2 altered natural bacterioplankton communities and led to differential abundance of community functions. The shift in community structure and disproportionate effects of elevated pCO_2 on amino acid and carbohydrate metabolism provide a potential mechanism to explain why we observed enhanced organic carbon removal with elevated pCO_2. In addition, greater abundance of functions related to phospholipid and membrane maintenance, and toxin and antibiotic

resistance, provide a potential mechanistic explanation for increased bacterial respiration with elevated pCO_2, as these mechanisms require energy that could otherwise be used for growth. Collectively, the combined effects of pCO_2 on bacterioplankton community composition and metabolic functionality presented in Chapter I and II suggest that elevated pCO_2 can alter bacterial ecological function by enhancing rates of bacteria-mediated removal of surface organic carbon and production of carbon dioxide in the surface ocean through direct effects on community composition and community functions.

Critical to predicting the magnitude of the impact of short-term increases in pCO_2 on bacteria-mediated carbon dynamics on carbon-cycling in the surface ocean, is understanding the physical and biogeochemical processes currently controlling carbon dynamics in marine ecosystems. A subset of experiments conducted as part of the experimental work reported in Chapter I, in addition to the experiment conducted for Chapter II, were conducted using surface seawater collected in the oligotrophic waters near the islands of Moorea and Tahiti, French Polynesia, in the South Pacific Subtropical Gyre. To gain an understanding of the physical and biogeochemical processes controlling carbon dynamics in the upper 300 m of the water column near these islands, I took part in a 3-week oceanographic research cruise conducted as part of the Moorea Coral Reef Long Term Ecological Research effort to map key physical and biogeochemical constituents in the waters around the islands of Moorea and Tahiti. Chapter III describes the vertical patterns in hydrographic conditions, inorganic nutrients, rates of productivity, and stocks of organic matter resulting from this high-resolution sampling effort.

Overall, results from Chapters I and II contribute to the growing understanding of the effects of elevated pCO_2 on bacterioplankton-mediated carbon cycling in the marine environment. In addition, Chapter III provides the first high-resolution evaluation of key physical and biogeochemical dynamics controlling carbon dynamics in the highly oligotrophic waters surrounding the islands of Moorea and Tahiti, French Polynesia.

References

Allgaier, M., Riebesell, U., Vogt, M., Thyrhaug, R., and Grossart, H.-P. (2008). Coupling of heterotrophic bacteria to phytoplankton bloom development at different pCO2 levels: a mesocosm study. Biogeosciences 5, 1007–1022.

Arnosti, C., Grossart, H., Mühling, M., Joint, I., and Passow, U. (2011). Dynamics of extracellular enzyme activities in seawater under changed atmospheric pCO2: a mesocosm investigation. Aquatic Microbial Ecology 64, 285–298.

Azam, F., Fenchel, T., Field, J.G., Gray, J.S., Meyer-Reil, L.A., and Thingstad, F. (1983). The ecological role of water-column microbes in the sea. Marine Ecology Progress Series 257–263.

Bates, N.R., Best, M.H.P., Neely, K., Garley, R., Dickson, A.G., and Johnson, R.J. (2012). Detecting anthropogenic carbon dioxide uptake and ocean acidification in the North Atlantic Ocean. Biogeosciences 9, 2509–2522.

Beardall, J., Stojkovic, S., and Larsen, S. (2009). Living in a high CO 2 world: impacts of global climate change on marine phytoplankton. Plant Ecology & Diversity 2, 191–205.

Bernstein, L., Bosch, P., Canziani, O., Chen, Z., Christ, R., Davidson, O., Hare, W., Huq, S., Karoly, D., and Kattsov, V. (2008). Climate change 2007: Synthesis report: An assessment of the intergovernmental panel on climate change (IPCC).

Borch, N.H., and Kirchman, D.L. (1977). Concentration and composition of dissolved combine nuetral sugars (polysaccharides) in seawater determined by HPLC-PAD. Marine Chemistry 57, 85–95.

Broecker, W., and Clark, E. (2001). A dramatic Atlantic dissolution event at the onset of the last glaciation. Geochem. Geophys. Geosyst. 2, 1065.

Bunse, C., Lundin, D., Karlsson, C.M.G., Vila-Costa, M., Palovaara, J., Akram, N., Svensson, L., Holmfeldt, K., González, J.M., Calvo, E., et al. (2016). Response of marine bacterioplankton pH homeostasis gene expression to elevated CO2. Nature Climate Change.

Caldeira, K., and Wickett, M.E. (2003). Anthropogenic carbon and ocean pH. Nature 425, 365.

Cameron, D.R., Lenton, T.M., Ridgwell, A.J., Shepherd, J.G., Marsh, R., and Yool, A. (2005). A factorial analysis of the marine carbon cycle and ocean circulation controls on atmospheric CO 2: Marine carbon cycle control on atmospheric CO2. Global Biogeochemical Cycles 19.

Carlson, C.A., and Ducklow, H.W. (1996). Growth of bacterioplankton and consumption of dissolved organic carbon in the Sargasso Sea. Aquatic Microbial Ecology 10, 69–85.

Carlson, C., Giovannoni, S., Hansell, D., Goldberg, S., Parsons, R., Otero, M., Vergin, K., and Wheeler, B. (2002). Effect of nutrient amendments on bacterioplankton production, community structure, and DOC utilization in the northwestern Sargasso Sea. Aquatic Microbial Ecology 30, 19–36.

Carlson, C.A., Ducklow, H.W., and Michaels, A.F. (1994). Annual flux of dissolved organic carbon from the euphotic zone in the northwestern Sargasso Sea. Nature 371, 405–408.

Del Giorgio, P.A., and Cole, J.J. (1998). Bacterial growth efficiency in natural aquatic systems. Annual Review of Ecology and Systematics 29, 503–541.

del Giogrio, PA and JJ Cole. 2000. Bacterial energetics and growth efficiency. In Microbial Ecology of the Oceans, First Edition. DL Kirchman, ed. Wiley-Liss, New York, 542 pp.

Doney, S.C., Fabry, V.J., Feely, R.A., and Kleypas, J.A. (2009). Ocean Acidification: The Other CO 2 Problem. Annual Review of Marine Science 1, 169–192.

Ducklow, HW, DA Purdie, PJ LeB Williams and JM Davies. 1986. Bacterioplankton: a sink for carbon in a coastal marine plankton community. Science 232, 865-867.

Ducklow, H.W. (1999). The bacterial component of the oceanic euphotic zone. FEMS Microbiology Ecology 30, 1–10.

Endres, S., Galgani, L., Riebesell, U., Schulz, K.-G., and Engel, A. (2014). Stimulated Bacterial Growth under Elevated pCO2: Results from an Off-Shore Mesocosm Study. PLoS ONE 9, e99228.

Feely, R.A., Sabine, C.L., Hernandez-Ayon, J.M., Ianson, D., and Hales, B. (2008). Evidence for Upwelling of Corrosive “Acidified” Water onto the Continental Shelf. Science 320, 1490–1492.

Feely, R.A., Doney, S.C., and Cooley, S.R. (2009). Ocean acidification: Present conditions and future changes in a high-CO_2 world. Oceanography 22, 36–47.

Goldberg, S.J., Carlson, C.A., Hansell, D.A., Nelson, N.B., and Siegel, D.A. (2009). Temporal dynamics of dissolved combined neutral sugars and the quality of dissolved

organic matter in the Northwestern Sargasso Sea. Deep Sea Research Part I: Oceanographic Research Papers 56, 672–685.

Goldberg, S.J., Carlson, C.A., Bock, B., Nelson, N.B., and Siegel, D.A. (2010). Meridional variability in dissolved organic matter stocks and diagenetic state within the euphotic and mesopelagic zone of the North Atlantic subtropical gyre. Marine Chemistry 119, 9–21.

Goldberg, S.J., Carlson, C.A., Brzezinski, M., Nelson, N.B., and Siegel, D.A. (2011). Systematic removal of neutral sugars within dissolved organic matter across ocean basins: Systematic Removal of Neutral Sugars. Geophysical Research Letters 38.

Grossart, H.-P., Allgaier, M., Passow, U., and Riebesell, U. (2006). Testing the effect of CO2 concentration on the dynamics of marine heterotrophic bacterioplankton. Limnol. Oceanogr. 51, 1–11.

Hansell and Carlson (2015). Biogeochemistry of marine dissolved organic matter (Amsterdam ; Boston: Academic Press).

Hansell, D.A., Carlson, C.A., and Schlitzer, R. (2012). Net removal of major marine dissolved organic carbon fractions in the subsurface ocean: Removal of Exported DOC. Global Biogeochemical Cycles 26.

Hedges, JI. 2002. Why dissolved organics matter. In Biogeochemistry of Dissolved Organic Matter. DA Hansell and CA Carlson, eds. Academic Press, New York, 774 pp.

Hofmann, G.E., Smith, J.E., Johnson, K.S., Send, U., Levin, L.A., Micheli, F., Paytan, A., Price, N.N., Peterson, B., Takeshita, Y., et al. (2011). High-Frequency Dynamics of Ocean pH: A Multi-Ecosystem Comparison. PLoS ONE 6, e28983.

Joint, I., Doney, S.C., and Karl, D.M. (2011). Will ocean acidification affect marine microbes? The ISME Journal 5, 1–7.

Kirchman, D. L., C. Lancelot, M. Fasham, L. Legendre, G. Radach, and M. Scott (1993), Dissolved organic matter in biogeochemical models of the ocean, in Towards a Model of Ocean Biogeochemical Processes, edited by G. T. Evans and M. J. R. Fasham, pp. 209–225, Springer, Berlin

Krause, E., Wichels, A., Giménez, L., Lunau, M., Schilhabel, M.B., and Gerdts, G. (2012). Small Changes in pH Have Direct Effects on Marine Bacterial Community Composition: A Microcosm Approach. PLoS ONE 7, e47035.

Le Quéré, C., Andrew, R.M., Canadell, J.G., Sitch, S., Korsbakken, J.I., Peters, G.P., Manning, A.C., Boden, T.A., Tans, P.P., Houghton, R.A., et al. (2016). Global Carbon Budget 2016. Earth System Science Data 8, 605–649.

Lomas, M.W., Bates, N.R., Johnson, R.J., Knap, A.H., Steinberg, D.K., and Carlson, C.A. (2013). Two decades and counting: 24-years of sustained open ocean biogeochemical measurements in the Sargasso Sea. Deep Sea Research Part II: Topical Studies in Oceanography 93, 16–32.

Lüthi, D., Le Floch, M., Bereiter, B., Blunier, T., Barnola, J.-M., Siegenthaler, U., Raynaud, D., Jouzel, J., Fischer, H., Kawamura, K., et al. (2008). High-resolution carbon dioxide concentration record 650,000–800,000 years before present. Nature 453, 379–382.

Maas, E., Law, C., Hall, J., Pickmere, S., Currie, K., Chang, F., Voyles, K., and Caird, D. (2013). Effect of ocean acidification on bacterial abundance, activity and diversity in the Ross Sea, Antarctica. Aquatic Microbial Ecology 70, 1–15.

Motegi, C., Tanaka, T., Piontek, J., Brussaard, C.P.D., Gattuso, J.-P., and Weinbauer, M.G. (2013). Effect of CO2 enrichment on bacterial metabolism in an Arctic fjord. Biogeosciences 10, 3285–3296.

Newbold, L.K., Oliver, A.E., Booth, T., Tiwari, B., DeSantis, T., Maguire, M., Andersen, G., van der Gast, C.J., and Whiteley, A.S. (2012). The response of marine picoplankton to ocean acidification: Response of picoplankton to ocean acidification. Environmental Microbiology 14, 2293–2307.

Oliver, A.E., Newbold, L.K., Whiteley, A.S., and van der Gast, C.J. (2014). Marine bacterial communities are resistant to elevated carbon dioxide levels: Marine bacterial communities and elevated CO 2. Environmental Microbiology Reports 6, 574–582.

Orr, J.C., Fabry, V.J., Aumont, O., Bopp, L., Doney, S.C., Feely, R.A., Gnanadesikan, A., Gruber, N., Ishida, A., Joos, F., et al. (2005). Anthropogenic ocean acidification over the twenty-first century and its impact on calcifying organisms. Nature 437, 681.

Passow, U., and Carlson, C. (2012). The biological pump in a high CO<sub>2 world. Marine Ecology Progress Series 470, 249–271.

Piontek, J., Lunau, M., Händel, N., Borchard, C., Wurst, M., and Engel, A. (2010). Acidification increases microbial polysaccharide degradation in the ocean. Biogeosciences 7, 1615–1624.

Piontek, J., Handel, N., De Bodt, C., Harlay, J., Chou, L., and Engel, A. (2011). The utilization of polysaccharides by heterotrophic bacterioplankton in the Bay of Biscay (North Atlantic Ocean). Journal of Plankton Research 33, 1719–1735.

Piontek, J., Borchard, C., Sperling, M., Schulz, K.G., Riebesell, U., and Engel, A. (2013). Response of bacterioplankton activity in an Arctic fjord system to elevated pCO2: results from a mesocosm perturbation study. Biogeosciences 10, 297–314.

Pomeroy, L.R. (1974). The Ocean's Food Web, A Changing Paradigm. BioScience 24, 499–504.

Riebesell, U. (2004). Effects of CO2 enrichment on marine phytoplankton. Journal of Oceanography 60, 719–729.

Roy, A.-S., Gibbons, S.M., Schunck, H., Owens, S., Caporaso, J.G., Sperling, M., Nissimov, J.I., Romac, S., Bittner, L., Mühling, M., et al. (2013). Ocean acidification shows negligible impacts on high-latitude bacterial community structure in coastal pelagic mesocosms. Biogeosciences 10, 555–566.

Royal Society (Great Britain) (2005). Ocean acidification due to increasing atmospheric carbon dioxide. (London: Royal Society).

Sabine, C.L., and Tanhua, T. (2010). Estimation of Anthropogenic CO 2 Inventories in the Ocean. Annual Review of Marine Science 2, 175–198.

Sabine, C.L., Feely, R.A., Gruber, N., Key, R.M., Lee, K., Bullister, J.L., Wanninkhof, R., Wong, C.S., Wallace, W.R., Tilbrook, B., et al. (2004). The Oceanic Sink for Anthropogenic CO2. Science 305, 367–371.

Siu, N., Apple, J.K., and Moyer, C.L. (2014). The Effects of Ocean Acidity and Elevated Temperature on Bacterioplankton Community Structure and Metabolism. Open Journal of Ecology 04, 434–455.

Skoog, A., and Benner, R. (1997). Aldoses in various size fractions of marine organic matter: Implications for carbon cycling. Limnology and Oceanography 42, 1803–1813.

Sperling, M., Piontek, J., Gerdts, G., Wichels, A., Schunck, H., Roy, A.-S., La Roche, J., Gilbert, J., Nissimov, J.I., Bittner, L., et al. (2013). Effect of elevated CO2 on the dynamics of particle-attached and free-living bacterioplankton communities in an Arctic fjord. Biogeosciences 10, 181–191.

Taucher, J., Jones, J., James, A., Brzezinski, M.A., Carlson, C.A., Riebesell, U., and Passow, U. (2015). Combined effects of CO 2 and temperature on carbon uptake and partitioning by the marine diatoms Thalassiosira weissflogii and Dactyliosolen fragilissimus: Combined effects of CO 2 and temperature. Limnology and Oceanography 60, 901–919.

Weinbauer, M.G., Mari, X., and Gattuso, J.-P. (2011). Effect of ocean acidification on the diversity and activity of heterotrophic marine microorganisms. Ocean Acidification. Oxford University Press, Oxford 83–98.

Yamada, N., Tsurushima, N., and Suzumura, M. (2013). Effects of CO2-Induced Seawater Acidification on Microbial Processes Involving Dissolved Organic Matter. Energy Procedia 37, 5962–5969.

Zhang, R., Xia, X., Lau, S.C.K., Motegi, C., Weinbauer, M.G., and Jiao, N. (2013). Response of bacterioplankton community structure to an artificial gradient of pCO2 in the Arctic Ocean. Biogeosciences 10, 3679–3689.

Williams, P.J.l, 2000. Heterotrophic bacteria and the dynamics of dissolved organic material. In: Kirchman, D.L. (Ed.), Microbial Ecology of the Oceans. Wiley-Liss, New York, pp. 153–200 pp.

II. CHAPTER I

Elevated pCO_2 Enhances Bacterioplankton Removal of Organic Carbon

Anna K. James[1], Uta Passow[1], Mark A. Brzezinski[1], Rachel J. Parsons[2], Jennifer N. Trapani[2], and Craig A. Carlson[1]

[1] Marine Science Institute, Department of Ecology, Evolution, and Marine Biology, University of California, Santa Barbara, CA, United States of America

[2] Bermuda Institute of Ocean Science (BIOS), St. George's, GE 01, Bermuda

PLoS ONE 12(3): e0173145. doi:10.1371/journal.pone.0173145

Abstract

Factors that affect the removal of organic carbon by heterotrophic bacterioplankton can impact the rate and magnitude of organic carbon loss in the ocean through the conversion of a portion of consumed organic carbon to CO_2. Through enhanced rates of consumption, surface bacterioplankton communities can also reduce the amount of dissolved organic carbon (DOC) available for export from the surface ocean. The present study investigated the direct effects of elevated pCO_2 on bacterioplankton removal of several forms of DOC ranging from glucose to complex phytoplankton exudate and lysate, and naturally occurring DOC. Elevated pCO_2 (1000 – 1500 ppm) enhanced both the rate and magnitude of organic carbon removal by bacterioplankton communities compared to low (pre-industrial and ambient) pCO_2 (250 – ~400 ppm). The increased removal was largely due to enhanced respiration, rather than enhanced production of bacterioplankton biomass. The results suggest that elevated pCO_2 can increase DOC consumption and decrease bacterioplankton

growth efficiency, ultimately decreasing the amount of DOC available for vertical export and increasing the production of CO_2 in the surface ocean.

Introduction

Marine heterotrophic bacterioplankton play a key role in the biogeochemical cycling of carbon through their use of dissolved organic carbon (DOC) [1]. These communities convert a portion of consumed DOC into biomass and respire the remainder to CO_2, thereby, decreasing total organic carbon concentrations in the ocean through the production of CO_2. Via air – sea exchange, the production of CO_2 in the surface ocean could lead to the loss of carbon from the ocean [2]. DOC that escapes bacterioplankton consumption and persists on the timescales of months to years has the potential to be exported out of the surface ocean by physical processes and represents a major export pathway in the biological pump [3, 4, 5]. Thus, factors that affect bacterioplankton consumption of DOC impact surface-ocean carbon inventories and the amount of organic carbon available for export as either DOC or organic carbon associated with bacterioplankton biomass.

How ocean acidification affects marine bacterioplankton directly or indirectly remains a topic of interest [6]. Recent mesocosm and culture experiments comprised of photoautotrophs, heterotrophic bacterioplankton, and grazers have demonstrated clear effects of elevated pCO_2 on bacterioplankton growth [7-9] and extracellular enzyme activities [9-13]. Bacterioplankton protein production [9] and abundance [10] were shown to increase as a function of elevated pCO_2, while Motegi et al. [8] observed no effect of pCO_2 on other aspects of bacterioplankton activity (i.e. respiration, growth efficiency, and carbon

demand). Multiple studies observed enhanced rates of extracellular enzyme activity such as leucine-aminopeptidase [10, 12], protease [9], and glucosidase [9, 11-13], suggesting accelerated hydrolysis of various components of dissolved organic material as a function of increasing pCO_2. These studies provide valuable insight to the net community effects of pCO_2 on organic carbon cycling. However, the effects of pCO_2 on heterotrophic bacterioplankton for these studies were evaluated during nutrient-induced phytoplankton blooms (mesocosm studies) [7 – 10, 12, 13] or by inoculating pH-manipulated phytoplankton cultures with natural bacterioplankton communities (culture study) [11]. Both of these experimental designs make it difficult to differentiate the direct effects of pCO_2 on heterotrophic bacterioplankton physiology and organic carbon removal from the indirect effects that pCO_2 may have had on the quantity and quality of the organic carbon produced by the phytoplankton [14, 15], which could potentially also alter microbial organic carbon removal.

Studies conducted in the absence of phytoplankton showed somewhat different results: Yamada and Suzumura [16] observed no effect of elevated pCO_2 on extracellular glucosidase activity of the free-living bacterioplankton communities. They did, however, observe an increase in extracellular leucine-aminopeptidase and lipase activity, suggesting an increase in the processing of protein and lipid substrates and no effect on polysaccharide use. Siu et al. [17] observed a decrease in bacterioplankton respiration and bacterioplankton production, as measured via ^3H –thymidine incorporation, and a clear shift from more diverse bacterioplankton communities at ambient pH to less diverse communities under elevated pCO_2 conditions. These studies provide insight to the direct effects of elevated

pCO_2 on bacterioplankton extracellular enzyme activity and community structure but did not address the effects of pCO_2 on bacterioplankton removal of organic carbon.

Here we present results from seawater culture experiments that were designed to examine the direct effect of pCO_2 on net removal of organic carbon by bacterioplankton and discuss resulting implications for bacterioplankton respiration and biomass production. Laboratory perturbation experiments using natural bacterioplankton communities were conducted at three contrasting sites: the Sargasso Sea, the Santa Barbara Channel, and the South Pacific Subtropical Gyre. In the oligotrophic Sargasso Sea, deeper waters with elevated pCO_2 are brought to the surface through convective mixing annually [18, 19]. Coastal upwelling off the west coast of North America can induce higher-frequency variability in pCO_2 [20] and result in strong shifts in pH on timescales of days in places like the Santa Barbara Channel, CA [21]. In contrast, seasonal or higher-frequency pulses of elevated pCO_2 are less likely in the more permanently stratified oligotrophic systems such as the waters surrounding the islands of Moorea and Tahiti, within the South Pacific Subtropical Gyre [21]. All ocean surface waters are also subject to rising atmospheric CO_2 concentrations and are expected to be impacted gradually. How this broad range in the frequency and magnitude of elevated pCO_2 exposure impacts DOC processing by bacterioplankton remains largely unknown. The objective of this study was to assess the direct effect of short-term exposure to elevated pCO_2 on bacterioplankton organic carbon removal, across a variety of ocean sites.

Our results show that short-term perturbations of elevated pCO_2 can result in an increased rate and magnitude of organic carbon removal by bacterioplankton, independent of the

environmental origin of the bacterioplankton communities. These results suggest that short-term increases in pCO_2 can lead to an increased loss of organic carbon due to respiration, which may ultimately reduce surface ocean carbon inventories and the amount of DOC available for vertical export from the surface ocean.

Materials and Methods

General experimental set-up and design

The same general approach was used for all three study sites. Experiments consisted of 0.2 µm-filtered (0.2 µm GSWP, Millipore, Billerica, MA) seawater or 0.2 µm-filtered phytoplankton exudate that was inoculated with natural bacterial communities. The inoculum of natural bacterial communities consisted of either unfiltered whole seawater (Sargasso Sea and South Pacific Subtropical Gyre experiments) or 1.2 µm filtrate (Santa Barbara Channel experiments; 1.2 µm RAWP, Millipore, Billerica, MA). Particulate organic carbon concentration in oligotrophic gyres is low (1-3 µmol C L^{-1}) so to avoid filtration artifacts such as reduced bacterial production (unpublished data) and contamination of DOC due to handling, the inoculum was not pre-filtered for the experiments conducted in oligotrophic waters. Because particulate organic carbon concentration can be much greater in coastal upwelling systems it was necessary to remove large particles and organisms from the inoculum. Inoculum was added at 25 – 30% of final volume (Table 1), effectively diluting grazer concentrations and grazing pressure. All filters were pre-rinsed with ~2 L of deionized distilled water and sample water prior to use in order to remove organic contaminants from the filters.

Treatments

The four types of DOC treatments used in the experiments included either: (1) unamended seawater, which provided naturally occurring DOC, (2) naturally occurring DOC amended with glucose (~10 μM C), NH_4Cl (1μM) and K_2HPO_4 (0.1μM) (CNP) [22], or one of two phytoplankton-derived DOC mixtures: (3) phytoplankton exudate or (4) naturally occurring DOC amended with phytoplankton lysate (~10 μM C). There was no attempt to standardize the initial concentration of DOC in the phytoplankton exudate treatments; thus, those treatments contained total organic carbon concentrations that were 2 – 3 fold greater than those in the unamended seawater at the beginning of the experiments (Table 1).

The various treatments were generated by inoculating the 0.2 μm pre-filtered seawater or exudate with the microbial community; this solution was then divided into two polycarbonate (PC) containers to adjust pCO_2 (Table 1). pCO_2 levels were adjusted via chemical additions (Sargasso Sea experiment) or by bubbling with CO_2-mixed air (Santa Barbara Channel and South Pacific Subtropical Gyre experiments). Adjusted seawater incubations were then transferred into new PC carboys and CNP or lysate was added, if appropriate. A very small volume of lysate (1.2 mL to 11.5 L of experimental volume) or CNP (12 mL to 10 L of experimental water for the Sargasso Sea experiment; 0.28 mL to 10 L of experimental volume for the Santa Barbara Channel experiment) was added to minimize perturbing the carbonate chemistry. All experiments were conducted in duplicate, at in situ temperatures, and in the dark to eliminate photoautotrophic production (Table 1). All PC bottles had been acid-washed (5 % or 10 % HCL) and rinsed with deionized distilled water and sample water before use.

pCO_2 adjustments

Except in the Sargasso Sea, the pCO_2 was adjusted by bubbling with CO_2-mixed air (Scott Marrin Inc.) at ~100 mL min^{-1} through an air stone to produce fine bubbles for 45 min – 4 hours depending on volume. The pCO_2 adjustment via bubbling was conducted only once, prior to the start of the experiment, to eliminate the possibility of abiotic removal of organic matter as a result of continued bubbling. The air in the headspace of each sample bottle was exchanged with target CO_2-mixed air every 24 hours to minimize the change in pCO_2 levels throughout the experiment. Bubbling was conducted at experimental temperatures, which were identical to the in situ temperatures of the inoculums. In the Sargasso Sea experiment, pCO_2 was adjusted through the addition of 0.206 g $CaCO_3$, 0.032 g $NaHCO_3$, and 29 mL of 0.1 N HCL according to the best practices guide [23]. This closed system approach results in an inorganic carbon perturbation that is chemically identical to bubbling [24].

To maintain pCO_2 over the course of the experiments, the incubation bottle lids used for the Santa Barbara Channel and South Pacific Subtropical Gyre experiments were equipped with built-in gas and sampling ports to allow for sampling via positive pressure displacement in which the treatment pCO_2 gas was used to pressurize the head space (< 3 PSI); thus displacing the sample volume from the incubation vessel through the sample line directly into a collection vessel. In the Sargasso Sea, samples were collected by decanting directly from the incubation bottles into sample bottles.

To assess the potential change in pH over the course of an incubation we measured pH as described below for experiments # 1 – 4. We found that pH changes, within a given incubation, were minimal (0 – 0.04 pH units) over the course of the experiments. These pH changes correspond to changes in pCO_2 of ~ 1 – 60 ppm, which is much less than the differences in pCO_2 between low and elevated-pCO_2 treatments (~370 – ~1100 ppm). Thus, we concluded that pH adjustments were maintained throughout experiments with very little drift in pCO_2.

Sargasso Sea experiment

Water was collected from Hydrostation S (32° 10'N, 64° 30'W) in the northwestern Sargasso Sea at a depth of 10 m using a conductivity, temperature, depth (CTD) rosette. Sampling met the limited impact research requirements under the Bermuda Institute of Sciences Collection and Experimental Ethics Policy. As a result, collection and export permits were not required from the Bermuda Government at the time of this study. Seawater culture experiments were set-up in the lab at the Bermuda Institute of Ocean Science within hours of collection. The experiment consisted of four treatments, each in duplicate: two pCO_2 treatments (ambient and elevated) combined with two DOC treatments (CNP amended and unamended) as a full factorial design (experiment # 1, Table 1). The inoculated seawater was partitioned into two 10 L PC carboys, one remaining unadjusted (ambient pCO_2 treatment); the pCO_2 of the second carboy was adjusted to ~760 ppm using the closed system approach (23). Duplicate 2 L PC bottles were filled with each pCO_2 treatment for the unamended DOC treatments. CNP was added to the seawater remaining in the 10 L carboys to a final concentration of 10 μM C, 1 μM N, and 0.1 μM P (as described above) and each

was then split into duplicate 2 L PC bottles, representing the amended DOC treatments. All eight bottles were incubated within a temperature controlled upright incubator (Table 1).

Santa Barbara Channel experiments

Five experiments were conducted with surface seawater collected from the Santa Barbara Channel between 2012 and 2014 (experiments # 2-6, Table 1). No specific permissions were required for near-shore seawater collection in the Santa Barbara Channel. Each time, surface seawater was collected using a PC carboy from a near-shore site along the coast of Santa Barbara, CA (34° 24'N, 119° 50'W). The DOC source and starting pCO_2 conditions, as well as the bacterioplankton inoculum varied between experiments (Table 1). pCO_2 of seawater incubations were adjusted to pre-industrial (250 ppm) and elevated (1000 ppm or 1500 ppm) levels by bubbling with CO_2-mixed air in two 8 L or 20 L PC carboys (see above) depending on experimental water requirements (Table 1). pCO_2 adjusted seawater was split into duplicate 0.5 L or 2 L PC bottles and placed within a temperature controlled upright incubator (Table 1).

South Pacific Subtropical Gyre experiments

Three separate experiments were conducted in July 2014 with water collected near French Polynesia in the South Pacific Subtropical Gyre (17° 36'S, 149° 43'W) (experiments # 7-9, Table 1). All research was performed under annual research permits (permit no. 438/AME) issued by the French Polynesian Ministry of Foreign Affairs of International Development of the French Republic, Americans and Caribbean Islands Division. Seawater was collected from a depth of 25 m using a CTD rosette and seawater cultures were prepared in two 20 L

PC carboys. Treatments for each of the three experiments included unamended and amended DOC treatments and pre-industrial (250 ppm) and elevated (1000 ppm) pCO_2 in a full factorial design. One of two 20 L carboys was bubbled with pre-industrial (250 ppm) CO_2-mixed air and the other with elevated (1000 ppm) CO_2-mixed air as described below. pCO_2 adjusted seawater was then amended with phytoplankton-lysate to a final addition of ~10 μM C and placed within an upright incubator (Table 1). We were unable to measure pCO_2 at sea but applied the same flow rate and bubbling time that resulted in effective pCO_2 adjustment previously.

Production of phytoplankton-derived DOC

Phytoplankton exudates and lysates were derived from phytoplankton cultures in order to assess the impact of varying pCO_2 on the microbial consumption of complex DOC. Exudates from five different diatom cultures (*Dactyliosolen fragilissimus, Thalassiosira weissflogii, Chaetoceros socialis, Asterionellopsis glacialis*) and one coccolithophore (*Emiliana huxleyi*) were used in the Santa Barbara Channel experiments where diatoms are often abundant. In addition, phytoplankton lysate was produced from *Emiliana huxleyi* and used for the experiments conducted in the South Pacific Subtropical Gyre where coccolithophores are often present [25].

Phytoplankton cultures were grown in sterilized (double 0.2 μm filtered) seawater collected from the Santa Barbara Channel and enriched with inorganic nutrients in a modified version of f/2 medium [26]. Preliminary growth experiments were used to determine the ratio of N:P:Si nutrient additions needed to induce nitrate limitation within each culture. This was

done to enhance the production of DOC in the phytoplankton cultures and to minimize the addition of nitrate to the culture experiments. A light/ dark cycle of 14/10 hours, a photon flux density of ~100 μmol m^{-2} s^{-1}, and a temperature of 18 °C was maintained for all cultures throughout the growth period.

Nitrate concentration was monitored over the course of phytoplankton growth via UV detection using an HP452A spectrophotometer (Hewlett Packard 8452A) [27] and calibrated against a series of chemical nitrate standards (4 point curve; 0 – 100 μmol N L^{-1}). Exudate and lysate was harvested from the cultures two days after nitrate concentration fell below 2.4 ± 1 μmol N L^{-1} according to Nelson and Carlson [28]. Briefly, exudate was harvested via filtration (0.2 μm GSWP, Millipore, Billerica, MA), whereas lysate was harvested through a series of steps including cell concentration via centrifugation (10,000 rpm) and freeze-thaw cycles. After final centrifugation the cell pellet was abraded with a pre-combusted glass rod to generate cell lysate. Final lysate volume was 0.2 μm filtered and then acidified (4 M HCl) to a pH of ~3 and stored at -20 °C for one week prior to use in the South Pacific Subtropical Gyre experiments.

Experimental samples

Experimental samples were not filtered upon removal from experimental incubations in order to minimize contamination due to transfer and handling. Samples for total organic carbon (TOC; carbon content of bacterioplankton biomass plus DOC) and bacterioplankton abundance were collected throughout the incubations. pH was monitored over regular intervals for the Sargasso Sea experiments and experiments # 2 – 5 in the Santa Barbara

Channel. pCO_2 was measured at the start of the incubations for Santa Barbara Channel experiments # 2 and 4 - 6. Measurements of pCO_2 and pH were not made for the South Pacific Subtropical Gyre experiments or the Santa Barbara Channel #10 experiment due to logistical constraints. However, our ability to effectively alter the pCO_2 from ambient to target levels was demonstrated numerous times prior to these experiments (Table 1, experiments # 2 – 6). Thus, we used previously determined bubbling rates and duration to achieve target pCO_2 levels. The direct effect of pCO_2 on carbon content of bacterioplankton cells was determined during the Santa Barbara Channel follow-up experiment # 10.

Sample processing

TOC measurements – The procedures used to set up each experiment (inoculum filtration and dilution with 0.2 μm filtrate) removed the majority of particulate organic carbon such that changes in bacterioplankton carbon production and DOC removal were mainly a function of the growth of the bacterioplankton. Ideally, samples collected for organic carbon would be filtered in order to directly assess DOC removal independently from bacterioplankton carbon production. However, sample handling during filtration can result in contamination that obscures changes in DOC on the scale of a few micro-molar C. To avoid contamination, seawater samples from the incubation experiments were not filtered. Therefore, measured values of organic carbon include both DOC and bacterioplankton carbon and are considered TOC.

TOC samples were collected into 60 mL high-density polyethylene bottles (Sargasso Sea and South Pacific Subtropical Gyre) or in combusted 40 mL glass EPA vials with Teflon

coated silicone septa (Santa Barbara Channel). All TOC samples were frozen at -20 °C until analysis. Samples were analyzed via high temperature combustion method on a modified Shimadzu TOC-V or Shimadzu TOC-L using the standardization and referencing approaches described in Carlson et al. [29].

Bacterioplankton abundance measurement – Samples for bacterioplankton abundance were analyzed by epifluorescence microscopy with 0, 6-diamidino -2-phenyl dihydrochloride (5µg mL^{-1}, DAPI, SIGMA-Aldrich, St. Louis, MO, USA) according to Porter and Feig [30] (experiments # 1 and 10), or by Flow Cytometry (FCM) on an LSR II with SYBR Green I according to Nelson et al. [31] (experiments # 2 – 9). See Parsons et al. [32] and Nelson et al. [31] regarding sample preparation and instrument settings for epifluorescence microscopy and FCM analyses, respectively. DAPI direct counts and FCM analysis enumerate total prokaryotic abundance. We were not able to differentiate between bacterial and archaeal domains and refer to the combined cell densities as bacterioplankton abundance [33].

Bacterioplankton carbon measurement – To assess the direct effect of pCO_2 on the carbon content of bacterioplankton cells a follow-up experiment was conducted with water collected from the Santa Barbara Channel during December 2015 (experiment # 10, Table 1). The experimental procedure used was identical to that for all other experiments. Surface seawater was collected using a PC carboy from a near-shore site along the coast of Santa Barbara, CA (34° 24'N, 119° 50'W). One of two 20 L carboys filled with 0.2 µm- and 1.2 µm-filtered seawater was bubbled with pre-industrial (250 ppm) CO_2-mixed air and the

other with elevated (1500 ppm) CO_2-mixed air. pCO_2 adjusted seawater was then amended with phytoplankton-lysate to a final addition of ~20 μmol C L^{-1} and placed within a temperature controlled incubator in the dark (Table 1).

Samples for determining the carbon content of bacterioplankton cells were collected at the beginning of stationary phase to maximize bacterioplankton abundance and to minimize the contribution of nanoflagellate grazers to carbon estimates. A one-liter sample was filtered onto combusted GF75 filters (Advantec®; Dublin CA). GF75 filters were used because they have a nominal pore size of 0.3 μm and demonstrated 92 ± 2 % (range = 3.7 %; n = 5) cell retention. DOC-blanks were collected simultaneously to account for adsorption of organic carbon to the filters and were collected by filtering ~1 L of pre-filtered (0.2 μm) experimental volume onto a 0.3 μm GF75. Filters were placed into pre-combusted (4 hr at 400 ˚C) glass vials, and frozen at -40 ˚C. Filters were shipped on dry ice to Bigelow Analytics (Bigelow Laboratories for Ocean Sciences) and particulate organic carbon was determined using a Costech ECS 4010 elemental analyzer (980˚ combustion). Filters were analyzed within two weeks of collection and DOC-blank values were subtracted from experimental particulate organic carbon values. Carbon content of bacterioplankton cells (i.e. the carbon conversion factor) was calculated as particulate organic carbon concentration divided by bacterioplankton abundance.

Carbonate parameters

pH – Spectrophotometric pH measurements were made via absorbance of seawater sample at 25 °C with m-cresol purple indicator dye (unpurified) following Dickson et al. [34] for the

Santa Barbara Channel experiments. The dye was frequently calibrated against certified reference material (Batch # 10, Dickson, La Jolla, California). pH was measured using a Corning 430 pH meter for the Sargasso Sea experiments.

pCO_2 – Samples for pCO_2 analysis were collected into ~400 mL borosilicate bottles according to Dickson et al. [34]. The bottles were capped immediately upon collection and pCO_2 analysis was conducted within 24 hrs of sampling on a custom pCO_2 system according to Hales et al. [35]. All pCO_2 samples were systematically referenced against standard quality gasses (Scott Marrin Inc.).

Measurements of carbonate parameters were not made for the South Pacific Subtropical Gyre and Santa Barbara Channel # 10 experiments due to logistical constraints. We used bubbling flow rates and duration determined from previous experimental volumes to achieve target elevated and pre-industrial pCO_2 levels for these experiments. For all other experiments where pCO_2 was not directly measured (experiments # 1 and 3), it was calculated based on pH and a recent local in situ measurement of total alkalinity using CO2SYS [36] and the dissociation constants for carbonic acid as refitted by Dickson and Millero [37].

Calculations

Cell-specific TOC removal – Cell-specific TOC removal was calculated as the difference in TOC concentration (ΔTOC) from the start of the experiment to the beginning of stationary phase divided by the concomitant change in bacterioplankton abundance.

Bacterioplankton carbon demand – Bacterioplankton carbon demand (BCD) is equivalent to the carbon required for bacterioplankton biomass production (ΔBC) plus bacterioplankton respiration (BR; BCD = ΔBC + BR), over a given period of time. BCD is also equivalent to the total amount of DOC consumed by heterotrophic microbial communities. Therefore, bacterioplankton carbon demand was calculated as the change in the concentration of DOC from the start of the incubations to stationary phase. DOC concentration was calculated as the difference between the concentrations of TOC and BC (i.e. DOC = TOC – BC).

Bacterioplankton growth efficiency – Bacterioplankton growth efficiency, which provides an estimate of how much of the consumed organic carbon is partitioned into cellular biomass (BC) versus respiration [38, 39], was calculated as the increase in BC from the start of the incubations to stationary growth phase divided by bacterioplankton carbon demand. For the Santa Barbara Channel experiments, bacterioplankton abundance was converted to BC using the carbon conversion factor of 30 fgC $cell^{-1}$ measured during Santa Barbara Channel experiment # 10. This is comparable to other published carbon conversion factors ([40], A Cano, unpublished). A lower conversion factor of 10 fgC $cell^{-1}$ was used for communities from the Sargasso Sea and the South Pacific Subtropical Gyre to reflect smaller cells in oligotrophic regions [41, 42].

Bacterioplankton respiration – Bacterioplankton respiration can be equated to the change in ΔTOC by the following argument. The change in TOC between time 1 and time 2 is given by:

$$\Delta TOC = (DOC_1 + BC_1) - (DOC_2 + BC_2) \quad (1)$$

Then because bacterioplankton grow by consuming DOC, converting a portion of consumed DOC into BC and respiring the remainder to CO_2, the change in DOC between two time points (ΔDOC) is given by:

$$\Delta DOC = (BC_2 - BC_1) + BR \quad (2)$$

Note that in this formulation ΔDOC is a positive value such that when equation 1 is rearranged as:

$$\Delta TOC = (DOC_1 - DOC_2) + (BC_1 - BC_2) \quad (3)$$

the right-hand side of equation 2 can be substituted for $(DOC_1 - DOC_2)$ in equation 3 yielding:

$$\Delta TOC = (BC_2 - BC_1) + BR + (BC_1 - BC_2) = BR \quad (4)$$

Results

Growth patterns of the natural bacterioplankton communities within all experiments demonstrated typical batch culture patterns of lag, exponential, and stationary growth (Figs

1, 2, and 3). However, the magnitude of the response differed between sites and treatments as described below.

Experiments with naturally occurring DOC

Bacterioplankton communities in both elevated and pre-industrial pCO_2 treatments, grown on naturally occurring DOC in the Sargasso Sea, demonstrated a less than two-fold change in bacterioplankton abundance and no resolvable removal of TOC over the course of the incubations (Fig 1A). pCO_2 treatments showed no difference in cell yield ($4.8 \pm 0.8 \times 10^5$ cells mL^{-1}; elevated pCO_2 vs. $4.8 \pm 0.3 \times 10^5$ cells mL^{-1}; ambient pCO_2) or production rate ($6.0 \pm 2.2 \times 10^4$ cells mL^{-1} d^{-1}; elevated pCO_2 vs. $7.0 \pm 1.4 \times 10^4$ cells mL^{-1} d^{-1}; ambient pCO_2) (Fig 1A). A similar pattern was detected in the South Pacific Subtropical Gyre for the unamended experimental treatments (Fig 1B).

In contrast, the experiment with naturally occurring DOC from the Santa Barbara Channel demonstrated significant increases in bacterioplankton abundance and measurable removal of TOC in both pre-industrial and elevated pCO_2 treatments (Fig 1C). Although the initial rate of increase in bacterioplankton abundance was similar for both pCO_2 treatments, greater maximum abundance was obtained by stationary phase with elevated pCO_2 ($1.0 \pm 0.02 \times 10^6$ cells mL^{-1}), compared with pre-industrial (250 ppm) pCO_2 levels ($0.9 \pm 0.01 \times 10^6$ cells mL^{-1}) (Fig 1C). The rate of TOC removal was also greater in the elevated pCO_2 treatment (-2.8 ± 0.9 µmol C L^{-1} d^{-1}) relative to the pre-industrial pCO_2 treatment (-1.3 ± 0.5 µmol C L^{-1} d^{-1}) (Fig 1C). The enhanced TOC removal relative to the corresponding change in

bacterioplankton abundance led to greater cell-specific consumption of TOC at elevated pCO_2 (71.9 ± 24.4 fg C $cell^{-1}$) relative to pre-industrial pCO_2 (46.1 ± 17.7 fg C $cell^{-1}$; Fig 4).

Experiments with CNP

The addition of glucose in the CNP- Sargasso Sea experiment raised TOC concentration by 11.2 and 11.6 μmol C L^{-1} over the unamended treatment for the ambient and elevated pCO_2 treatments, respectively. This additional labile organic carbon (in combination with ammonium and phosphate) enhanced overall bacterioplankton yield by greater than an order of magnitude (Fig 1D) compared to the unamended treatment (Fig 1A). The bacterioplankton communities removed an amount of TOC equal to those carbon amendments in both elevated and ambient pCO_2 treatments implying that throughout the incubation little, if any, of the naturally occurring DOC was consumed, e.g. no priming effect was observed. However, TOC removal rates during exponential growth were greater under elevated pCO_2 compared to ambient pCO_2 (-4.3 ± 0.5 μmol C L^{-1} d^{-1} vs. -3.1 ± 1.2 μmol C L^{-1} d^{-1}, respectively; Fig 1D). Greater bacterioplankton abundance at elevated pCO_2 (1.4 ± 0.02 x10^6 cells mL^{-1}) relative to ambient pCO_2 (1.2 ± 0.04 x10^6 cells mL^{-1}) was proportionately smaller than enhanced TOC removal during the same period, resulting in greater cell-specific consumption of TOC at elevated pCO_2 (101.1 ± 15.6 fg C $cell^{-1}$) relative to ambient pCO_2 (81.9 ± 37.7 fg C $cell^{-1}$; Fig 4).

The addition of glucose in the CNP- Santa Barbara Channel experiment raised TOC concentration by 7.5 and 10.5 μmol C L^{-1} over the unamended treatment for the pre-industrial (250 ppm) and elevated (1000 ppm) pCO_2 treatments, respectively.

Bacterioplankton abundance increased by over an order of magnitude (Fig 1E) compared to the unamended treatment (Fig 1C). An amount of TOC greater than the amendments was removed in both pCO_2 treatments over the course of the experiment (compare initial TOC in Fig 1C with the final TOC in Fig 1E); however, both total TOC drawdown and the rate of TOC removal during exponential phase were greater under elevated pCO_2 (-8.0 ± 0.6 μmol C L^{-1} d^{-1}) relative to the pre-industrial pCO_2 treatment (-4.3 ± 1.1 μmol C L^{-1} d^{-1}). The bacterioplankton abundance in stationary phase was also greater at elevated pCO_2 (1.9 ± 0.1 x10^6 cells mL^{-1}) than at pre-industrial pCO_2 (1.7 ± 0.06 x10^6 cells mL^{-1}); however, the enhanced TOC removal relative to the increase in bacterioplankton, again resulted in greater cell-specific TOC consumption at elevated pCO_2 (84.1 ± 9.3 fg C $cell^{-1}$) relative to ambient pCO_2 (55.2 ± 14.2 fg C $cell^{-1}$; Fig 4).

Final TOC concentration in the Santa Barbara Channel experiment was drawn down to the same final concentration with and without CNP in elevated pCO_2 incubations (compare Fig 1C and E) indicating that CNP addition did not enhance the consumption of naturally occurring DOC under elevated pCO_2. In contrast, final TOC concentration in the pre-industrial pCO_2 CNP incubations was ~3 μmol C L^{-1} lower than in the unamended incubations (compare Fig 1C and E), indicating that the addition of CNP allowed for greater consumption of the naturally occurring DOC (a priming effect) under pre-industrial pCO_2.

Experiments with phytoplankton-derived DOC

TOC removal rates and the magnitude of TOC removal through stationary growth phase were enhanced in elevated pCO_2 treatments for all experiments with phytoplankton-derived

DOC (Figs 2 and 3), indicating greater consumption of the exudates and lysates at elevated pCO_2 compared to pre-industrial levels. While trends in TOC removal were consistent across experiments and DOC sources, the bacterioplankton abundance yield was variable with some treatments having elevated yield in high pCO_2 treatments (Figs 2E, F; Fig 3B), and others showing no difference (Figs 1A, B, C, D; Fig 3A and C) between pCO_2 treatments. Despite variability in bacterioplankton abundance yield, elevated pCO_2 resulted in TOC removal by bacterioplankton that was always proportionately greater than the corresponding increases in abundance, leading to greater cell-specific removal at elevated pCO_2 (Fig 4).

Carbon content of bacterioplankton cells

Trends in TOC removal and bacterioplankton abundance in the Santa Barbara Channel experiment # 10 were consistent with all previous Santa Barbara Channel experiments: Greater TOC removal through stationary growth phase was observed in elevated pCO_2 incubations (-18.0 ± 0.6 μmol C L^{-1}) relative to pre-industrial pCO_2 incubations (-15.6 ± 0.1 μmol C L^{-1}), while bacterioplankton abundance yield was similar across pCO_2 treatments (4.0 ± 0.5 x10^6 cells mL^{-1}; elevated pCO_2 vs. 3.8 ± 0.1 x10^6 cells mL^{-1}; pre-industrial pCO_2). No resolvable difference in the carbon content of bacterioplankton cells was observed between cells as a function of pCO_2 (31.4 ± 1.2 fg C $cell^{-1}$; pre-industrial pCO_2 vs. 31.8 ± 1.8 fg C $cell^{-1}$; elevated pCO_2; p-value > 0.66, t-test).

Bacterioplankton carbon removal and growth dynamics

Bacterioplankton carbon removal and growth dynamics were evaluated for experiments in which TOC removal was measureable. Effects of pCO_2 on carbon removal and bacterioplankton growth dynamics within experiments were tested for significance by the Alexander-Govern test. This first approximation, unequal variance test was used to account for small sample sizes (n = 2 for each pCO_2 level) and, therefore, an inability to test for normality and homoscedasticity with substantial power (p-values are reported in Table 2). Despite the fact that few within experiment comparisons resulted in significant effects of pCO_2, patterns in carbon removal and bacterioplankton growth dynamics were consistent across all experiments and locations, and are highly significant: cell-specific TOC removal (Fig 4) and bacterioplankton carbon demand (Fig 5) were consistently enhanced at elevated pCO_2 (p-value = 0.0003, Fisher's sign test; p-value < 0.0001, t-test, respectively), while bacterioplankton growth efficiency (Fig 6) was significantly reduced at elevated pCO_2 (p-value = 0.0003, Fisher's sign test). Significance of these consistent patterns was tested using the consensus t-test or the Fisher's sign-test, when tests for normality and homoscedasticity failed. Thus, while our measurement precision was inadequate to demonstrate statistically significant differences at any given location, the ecological and biogeochemical significance across all sites is statistically clear in that the consistency of the response shows that an enhancement of cell-specific TOC removal and carbon demand, and a reduction in bacterioplankton growth efficiency, under elevated pCO_2 is a common feature across the wide range of ocean habitats examined.

Discussion

The results indicate that elevated pCO_2 can directly influence bacterioplankton removal of organic carbon. Elevated pCO_2 led to greater TOC removal by bacterioplankton communities growing on a range of DOC from glucose to more complex DOC, consisting of phytoplankton products or naturally occurring DOC. This result was observed across all ocean regions for experiments where DOC was amended. Similar results were observed in the unamended Santa Barbara Channel incubations at elevated pCO_2 but it was not possible to discern whether pCO_2 affected consumption of naturally occurring DOC in the South Pacific Subtropical Gyre and Sargasso Sea, as changes in TOC were below analytical detection limits in these more oligotrophic environments.

Our results suggest that short-term increases in pCO_2 will lead to enhanced removal of bioavailable surface organic carbon by heterotrophic bacterioplankton communities. Through observations of enhanced extracellular glucosidase activity, previous mesocosm and culture studies suggested that elevated pCO_2 conditions might lead to greater removal of organic carbon [9, 11-13]. Here we show a clear, direct effect of elevated pCO_2 on bacterioplankton-mediated organic carbon removal. Both our work and that of the mesocosm and culture studies [9, 11-13] suggest that short-term exposure to elevated pCO_2 will enhance the bacterioplankton removal of bioavailable DOC in the surface ocean.

Experimental design considerations

In order to investigate the direct effect of pCO_2 on organic carbon consumption by natural bacterioplankton communities, we employed the following in our experimental design: (1)

Experiments were conducted in the dark to eliminate photoautotrophic organic carbon production; (2) To ensure that the majority of organic carbon removal could be attributed to heterotrophic bacteria, we used seawater culture dilution methods [43] to dilute and minimize the effects of protistan grazer populations [44, 45, 46]; (3) To further minimize the potential effects of grazers on organic carbon consumption, calculations were made from the start of the incubations to stationary growth phase, ensuring low grazer densities and high bacterial densities during the period over which bacterioplankton physiological parameters were estimated. However, we cannot rule out the possibility that groups other than heterotrophic bacteria (e.g. archaea and marine protists) contributed to organic carbon removal in these experiments because we were unable to resolve changes in their abundance. The consumption of specific organic compounds (i.e. amino acids) by other members of marine plankton has been observed [47-49] but their effect on removal of bulk dissolved organic material remains largely unquantified [50].

To minimize the potential for abiotic removal of organic carbon (e.g. via adhesion to the incubation-bottle walls or accumulation at the air-water interface) our seawater cultures were only bubbled before the start of the experiments (before T_0). pCO_2 levels were maintained over the course of the experiments through the use of gas-tight sampling ports (see methods) and by replacing the headspace with target pCO_2 – gas, daily. We cannot rule out the possibility that abiotic removal of organic carbon occurred during bubbling; however, continued abiotic removal over the course of the experiment did not occur as is evidenced by the fact that no resolvable removal of TOC was detected in experiments in

which bacterioplankton growth was minimal (Fig 1A and B, Table 1: experiments #1A, and 7A, 8A, and 9A).

We attribute organic carbon removal (ΔTOC) to consumption by heterotrophic bacterioplankton in our experiments. The filtration and dilution steps used in our experimental set-up were designed to minimize or eliminate the contribution of non-living particulate organic carbon in experimental incubations. That means that a measurement of TOC represents the sum of DOC and the carbon content of bacterioplankton biomass. It also means that the change in TOC (ΔTOC) is a measure of the amount of carbon lost to bacterioplankton respiration by the argument described in the materials and methods section (see *bacterioplankton respiration* calculation). This tight coupling between the direct measurement of ΔTOC and the production of CO_2 (i.e. bacterioplankton respiration) was shown empirically in similar seawater culture experiments, supporting the use of ΔTOC as a proxy for heterotrophic bacterioplankton respiration in this type of experiment [45].

Bacterioplankton removal of organic carbon

Highly productive systems like the coastal upwelling regions of the Santa Barbara Channel can create food-webs that allow for greater DOC production than heterotrophic bacterioplankton consumption, resulting in the accumulation of bioavailable DOC [51, 52, 40]. In the present study we show enhanced removal of naturally occurring organic carbon by Santa Barbara Channel heterotrophic bacterioplankton communities under increased pCO_2, suggesting that rapid increases in pCO_2, common in upwelling systems, can accelerate the consumption of DOC in the surface ocean.

In contrast, removal of TOC in the naturally occurring DOC treatments conducted in the Sargasso Sea and the South Pacific Subtropical Gyre was below limits of detection, indicating that only a very small fraction of the naturally occurring DOC was available to the extant bacterioplankton on the time-scale of these experiments. This result is consistent with previous observations indicating that because DOC production and consumption processes in the oligotrophic gyres are so tightly coupled little, if any, of the DOC that accumulates in these regions is bioavailable to surface bacterioplankton communities on the time scale of hours to days [44, 53].

To assess the effect of pCO_2 on the removal of recently produced DOC in systems where DOC use is difficult to resolve, we simulated food-web production of complex DOC by adding phytoplankton-derived DOC to seawater culture experiments. These amendment experiments were conducted in both coastal (Santa Barbara Channel) and open ocean systems (South Pacific Subtropical Gyre) and show a consistent pattern of an increased magnitude of TOC removal with elevated pCO_2. While these results show clear short-term trends regarding the removal of phytoplankton-derived DOC, longer-term experiments (weeks to months) must be conducted to properly evaluate whether exposure to elevated pCO_2 sustains an offset in the magnitude of TOC removal compared to ambient and pre-industrial pCO_2 conditions.

Collectively, our experiments indicate that short-term increases in pCO_2 directly influence bacterioplankton removal of organic carbon. Elevated pCO_2 led to greater TOC removal by

natural bacterioplankton communities growing on a range of organic carbon compounds from glucose, to more complex phytoplankton products, to naturally occurring DOC. Assuming that heterotrophic bacterioplankton are driving the removal of TOC, then these results suggest that short-term exposure to elevated pCO_2 leads to enhanced bacterioplankton respiration relative to pre-industrial pCO_2. Enhanced respiration under elevated pCO_2 coupled with minimal change in bacterioplankton abundance yielded systematically greater cell-specific respiration (i.e. cell-specific TOC removal) in elevated pCO_2 treatments (Fig 4). Even in cases where bacterioplankton yield was greater under elevated pCO_2, that effect was outweighed by enhanced respiration leading to greater amounts of carbon respired per cell. This result suggests that during periods of acidified conditions, more bioavailable organic carbon in surface waters will be converted to CO_2, decreasing the amount of organic carbon available for potential export and increasing the likelihood that carbon will be lost from the surface ocean to the atmosphere through outgassing of CO_2.

Bacterioplankton growth dynamics

Organic carbon removal was tracked by measuring TOC; as a result, these seawater experiments do not directly address the effect of pCO_2 on BC production or DOC consumption. However, these components were evaluated using the direct estimates of the carbon content of bacterioplankton cells from the December 2015 Santa Barbara Channel experiment. Knowledge of the carbon content of bacterioplankton cells enables the calculation of BC to be easily extrapolated from cell abundance data and also enables DOC to be calculated as the difference between TOC and BC. Estimates of BC and DOC removal

can then be used to inform aspects of bacterioplankton physiology by providing estimates of bacterioplankton carbon demand (i.e. DOC consumption) and the fraction of consumed DOC that is converted to BC (i.e. bacterioplankton growth efficiency). Thus, understanding how pCO_2 affects the carbon content of bacterioplankton cells enabled us to extend our results beyond carbon loss via respiration, to the partitioning of surface organic carbon between dissolved (that which escapes or resists bacterioplankton consumption) and particulate (as BC) organic carbon.

We observed no direct effect of pCO_2 on the carbon content of bacterioplankton cells. Assuming this equivalency across all experiments, we calculated bacterioplankton carbon demand for all of the experiments where a change in TOC was resolvable. Bacterioplankton carbon demand was estimated as the change in DOC from the start of the incubations to stationary growth phase and DOC was estimated as TOC – BC. These calculations revealed a consistent pattern across DOC amendments and experimental location: bacterioplankton communities grown at elevated pCO_2 exhibited enhanced carbon demand relative to communities at pre-industrial and ambient pCO_2 (Fig 5). These results suggest that bacterioplankton communities exposed to short-term increases in pCO_2 reduce the amount of DOC available for vertical export through enhanced consumption of recently produced DOC (Fig 7).

Estimates of bacterioplankton growth efficiency revealed a consistent pattern across DOC amendment and experimental location: growth efficiencies were consistently lower at elevated pCO_2 than at pre-industrial or ambient pCO_2 (Fig 6). This implies that a greater

portion of consumed DOC is converted to CO_2 by bacterioplankton communities exposed to elevated pCO_2 (Fig 7). It is important to note that variable initial bacterioplankton communities likely resulted in variable BC and that our estimate of cellular carbon conversion factor may not accurately represent communities across experiments; however, only the absolute magnitude of the growth efficiency values will be affected if, as our results suggest, BC is similar across pCO_2 levels. Enhanced bacterioplankton respiration at elevated pCO_2 will consistently result in lower growth efficiencies, regardless of the exact carbon conversion factor used.

Our estimates of bacterioplankton carbon demand and growth efficiency demonstrate a direct effect of pCO_2 on bacterioplankton processing of organic carbon in the surface ocean. While elevated pCO_2 had little impact on BC production, enhanced DOC removal through accelerated bacterioplankton consumption and reduced growth efficiencies reduced the amount of DOC available for export, relative to pre-industrial pCO_2 conditions (Fig 7). Enhanced removal of DOC could also lead to increased production of recalcitrant organic compounds via the microbial carbon pump [54]. Further experiments and measurements of long-term DOC removal and DOC characterization are required to evaluate this possibility.

Possible mechanisms

Consumption of organic carbon is often a function of bacterioplankton community structure and a number of studies have demonstrated that slight variations in DOC may select for specific bacterioplankton populations over timescales of hours to days [28, 40, 53, 55]. It is likely that bacterioplankton community composition shifted over time in our experiments

and it is also possible that a shift in community composition between pCO_2 treatments contributed to the consistent differences in TOC removal. A recent study by Siu et al. [17] indicated that elevated pCO_2 (~1050 ppm) could induce shifts in bacterioplankton composition. However, pCO_2 manipulations in mesocosm experiments in Bergen [56, 57] and Svalbard, Norway [58 - 60] showed that the free-living bacterioplankton community structure was mostly unaffected by elevated pCO_2, which ranged from ~750 – 1085 ppm, depending on the experiment. In the present study the trend of enhanced bacterioplankton respiration in the presence of elevated pCO_2 was observed across DOC experiments for which water was collected at various times of the year and presumably contained different initial bacterioplankton communities. While it is possible that the bacterioplankton community structure shifted under elevated pCO_2 conditions, the response of enhanced respiration at elevated pCO_2 appeared universal despite likely differences in initial microbial composition sampled across sites and time.

Alternatively, enhanced bacterioplankton respiration combined with low bacterioplankton growth efficiency in elevated pCO_2 treatments may be a physiological response to decreased pH. A recent study examined the expression of bacterioplankton transcripts in response to elevated pCO_2 and showed that transcripts associated with respiration were significantly enhanced in elevated pCO_2 mesocosms [61]. The authors specifically showed upregulation of respiratory proton pumps that aid in translocating protons across the cell membrane. These results suggest that as environmental pH decreases, heterotrophic bacterioplankton upregulate respiratory proton pumps to export protons that invade the cell as a result of low external pH. Consistent with our observations, Bunse et al. [61] suggested that upregulating

proton pumps under low pH would be energetically costly to heterotrophic bacterioplankton and thus reduce their overall efficiency.

There is also evidence to suggest that increasing pCO_2 may lead to increased removal of organic matter in the ocean through up-regulation and/or enhanced efficiencies of extracellular enzymes [9-12]. Extracellular enzymes convert high molecular weight organic compounds to low molecular weight compounds that can be used by heterotrophic bacterioplankton [62-64]. These enzymes are not buffered by the cell's cytoplasm and are directly impacted by external changes in pH. An increase in the concentration of hydrogen ions in an enzyme's environment, as a result of declining pH, may alter the three-dimensional protein structure of the enzyme's active site and thus affect enzymatic activity [65, 66]. Recent studies report that extracellular α and β-glucosidase activity increased in response to elevated hydrogen ion concentration, suggesting that a decline in pH of 0.2-0.3 pH units was closer to the pH optimum of glucosidase activity than ambient pH [11, 12]. It may be that up-regulation of enzymes like α and β-glucosidase by marine heterotrophic bacterioplankton in conjunction with altered enzymatic active sites led to the increased removal of DOC measured within elevated pCO_2 treatments. Further experimentation is required to explore these mechanisms.

Thus, while we do not exclude the possibility of a shift in the bacterioplankton community under elevated pCO_2 conditions, we suggest that the increased respiration at elevated pCO_2 is likely due to up-regulation of proton pumps and possibly the enhancement of extracellular enzyme activity (via up-regulation and/or enhanced efficiencies).

Conclusions

This study reveals a direct impact of pCO_2 on bacterioplankton removal of organic carbon. In all experiments for which TOC removal was measurable, enhanced bacterioplankton respiration under elevated pCO_2 coupled with minimal change in bacterioplankton biomass yield resulted in systematically greater cell-specific respiration in elevated pCO_2 treatments (i.e. cell-specific TOC removal; Fig 4). Even in cases where bacterioplankton abundance yield was greater under elevated pCO_2, enhanced respiration led to greater amounts of carbon respired per cell, increasing the likelihood that surface organic carbon will be lost to the atmosphere through outgassing of CO_2. Estimates of bacterioplankton carbon demand and growth efficiency suggest that acidified conditions may also increase the ability of bacterioplankton to consume DOC but with reduced growth efficiencies. The cumulative effect of enhanced consumption and enhanced respiration under elevated pCO_2 would increase the fraction of surface-ocean DOC respired to CO_2, ultimately decreasing the effectiveness of DOC as a sink of carbon in the ocean (Fig 7). Incorporation of these results into numerical models will enable more accurate understanding of current air-sea carbon exchange and the impact of elevated pCO_2 in surface waters on biogeochemical cycles.

Acknowledgments

We would like to thank Bigelow Analytics, Julia Sweet, Maverick Carey, Nick Huynh, Emma Wear, Ellie Halewood, and the officers and crew of the R.V. *Atlantic Explorer* and R.V. *Kilo Moana,* without whose laboratory assistance and expertise these projects would not be possible. We would also like to thank Dr. W. Rice for the invaluable and extensive

discussions regarding appropriate statistical analyses for this study. We also thank three anonymous reviewers and the editorial office for their helpful and constructive comments. Lastly, we would like to thank the Moorea Coral Reef LTER (NSF OCE 12-36905) and the Santa Barbara Channel LTER (NSF OCE – 1232779) for logistical assistance.

Tables for Chapter I

Table 1. Summary of experimental conditions and results (page 52 - 53).

		Conditions at the Start of the Experiment								Incubation Times		Results		
Exp #	Exp.	DOC Source	Volume of Incubation (L)	Ratio of 0.2µm: Inoculum SW	T (°C)	Target pCO_2 (ppm)	Actual pCO_2 (ppm)	In situ TOC (µmol C L^{-1})	Initial TOC (µmol C L^{-1})	Time from T_0 to Stationary-Growth (Days)	Duration of Exp. (Days)	TOC Removal (µmol C L^{-1}) From T_0 to Stationary-Growth	TOC Removal (µmol C L^{-1}) Over Duration of Exp.	BGE (%)
1A	SS Sept. 2012	Natural DOC	2	3:7	26.5	400	~389	73.1 ± 1.3	76.0 ± 0.2	2.13	6.7	ND	ND	ND
1A	–	–	–	–	–	800	~760	–	77.9 ± 0.8	2.13	–	ND	ND	ND
1B	SS Sept. 2012	CNP	2	3:7	26.5	400	~389	73.1 ± 1.3	87.3 ± 1.3	2.13	6.7	-6.7 ± 2.6	-10.2 ± 2.3	11.9 ± 4.9
1B	–	–	–	–	–	800	~760	–	89.5 ± 1.5	2.13	–	-9.2 ± 1.3	-10.6 ± 1.1	9.1 ± 1.3
2A	SBC Dec. 2012	Natural DOC	2	3:7	14.5	250	349 ± 10	85.4 ± 2.0	86.4 ± 0.1	1.34	3.6	-1.7 ± 0.7	-2.0 ± 1.9	40.5 ± 9.4
2A	–	–	–	–	–	1000	1064 ± 10	–	86.1 ± 0.3	1.34	–	-3.8 ± 1.2	-4.7 ± 0.1	30.3 ± 7.2
2B	SBC Dec. 2012	CNP	2	3:7	14.5	250	349 ± 10	85.5 ± 0.5	93.8 ± 0.8	1.34	3.6	-5.8 ± 1.5	-12.0 ± 1.1	35.7 ± 6.0
2B	–	–	–	–	–	1000	1064 ± 10	–	96.5 ± 0.3	1.34	–	-10.7 ± 0.8	-15.1 ± 0.3	26.4 ± 2.1
3	SBC May 2013	*D. frag.* Exudate	0.5	1:3	12	250	238 ± 2	88.0 ± 0.1	398.6 ± 3.4	2.75	8	-65.5 ± 1.6	-115.6 ± 3.9	9.1 ± 2.5
3	–	–	–	–	–	1500	1376 ± 45	–	389.6 ± 9.8	2.75	–	-69.9 ± 10.3	-119.2 ± 12.4	6.8 ± 2.8
4	SBC August 2013	*T. weiss.* Exudate	2	1:3	14	250	132 ±3	64.2 ± 1.6	157.4 ± 0.9	5.11	6.8	-3.2 ± 0.8	-2.4 ± 0.5	47.0 ± 2.3
4	–	–	–	–	–	1500	1262 ± 6	–	158.2 ± 0.1	5.11	–	-4.9 ± 0.6	-6.52 ± 1.0	36.4 ± 0.3
5A	SBC Oct. 2013	*T. weiss.* Exudate	0.5	1:3	16	250	233 ± 3	73.1	155.9 ± 0.3	4.42	12.9	-10.5 ± 0.3	-22.9 ± 3.7	35.6 ± 0.3
5A	–	–	–	–	–	1500	1563 ± 74	–	156.3 ± 0.1	4.42	–	-17.2 ± 0.5	-32.5 ± 13.9	27.1 ± 5.5
5B	SBC Oct. 2013	*C. soc.* Exudate	0.5	1:3	16	250	244 ± 5	73.1	141.2 ± 3.2	3.0	12.9	-4.0 ± 0.1	-24.1 ± 4.4	26.1 ± 1.1
5B	–	–	–	–	–	1500	1551 ± 10	–	140.0 ± 2.3	3.0	–	-8.0 ± 4.0	-29.9 ± 4.8	15.7 ± 5.8

5C	SBC Oct. 2013	*A. glac* Exudate	0.5	1:3	16	250	194 ± 10	73.1	142.9 ± 1.5	4.42	12.9	-2.7 ± 2.3	-21.5 ± 3.1	38.4
5C	–	–	–	–	–	1500	1363 ± 5	–	143.5 ± 0.9	4.42	–	-10.2 ± 0.5	-25.2 ± 0.7	31.3 ± 2.9
6	SBC May 2014	*E. hux.* Exudate	2	1:3	14.5	250	325 ± 23	ND	103.8 ± 0.1	4.92	14.7	-2.1 ± 1.7	-7.4 ± 1.3	58.4 ± 22.9
6	–	–	–	–	–	1500	1454 ± 14	–	106.9 ± 0.1	5.75	–	-7.5 ± 0.2	-13.5 ± 0.9	28.6 ± 0.6
7A	SPSG July 2014	Natural DOC	2.8	1:3	22	250	ND	70.6	75.4 ± 1.0	ND	10	ND	ND	ND
7A	–	–	–	–	–	1000	ND	–	73.8 ± 0.5	ND	–	ND	ND	ND
7B	SPSG July 2014	*E. hux.* Lysate	2.8	1:3	22	250	ND	70.6	85.8 ± 0.6	1.81	10	-4.8 ± 2.3	-11.1 ± 1.1	11.9 ± 5.2
7B	–	–	–	–	–	1000	ND	–	84.4 ± 1.3	1.81	–	-7.0 ± 0.7	-12.4 ± 0.5	8.4 ± 0.7
8A	SPSG July 2014	Natural DOC	2.8	1:3	22	250	ND	76.7	75.2 ± 0.4	ND	10.5	ND	ND	ND
8A	–	–	–	–	–	1000	ND	–	73.7 ± 0.9	ND	–	ND	ND	ND
8B	SPSG July 2014	*E. hux.* Lysate	2.8	1:3	22	250	ND	76.7	87.2 ± 0.4	0.92	10.5	-4.7 ± 1.0	-8.0 ± 2.1	24.7 ± 3.0
8B	–	–	–	–	–	1000	ND	–	84.8 ± 0.6	1.84	–	-7.0 ± 0.8	-8.8 ± 2.3	8.5 ± 1.8
9A	SPSG July 2014	Natural DOC	2.8	1:3	22	250	ND	70.9	75.0 ± 2.0	ND	9	ND	ND	ND
9A	–	–	–	–	–	1000	ND	–	75.0 ± 3.6	ND	–	ND	ND	ND
9B	SPSG July 2014	*E. hux.* Lysate	2.8	1:3	22	250	ND	70.9	83.7 ± 0.9	1.79	9	-6.7 ± 1.3	-8.9 ± 2.1	8.9 ± 0.7
9B	–	–	–	–	–	1000	ND	–	85.6 ± 0.7	1.79	–	-7.9 ± 0.6	-12.3 ± 0.6	7.3 ± 0.3
10	SBC BC Dec 2015	*T. weiss.* Lysate	5	3:7	14	250	ND	69.6	86.4 ± 2.8	2.8	17.5	-15.6 ± 0.1	-19.7 ± 3.0	36.4 ± 0.2
10	–	–	–	–	–	1500	ND	–	87.1 ± 0.5	2.8	–	-18.0 ± 0.6	-23.2 ± 0.5	34.1 ± 3.7

Table 1. Conditions at the start of the seawater culture experiments, total organic carbon (TOC) removal from T_0 to stationary phase, TOC removal over the duration of the incubations, and bacterioplankton growth efficiency (BGE). Mean BGE was calculated as the ratio of the change in the carbon content of bacterioplankton biomass (BC) to dissolved organic carbon (DOC) removal from T_0 to stationary phase. DOC was calculated as TOC –

BC. Bacterioplankton cell abundance was converted to BC carbon using a carbon conversion factor of 30 fg C $cell^{-1}$ for the Santa Barbara Channel (SBC) experiments and 10 fg C $cell^{-1}$ for the experiments conducted in the Sargasso Sea (SS) and South Pacific Subtropical Gyre (SPSG). Error refers to mean ± standard deviation and 'ND' refers to not determined. Only one value is recorded in the table when only one valid result was obtained. Dashes refer to the information in the cell above the dash.

Table 2. P values for Bacterioplankton Carbon Removal and Growth Dynamics.

Experiment #	Cell-specific TOC removal p-value	BCD p-value	BGE p-value
1B	0.62	0.39	0.57
2A	0.40	0.17	0.40
2B	0.18	0.07	0.25
3	0.52	0.80	0.51
4	0.05	0.33	0.08
5A	0.33	0.03*	0.27
5B	0.34	0.41	0.23
5C	0.30	0.03*	NA
6	0.19	0.12	0.32
7B	0.54	0.41	0.52
8B	0.64	0.02*	0.04*
9B	0.12	0.45	0.15
10	0.54	0.05	0.54

Table 2. Alexander-Govern approximate p-values, calculated for cell-specific TOC removal, bacterioplankton carbon demand (BCD) and bacterioplankton growth efficiency (BGE). Asterisks denote p-values < 0.05 and 'ND' refers to not determined, due to lack of replication.

Figures for Chapter I

Figure 1. Mean TOC concentration and mean bacterioplankton abundance for Sargasso Sea and Santa Barbara Channel CNP- and natural-DOC experiments.

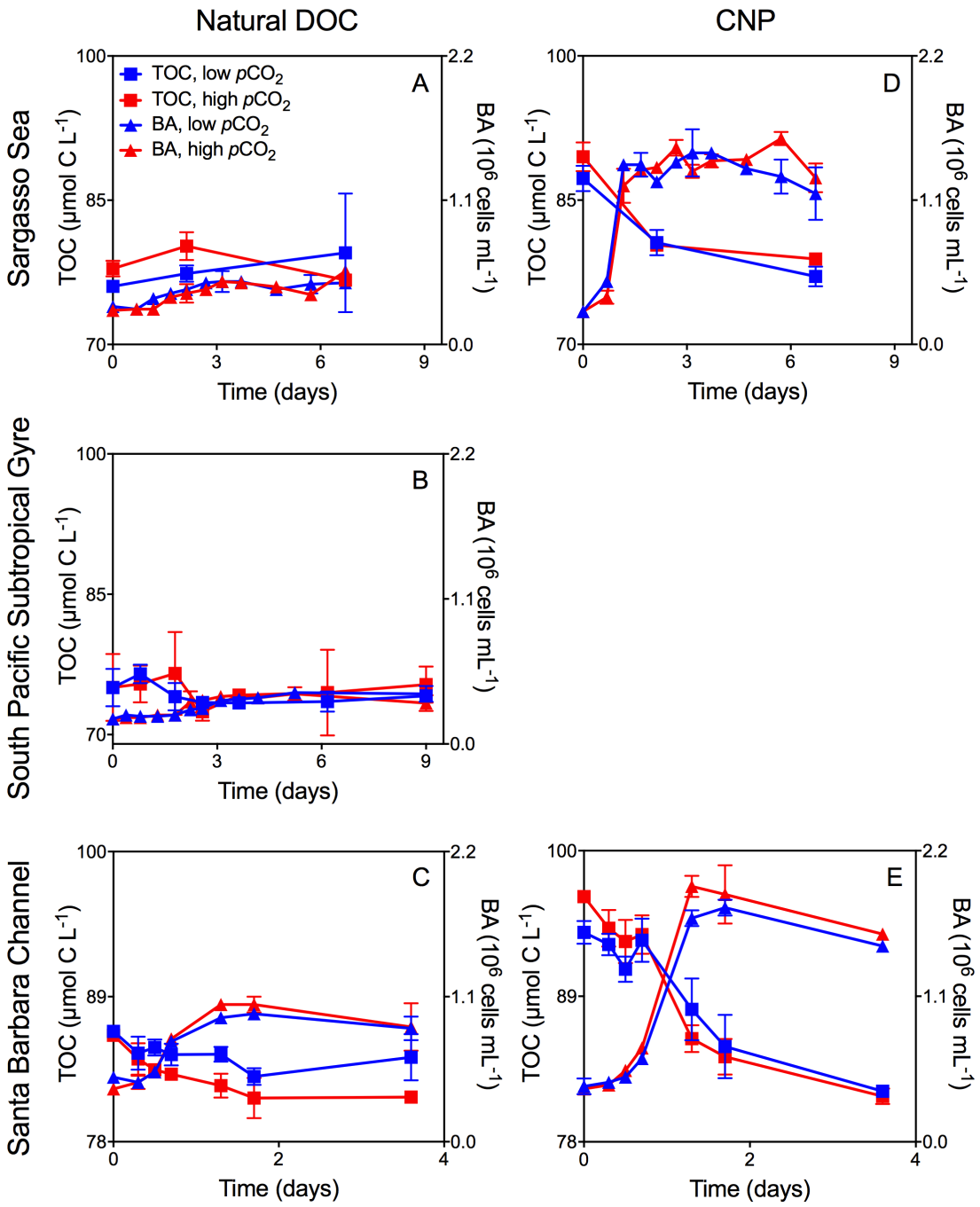

Mean TOC concentration (± SD) and mean bacterioplankton abundance (BA; ± SD) averaged across duplicate incubations through time and as a function of pCO_2 for natural

bacterioplankton assemblages incubated with: A: Natural DOC, Sargasso Sea Exp. #1A; B: Natural DOC, South Pacific Subtropical Gyre Exp. #7; C: Natural DOC, Santa Barbara Channel Exp. #2A; D. CNP, Sargasso Sea Exp. #1B; E. CNP, Santa Barbara Channel Exp. #2B. For treatments at all sites, red denotes elevated pCO_2, while blue denotes ambient pCO_2 in the Sargasso Sea experiment and pre-industrial pCO_2 in the Santa Barbara Channel and South Pacific Subtropical Gyre experiments. Squares represent TOC (μmol C L^{-1}) while triangles denote BA (10^6 cells mL^{-1}) over the course of the incubation.

Figure 2. Mean TOC concentration and mean bacterioplankton abundance for Santa Barbara Channel phytoplankton-DOC experiments.

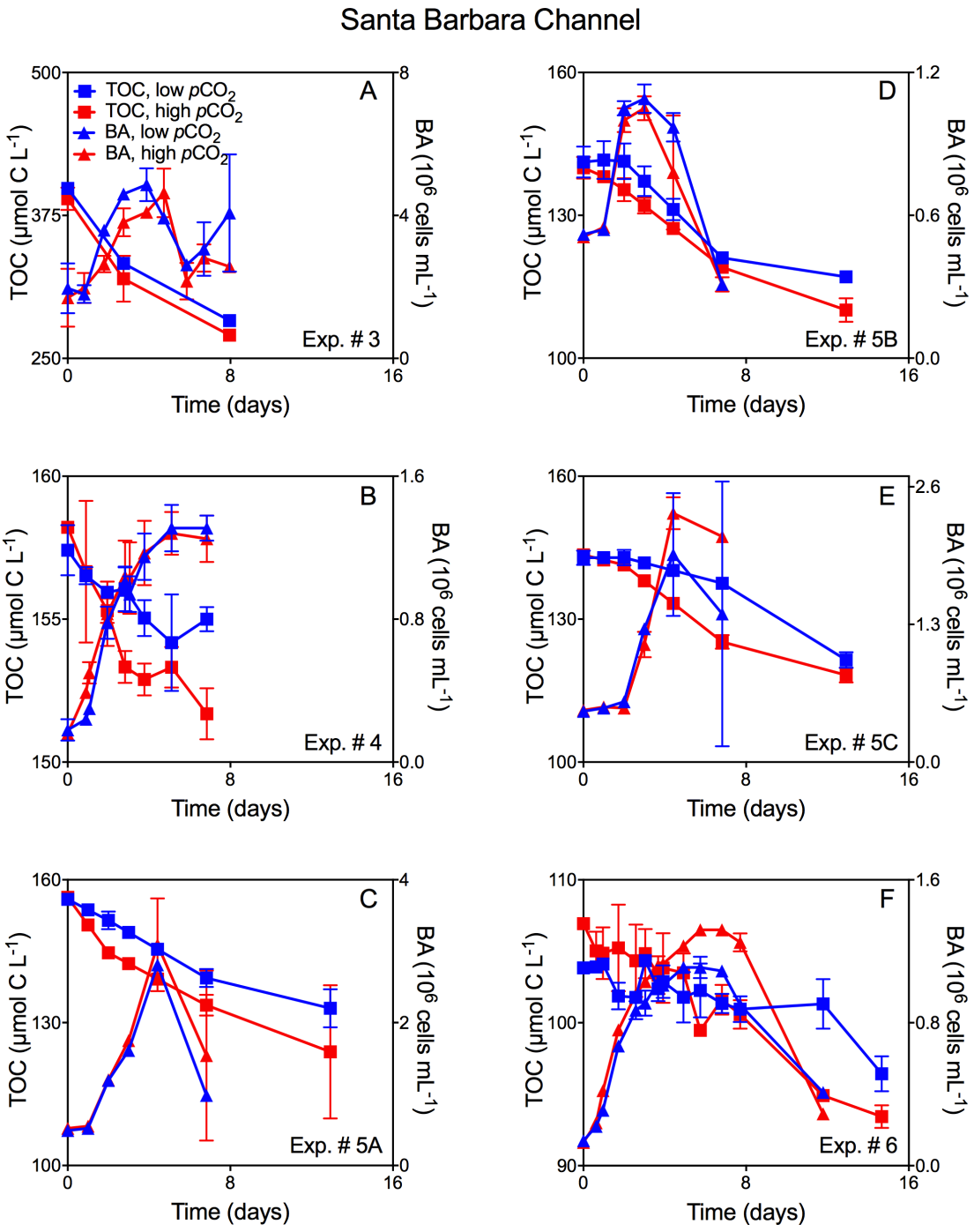

Mean TOC concentration (± SD) and mean bacterioplankton abundance (BA; ± SD) averaged across duplicate incubations through time and as a function of pCO_2 for natural

bacterioplankton assemblages in the Santa Barbara Channel experiments incubated with: A: *D. fragilissimus*-derived DOC, Exp. #3; B: *T. weissflogii*-derived DOC, Exp. #4; C: *T. weissflogii*-derived DOC, Exp. #5A; D: *C. socialis*-derived DOC, Exp. #5B; E: *A. glacialis*-derived DOC, Exp. #5C; F: *E. huxleyi*-derived DOC, Exp. #6. Red denotes elevated pCO_2, while blue denotes low (250 ppm) pCO_2. Squares represent TOC (μmol C L^{-1}) while triangles denote bacterioplankton abundance (10^6 cells mL^{-1}) over the course of the incubation.

Figure 3. Mean TOC concentration and mean bacterioplankton abundance for phytoplankton-DOC South Pacific Subtropical Gyre experiments.

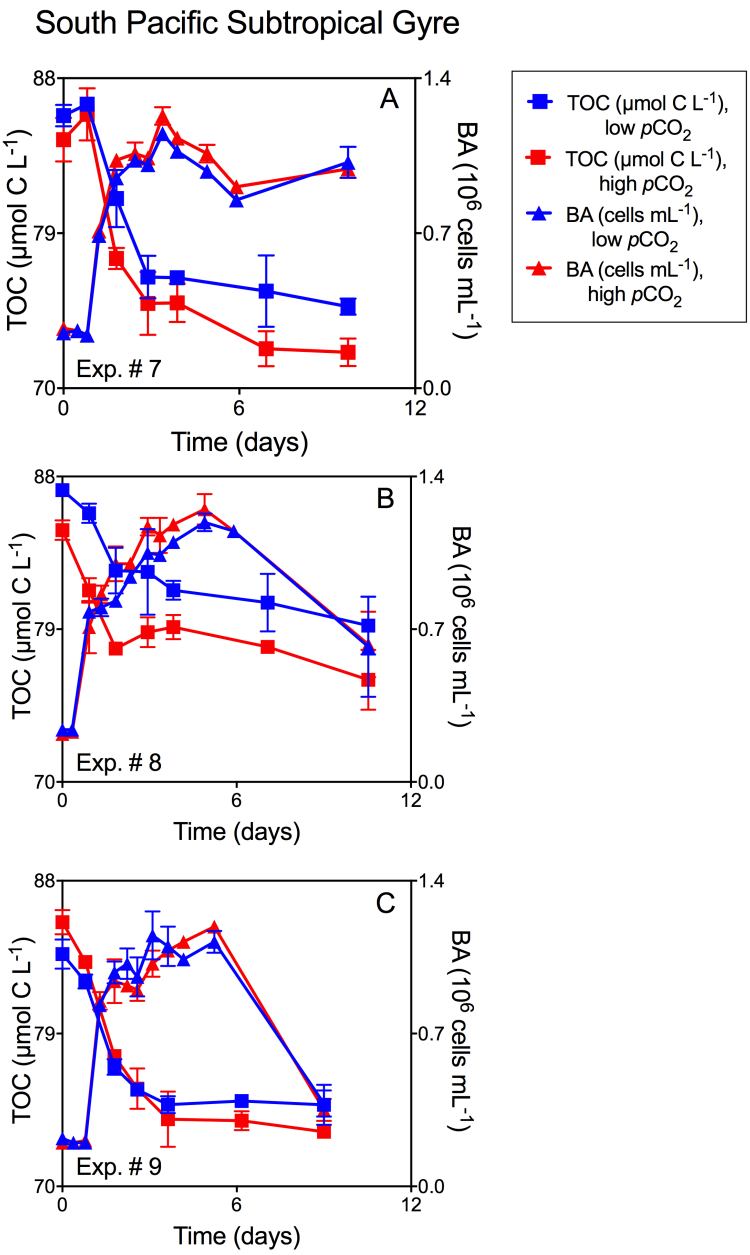

Mean TOC concentration (± SD) and mean bacterial abundance (BA; ± SD) averaged across duplicate incubations through time and as a function of pCO_2 for natural bacterioplankton assemblages in the South Pacific Subtropical Gyre experiments incubated with *E. huxleyi*-derived DOC: A: Exp. #7B; B: Exp. #8B; C: Exp. #9B. The same experimental design was

used for these experiments (note that only the amended treatments are shown). Red denotes elevated pCO_2, while blue denotes low (250 ppm) pCO_2. Squares represent TOC (µmol C L^{-1}) while triangles denote BA (10^6 cells mL^{-1}) over the course of the incubation.

Figure 4. Cell-specific TOC removal.

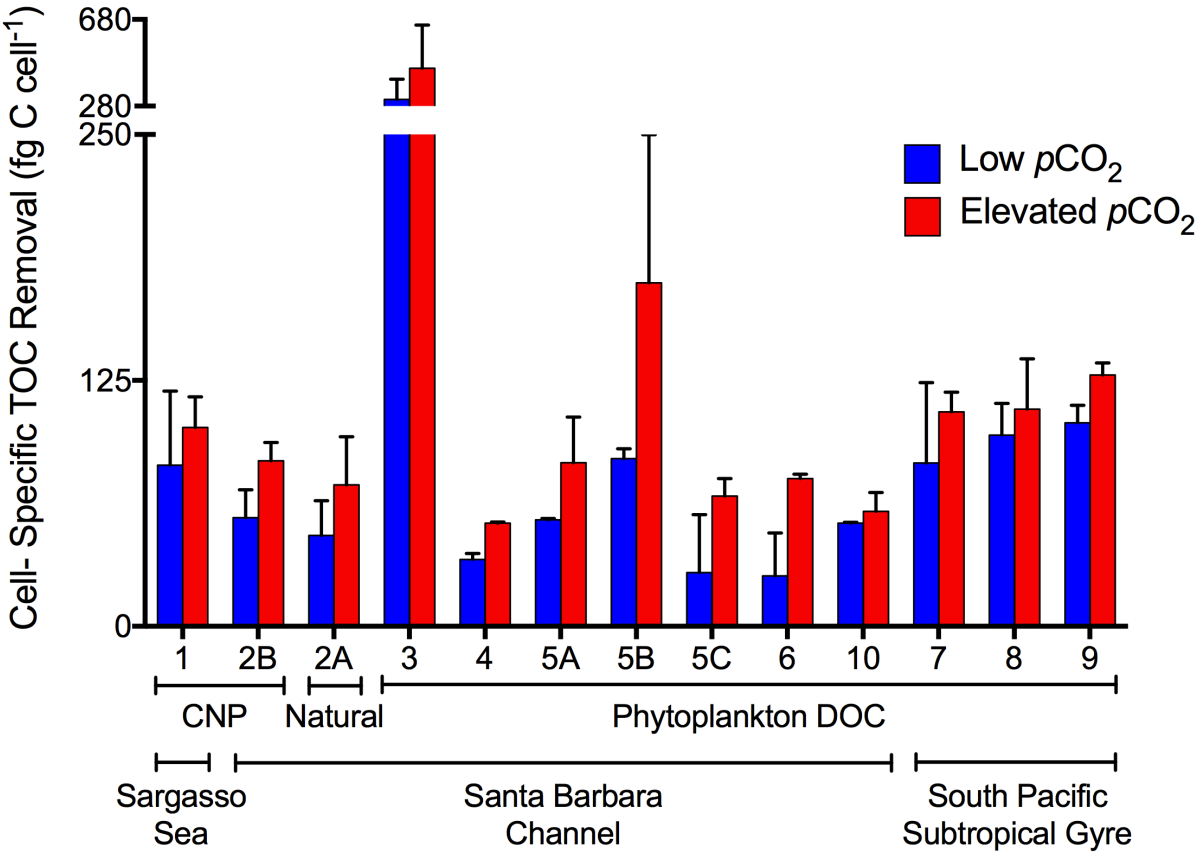

Mean (± SD) cell-specific TOC removal averaged across duplicate incubations and calculated as the change in TOC divided by the concurrent change in bacterioplankton abundance (BA) from the start of the incubations to stationary phase. Numbers on X-axis label refer to the experiment number (Table 1). Colors denote cell-specific TOC removal at elevated pCO_2 (red) and low (ambient or pre-industrial) pCO_2 (blue). Only experiments where a change in TOC was resolvable are shown.

Fig 5. Bacterioplankton Carbon Demand.

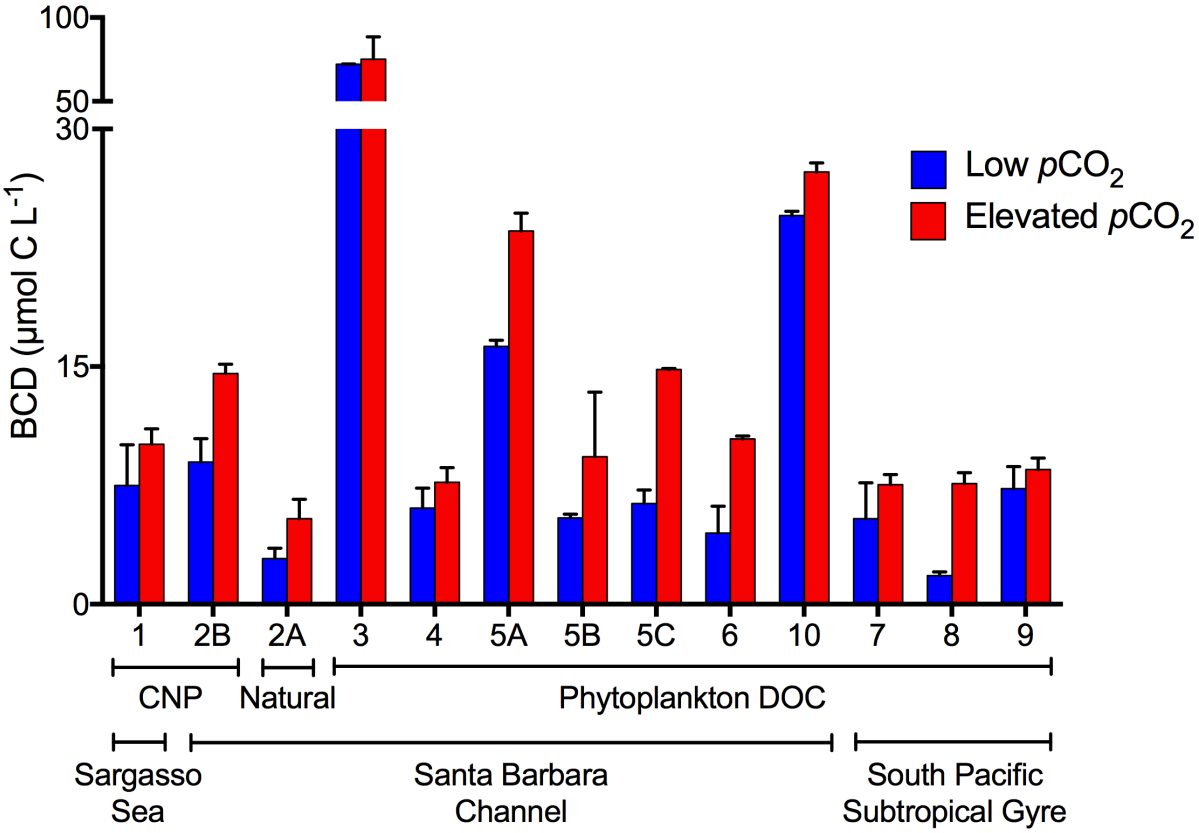

Mean (± SD) bacterioplankton carbon demand (BCD) averaged across duplicate incubations and calculated as the change in DOC from T_0 to stationary phase. Change in DOC was calculated as TOC less the carbon content of bacterioplankton biomass (using a carbon conversion factor of 30 fg C $cell^{-1}$ for bacterioplankton in the Santa Barbara Channel and 10 fg C $cell^{-1}$ for bacterioplankton in the Sargasso Sea and South Pacific Subtropical Gyre). Colors denote BCD at elevated pCO_2 (red) and low (ambient or pre-industrial) pCO_2 (blue). Numbers refer to the experiment number (Table 1). Only experiments where a change in TOC was resolvable are shown.

Fig 6. Bacterioplankton Growth Efficiency.

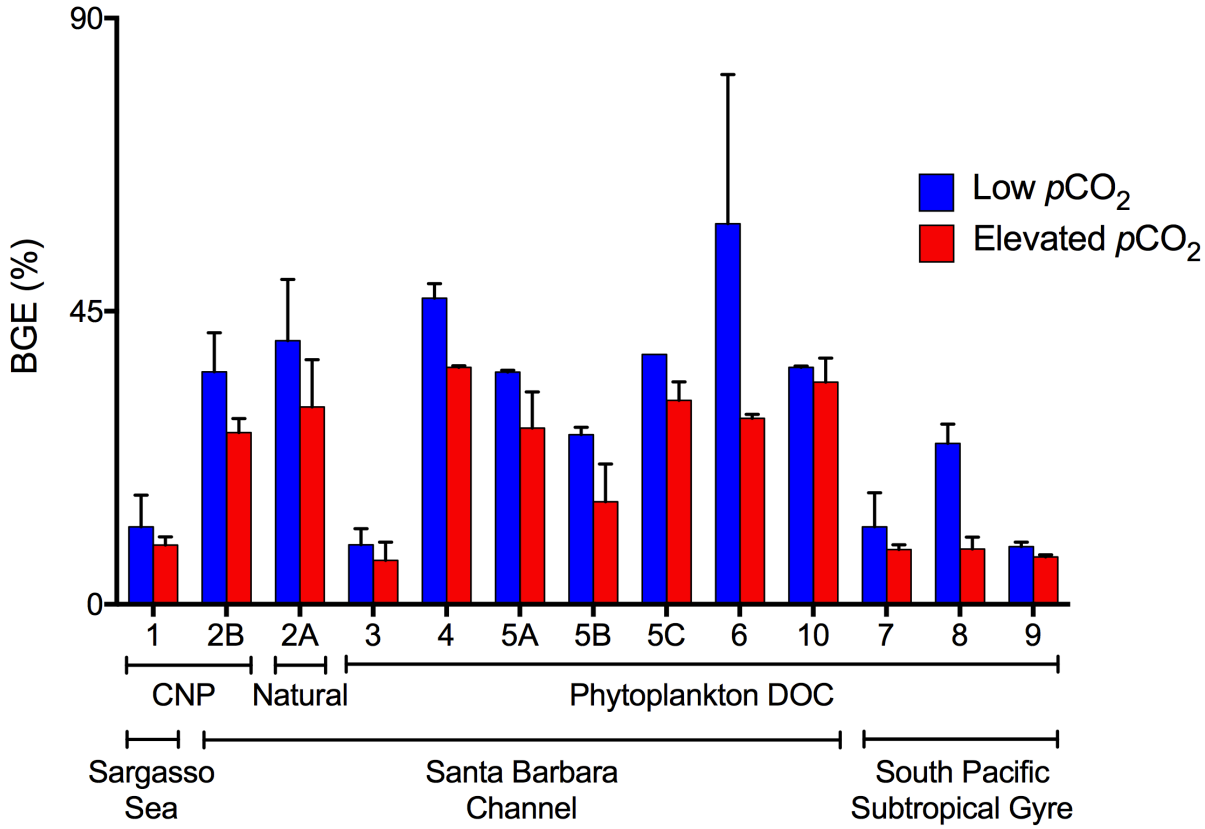

Mean (± SD) Bacterioplankton growth efficiency averaged across duplicate incubations and calculated as the change in bacterioplankton biomass carbon (using a carbon conversion factor of 30 fg C $cell^{-1}$ for bacterioplankton in the Santa Barbara Channel and 10 fg C $cell^{-1}$ for bacterioplankton in the Sargasso Sea and South Pacific Subtropical Gyre) divided by the concurrent change in DOC from T_0 to stationary phase. Colors denote bacterioplankton growth efficiency at elevated pCO_2 (red) and low (ambient or pre-industrial) pCO_2 (blue). Numbers refer to the experiment number (Table 1). Only experiments where a change in TOC was resolvable are shown.

Fig 7. Effects of pCO_2 on bacterioplankton removal of organic carbon.

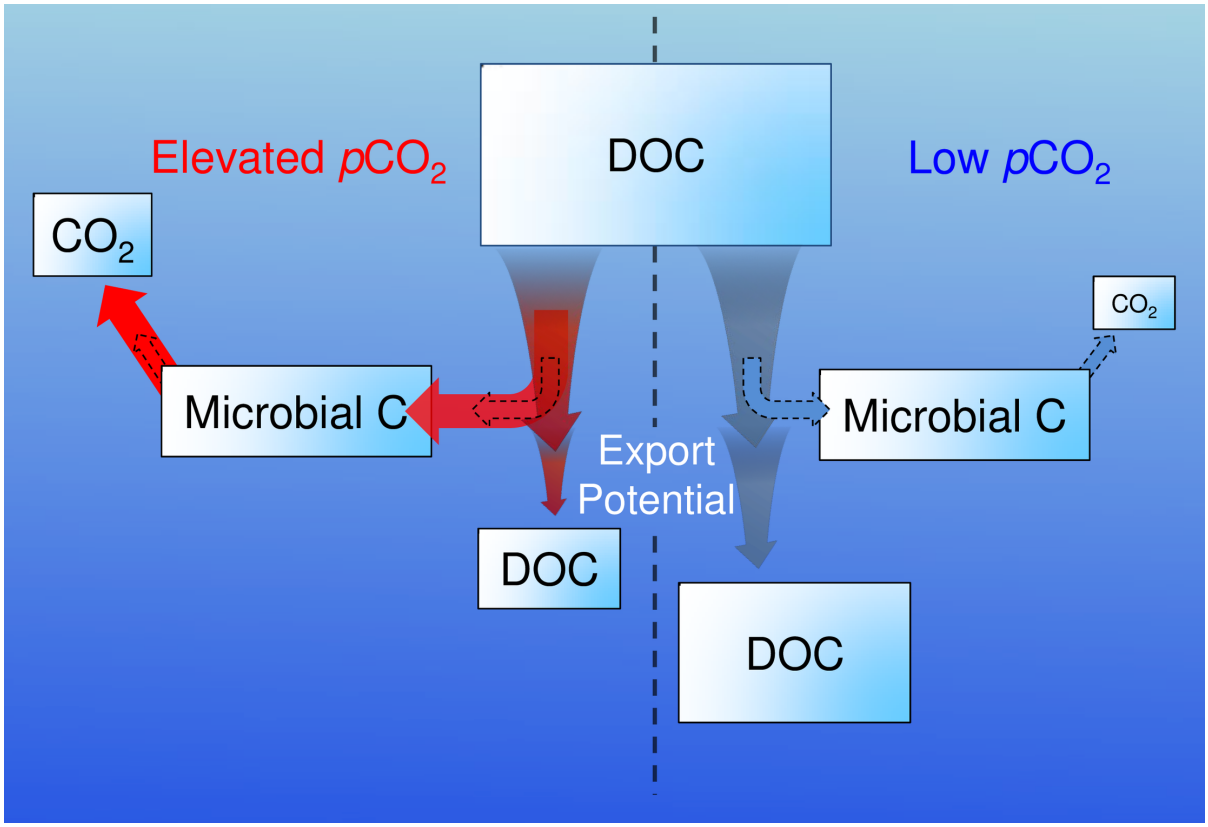

A depiction of the short-term effects of pCO_2 on the use of DOC by bacterioplankton communities in ocean surface waters. Elevated pCO_2 may increase the use of DOC at lowered bacterioplankton growth efficiencies by natural bacterioplankton communities, increasing the respiration of DOC and decreasing the magnitude of accumulated DOC in these regions, ultimately decreasing the amount of DOC available for vertical export (i.e. export potential). Arrows represent the flux of carbon between identified pools. Red represents processes occurring under elevated (> ambient) pCO_2 conditions while blue represents processes occurring under low (ambient or pre-industrial) pCO_2 conditions. Dotted black arrows denote the flux of carbon between identified pools at low pCO_2 to enable an easy comparison between elevated and low pCO_2 fluxes.

References

1. Azam F, Fenchel T, Field JG, Gray JS, Meyer-Reil LA, and Thingstad F. The ecological role of water-column microbes in the sea. Mar. Ecol. Prog. Ser. 1983;10: 257-263.
2. Zeebe RE and Wolf-Gladgrow D. CO_2 in seawater: Equilibrium, kinetics, isotopes. Elsevier Oceanography Series, 2001;65, pp. 346. Amsterdam, Book.
3. Carlson CA, Ducklow HW, and Michaels AF. Annual flux of dissolved organic carbon from the euphotic zone in the northwestern Sargasso Sea. Nature 1994;371: 405-408.
4. Hansell DA, Carlson CA, Repeta DJ, and Schlitzer R. Dissolved organic matter in the ocean: a controversy stimulates new insights. Oceanogr. 2009;22: 202-211.
5. Passow U and Carlson CA. The biological pump in a high CO_2 world. Mar. Ecol. Prog. Ser. 2012; doi: 10.3354meps09985.
6. Joint I, Doney SC, and Karl DM. Will ocean acidification affect marine microbes? ISME J 2009;5: 1-7.
7. Riebessell U, Gattusho J-P, Thingstad TF, and Middelburg JJ. Arctic ocean acidification: pelagic ecosystem and biogeochemical responses during a mescocosm study. Biogeosciences 2013; doi: 10.5194/bg-10-5619-2013
8. Motegi C, Tanaka T, Piontek J, Brussard CPD, Gatusso JP, and Weinbauer MG. Effect of CO_2 enrichment on bacterial metabolism in an Arctic fjord. Biogeosciences 2013;10: 3285-3296.
9. Grossart H-P, Allgaier M, Passow U, and Riebesell U. Testing the effect of CO_2 concentration on the dynamics of marine heterotrophic bacterioplankton. Limnol. Oceanogr. 2006;51(1): 1-11.
10. Endres S, Galgani L, Riebesell U, Schulz K-G, and Engel A. Stimulated bacterial growth

under elevated pCO_2: Results from an off-shore mesocosm study. PLoS ONE 2014;9(6): e99228.

11. Piontek J, Lunau M, Handel N, Borchard C, Wurst M, Engel A. Acidification increases microbial polysaccharide degradation in the ocean. Biogeosciences 2010;7: 1615-1624.
12. Piontek J, Borchard C, Sperling M, Schulz KG, Riebesell U, and Engel A. Response of bacterioplankton activity in an Arctic fjord system to elevated pCO_2: results from a mesocosm perturbation study. Biogeosciences, 2013;10: 297-314**.**
13. Mass EW, Law CS, Hall JA, Pickmere S, Currie KI, Chang FH, Voyles KM, and Caird D. Effect of ocean acidification on bacterial abundance, activity, and diversity in the Ross Sea, Antarctica. Aquat. Microb. Ecol. 2013; doi: 10.3354/ame01633.
14. Engel A, Delille B, Jacquet S, Riebesell U, Rochelle-Newall E, Terbrüggen A, and Zondervan I. Transparent exopolymer particles and dissolved organic carbon production by *Emiliana huxleyi* exposed to different CO_2 concentrations: a mesocosm experiment. Aquat. Microb. Ecol. 2004; doi: 10.3354/ame034093.
15. Taucher J, Jones J, James A, Brzezinski MA, Carlson CA, Riebesell U, and Passow U. Combined effects of CO_2 and temperature on carbon uptake and partitioning by the marine diatoms *Thalassiosira weissflogii* and *Dactyliosolen fragilissimus*. Limnol. Oceanogr. 2015; doi: 10.1002/lno.10063.Yamada N and Suzumura M. Effects of seawater acidification on hydrolytic enzyme activities. J. of Oceanogr. 2010;66: 233-241.
16. Yamada N and Suzumura M. Effects of seawater acification on hydrolytic enzyme activities. J of Oceanogr. 2010;66: 233-241.

17. Siu N, Apple JK, and Moyer CL. The effects of ocean acidity and elevated temperature on bacterioplankton community structure and metabolism. Open J. of Ecol. 2014;4: 434-455.
18. Bates N, Best M, Neely K, Garley R, Dickson A, and Johnson R. Detecting anthropogenic carbon dioxide uptake and ocean acidification in the North Atlantic Ocean. Biogeosciences Disc. 2012;9: 989-1019.
19. Lomas M, Bates N, Johnson R, Knap A, Steinberg D, and Carlson C. Two decades and counting: 24-years of sustained open ocean biogeochemical measurements in the Sargasso Sea. Deep Sea Res. Part 2 2013;93: 16-32.
20. Feely RA, Sabine CL, Hernandez-Ayon M, Ianson D, Hales B. Evidence for upwelling of corrosive "acidified" water onto the continental shelf. Science 2008;320: 1490-1492.
21. Hofmann GE, Smith JE, Johnson KS, et al. High-frequency dynamics of ocean pH: a multi-ecosystem comparison. PLoS ONE 2011;6: e28983- e28983.
22. Carlson CA, Giovannoni SJ, Hansell DA, Goldberg SJ, Parsons R, Otero MP, Vergin K, and Wheeler BR. The effect of nutrient amendments on bacterioplankton growth, DOC utilization, and community structure in the Northwestern Sargasso Sea. Aquat. Microb. Ecol. 2002;30: 19-36.
23. Gattuso J-P, Gao K, Lee K, Rost B, and Schulz KG. Approaches and tools to manipulate the carbonate chemistry. Guide to best practices for ocean acidification research and data reporting, eds. Riebesell U, Fabry VJ, Hansson L, and Gattuso JP (Luxembourg: Publications Office of the European Union). 2010; pp 41-52.

24. Rost B, Zondervan I, and Wolf-Gladrow D. Sensitivity of phytoplankton to future changes in ocean carbonate chemistry: current knowledge, contradictions and research directions. Mar. Ecol. Prog. Ser. 2008;373: 227-237.
25. Legendre L, Demers S, Delesalle B, and Harnois C. Biomass and photosynthetic activity of phototrophic picoplankton in coral reef waters (Moorea Island, French Polynesia). Mar. Ecol. Prog. Ser. 1988;47: 153-160.
26. Guillard, RRL and JH Ryther. Studies of marine planktonic diatoms. I. Cyclotella nana Hustedt and Detonula confervacea Cleve. Can. J. Microbiol. 1962;8: 229-239.
27. Johnson KS and Coletti LJ. In site ultraviolet spectrophotometry for high resolution and long-term monitoring of nitrate, bromide and bisulfide in the ocean. Deep Sea Res. Part 1 2002;49: 1291-1305.
28. Nelson C and Carlson C. Tracking differential incorporation of dissolved organic carbon types among diverse lineages of Sargasso Sea bacterioplankton. Environ. Microbiol. 2012;14: 1500-1516.
29. Carlson CA, Hansell D, Nelson N, Siegel D, Smethie W, Khatiwala S, Meyers MM, and Halewood E. Dissolved organic carbon export and subsequent remineralization in the mesopelagic and bathypelagic realms of the North Atlantic basin. Deep Sea Res. Part 2 2010;57(16): 1433-1445.
30. Porter KG and Feig YS. The use of DAPI for identifying and counting aquatic microflora. Limnol. Oceanogr. 1980;25: 943-948.
31. Nelson CE, Alldredge AL, McCliment EA, Amaral-Zettler LA, Carlson CA. Depleted dissolved organic carbon and distinct bacterial communities in the water column of a rapid-flushing coral reef ecosystem. ISME J. 2011;5: 1374-1387.

32. Parsons RJ, Nelson CE, Carlson CA, et al. Marine bacterioplankton community turnover within seasonally hypoxic waters of a subtropical sound: Devils Hole, Bermuda. Environ. Microbiol., 2014; doi: 10.1111/1462-2920.12445.
33. Glockner FO, Fuchs BM, & Amann R. Bacterioplankton compositions of lakes and oceans: a first comparison based on fluorescence in situ hybridization. Appl. Environ. Microbiol. 1999;65: 3721-3726.
34. Dickson AG, Sabine CL, Christian JR. Guide to best practices for ocean CO_2 measurements, PICES Special Publication, 2007; 3.
35. Hales B, Chipman D, Takahashi T. High-frequency measurement of partial pressure and total concentration of carbon dioxide in seawater using microporous hydrophobic membrane contactors. Limnol. Oceanogr. Methods 2004;2: 356-364.
36. Robbins LL, Hansen ME, Kleypas JA, Meylan SC. CO2calc—A user-friendly seawater carbon calculator for Windows, Max OS X, and iOS (iPhone): U.S. Geological Survey Open-File Report 2010; 2010–1280, 17 p. 13.
37. Dickson AG and FJ Millero. A comparison of the equilibrium constants for the dissociation of carbonic acid in seawater media, Deep-Sea Res. Pt. A. 1987;34(10): 1733-1743.
38. del Giorgio PA and Cole JJ. Bacterial growth efficiency in natural aquatic systems. Annu. Rev. Ecol. Syst. 1998;29: 503-541.
39. del Giorgio PA and Cole JJ. Bacterial growth energetics and growth efficiency, in Microbial Ecology of the Oceans, ed. Kirchman DL, pp. 289-325, John Wiley, NY. 2000.
40. Wear EK, Carlson CA, James AK, Brzezinski MA, Windecker LA, and Nelson CE.

Synchronous shifts in dissolved organic carbon bioavailability and bacterial community responses over the course of an upwelling phytoplankton bloom. Limnol. Oceanogr. 2015;00: 1-32.

41. Fukuda R, Ogawa H, Nagata T, Koike I. Direct determination of carbon and nitrogen contents of natural bacterial assemblages in marine environments. Appl. Environ. Microbiol. 1998;64: 3352-3358.
42. Gundersen K, Heldal M, Purdie DA, Knap AH. Elemental C, N, and P cell content of individual bacteria collected at the Bermuda Atlantic Time-series Study (BATS) site. Limnol. Oceanogr. 2002;47: 1525-1530.
43. Ammerman JW, Fuhrman JA, Hagstrom A, and Azam F. Bacterioplankton growth in seawater: I. Growth kinetics and cellular characteristics in seawater cultures. Mar. Ecol. Prog. Ser. 1984;18: 31-39.
44. Cherrier J, Bauer JE, Druffel ERM. Utilization and turnover of labile dissolved organic matter by bacterial heterotrophs in eastern North Pacific surface waters. Mar. Ecol. Prog. Ser. 1996;139: 267–279.
45. Carlson CA, Bates NR, Ducklow HW, and Hansell DA. Estimation of bacterial respiration and growth efficiency in the Ross Sea, Antarctica. Aquat Microb Ecol 1999;19: 229-244.
46. Letscher RT, Knapp AN, James AK, Carlson CA, Santoro AE, and Hansell DA. Microbial community composition and nitrogen availability influence DOC remineralization in the South Pacific Gyre. Mar. Chem. 2015; doi: 10.1016/j.marchem.2015.06.024

47. Sherr E and Sherr B. Roles of microbes in pelagic food webs: a revised concept. Limnol. Oceanogr. 1988;33(5): 1225-1257.

48. Tranvik L J, Sherr E, and Sherr BF. Uptake and utilization of'colloidal DOM by heterotrophic flagellates in seawater. Collections. 1993.

49. First M R and Hollibaugh JT. The model high molecular weight DOC compound, dextran, is ingested by the benthic ciliate *Uronema marinum* but does not supplement ciliate growth. Aquat. Microb. Ecol. 2009;57(1): 79.

50. Hansell DA and Carlson CA (Eds.) Biogeochemistry of marine dissolved organic matter, Second Edition. Academic Press. 2015; 693 pp.

51. Sintes E, Witte H, Stodderegger K, Steiner P, and Herndl GJ. Temporal dynamics in the free-living bacterial community composition in the coastal North Sea. FEMS Microbiol. Ecol. 2010;83: 413-424.

52. Halewood E, Carlson C, Brzezinski MA, Reed DC, Goodman J. Annual cycle of organic matter partitioning and its availability to bacteria across the Santa Barbara Channel continental shelf. Aquat. Microb. Ecol. 2012;67: 189-209.

53. Carlson CA, Giovannoni SJ, Hansell DA, Goldberg SJ, Parsons R, and Vergin K. Interactions among dissolved organic carbon, microbial processes, and community structure in the mesopelagic zone of the northwestern Sargasso Sea. Limnol. Oceanogr. 2004;49: 1073– 1083.

54. Jiao N and Zheng Q. The microbial carbon pump: from genes to ecosystems. AEM. 2011; doi:10.1128/AEM.05640-11.

55. Cotrell MT and Kirchman DL. Natural assemblages of marine proteobacteria and members of *Cytophaga-Flavobacteri* cluster consuming low- and high- molecular-

weight dissolved organic matter. Aquatic. Microb. Ecol. 2000;66: 1692-1697.

56. Newbold L, Oliver A, Booth T, Thwarl B, DeSantis R, Maguire M, Anderson G, van der Gast CJ, and Whiteley AS. The response of marine picoplankton to ocean acidification. Environ. Microbiol. 2012;14: 2293-2307.

57. Oliver AE, Newbold LK, Whiteley AS, van der Gast CJ. Marine bacterial communities are resistant to elevated carbon dioxide levels. Environ. Microbiol. Rep. 2014;6(6): 574-582.

58. Zhang R, Xia X, Lau SCK, Weinbauer MG, and Jiao N. Response of bacterioplankton community structure to an artificial gradient of pCO_2 in the Arctic Ocean. Biogeosciences 2013;6: 3679-3689.

59. Sperling M, Piontek J, Gerdts G, et al. Effect of elevated CO_2 on the dynamics of particle-attached and free-living bacterioplankton communities in an Arctic fjord. Biogeosciences 2013;10: 181-191.

60. Roy AS, Gibbons SM, Schunk H, et al. Ocean acidification shows negligible impacts on high-latitude bacterial community structure in coastal pelagic mesocosms. Biogeosciences 2013;10: 555-566.

61. Bunse C, Lundin D, Karlsson CMG, Akram N, Vila-Costa M, Palovaara J, et al. Response of marine bacterioplankton pH homeostasis gene expression to elevated CO_2. Nature Clim. Change. 2016; doi:10.1038/nclimate2914.

62. Hoppe HG. Significance of exoenzymatic activities in the ecology of brackish water: measurements by means of methylumbelliferyl-substrates. Mar. Ecol. Prog. Ser. 1983; doi: 10.3354/meps011299.

63. Chróst R. Environmental control for the synthesis and activity of aquatic microbial

ectoenzymes. In Microbial enzymes in aquatic environments, edited by: Chróst R, Springer, Heidelberg 1991;29-59.

64. Arnosti C. Microbial extracellular enzymes and the marine carbon cycle. Annu. Rev. Mar. Sci. 2011; doi: 10.1146/annurev-marine-120709-142731.
65. King GM. Characterization of ß-glucosidase activity in intertidal marine sediments. Appl. Environ. Microbiol. 1986;51: 373-380.
66. Münster U. Extracellular enzyme activity in eutrophic and polyhumic lakes. In Microbial enzymes in aquatic environments, edited by: Chróst R, Springer, Heidelberg 1991:96-122.

III. CHAPTER II

Exposure to Elevated pCO_2 Alters Bacterial Community Composition and Metabolic Potential

Anna K James[1], Linda W Kelly[2], Craig E Nelson[3], and Craig A Carlson[1]

[1] Marine Science Institute, University of California, Santa Barbara, CA, United States of America

[2]Department of Biology, San Diego State University, San Diego, CA, United States of America

[3]Department of Oceanography and University of Hawaii Sea Grant, University of Hawai'i at Manoa, Honolulu, HI, United States of America

Abstract

Factors that affect the removal of organic carbon by marine bacterial communities can alter the extent to which the oceans act as a sink of atmospheric carbon dioxide. We designed seawater culture experiments to assess the direct effect of pCO_2 on bacterial community structure and removal of total organic carbon (TOC). Experiments included treatments of elevated (1000 ppm) and low (250 ppm) pCO_2, and were conducted using surface water collected from the South Pacific Subtropical Gyre, where surface waters are exposed to rising atmospheric CO_2. Our results demonstrate a clear response in which elevated pCO_2 leads to more rapid removal of TOC by natural bacterial communities, indicating enhanced rates of bacterial respiration with elevated pCO_2. To assess differences in metabolic potential of bacterial communities, metagenomic libraries were sequenced from low and

elevated pCO_2 treatments collected at the start of the experiment and during stationary growth phase. Results indicate that a significant shift in the relative dominance of main clades of bacteria occurred in elevated pCO_2 treatments – higher relative abundance of Pseudoalteromonadaceae and Shewanellaceae were obtained by stationary growth phase with elevated pCO_2 treatments, while low pCO_2 treatments were characterized by higher relative abundance of Alteromonadaceae over the same time frame. Community metabolic functions also showed a significant response to changes in pCO_2. Elevated pCO_2 had disproportionate effects on multiple functions related to previously described pH homeostasis mechanisms, including functions for proton pumps, carbohydrate and amino acid metabolism, modifications of the phospholipid bilayer, and resistance to toxic compounds. In addition, we provide evidence for the contribution of functions related to conjugative transfer in response to elevated pCO_2. Disproportionate effects of elevated pCO_2 on amino acid and carbohydrate metabolism provide a potential mechanism to explain our observations of enhanced organic carbon removal with elevated pCO_2. In addition, greater abundance of functions related to phospholipid and membrane maintenance, and toxin and antibiotic resistance, provide a mechanistic explanation for increased bacterial respiration with elevated pCO_2, as these mechanisms require energy that could otherwise be used for growth. These results contribute to a growing understanding of the effects of elevated pCO_2 on bacteria-mediated carbon cycling in the marine environment.

Introduction

Heterotrophic bacteria play a critical role in the marine carbon cycle. They consume 50 % or more of the dissolved organic carbon (DOC) produced in the surface ocean by

photosynthesis (Azam et al. 1983; Ducklow 1999). Subsequent bacterial respiration results in the conversion of the majority of consumed organic carbon to carbon dioxide (CO_2). Collectively, these processes decrease the amount of DOC in the surface ocean and can affect the rate at which recently produced DOC accumulates in the surface ocean. A reduction in DOC accumulation can diminish the contribution of DOC to the vertical export of carbon via the biological pump (Passow and Carlson 2012). Thus, alterations to the marine system that affect bacterial consumption and subsequent respiration of organic carbon can have profound impacts on the marine carbon cycle.

James et al. (2017) recently reported that increases in pCO_2 (i.e. 1000 ppm) in short-term experiments enhanced bacterial removal of organic carbon and increased bacterial respiration from the start of the experiments to stationary growth phase. This result was observed for natural bacterial communities growing on a range of organic carbon compounds, from glucose to more complex phytoplankton products and naturally occurring DOC. Additionally, enhanced bacterial respiration and removal of organic carbon were observed for experiments conducted at various sites, and which represented oceanic regions that varied in their frequency and magnitude of exposure to elevated pCO_2 (e.g. subtropical gyres versus coastal upwelling systems). Collectively, these experiments suggest that short-term increases in pCO_2 can lead to enhanced rates of bacteria-mediated removal of organic carbon and respiration of DOC to CO_2, thus decreasing the rate at which DOC accumulates in the surface ocean. Despite the biogeochemical implications of this result, a mechanistic understanding of the taxonomic and physiological response of marine heterotrophic bacteria to elevated pCO_2 remains unclear.

Though recent experiments using microcosms and mesocosms have provided significant insight to the effects of elevated pCO_2 on natural bacterial communities, the results are often conflicting. For example, multiple studies report significant shifts in the composition of free-living bacterial communities in response to elevated pCO_2 and low pH (Krause et al. 2012, Maas et al. 2013, Siu et al. 2014, Bunse et al. 2016), while others observe negligible effects (Sperling et al. 2013, Newbold et al. 2012, Oliver et al. 2014, Allgaier et al. 2008). Experiments conducted as part of the Kiel Off-Shore Mesocosms for Ocean Simulations (KOSMOS) study also report insignificant effects of elevated pCO_2 on the composition of free-living bacterial communities (Zhang et al. 2013, Roy et al. 2013). However, Zhang et al. (2013) observed a significant negative relationship between the relative abundance of *Bacteroidetes* and pCO_2 levels, and Roy et al. (2013) found that 15 rare taxa were significantly more abundant in elevated pCO_2 mesocosms. These studies indicate that pCO_2 may influence the development of bacterial assemblages, and disproportionately affect rare taxa.

Recent studies of the consequences of elevated pCO_2 on bacterial physiology and metabolism also revealed variable results. Some studies suggest that low pH conditions lead to increased bacterial degradation of carbohydrates through enhanced extracellular enzymatic rates of ß- glucosidase (Grossart et al. 2006, Piontek et al. 2010, Maas et al. 2013, Piontek et al. 2013, Endres et al. 2014), while Yamada and Suzumura (2010) observed no effect of pCO_2 on rates of extracellular ß- glucosidase. The response of bacterial abundance to elevated pCO_2 is also variable, with some studies observing an increase in bacteria

(Endres et al 2014, Arnosti et al. 2011), in contrast to others (Grossart et al. 2006, Allgaier et al. 2008, Yamada and Zuzumura 2010). These studies suggest that the effects of elevated pCO_2 on the ecological function of bacteria remain poorly constrained.

The variable responses of marine bacteria to elevated pCO_2 reported in the literature highlights the need for studies that directly link measurements of bacteria-mediated carbon cycling to taxonomy and physiology in order to gain an understanding of the ecological function of bacteria during exposure to elevated pCO_2. Bunse et al. (2016) conducted an elegant phytoplankton-bloom mesocosm experiment that provides insight to the physiological response of Mediterranean bacterial communities to low pH. In the presence of phytoplankton communities, Bunse et al. showed that elevated pCO_2 stimulated respiratory proton pumps that aid in translocating protons across the cell membrane, suggesting that bacteria upregulate respiratory proton pumps to export protons that invade the cell as a result of high external pCO_2. Consistent with our results from the seawater culture experiments (James et al. 2017), Bunse et al. suggest that upregulation of respiratory pumps is energetically costly and may decrease overall efficiency of bacterial growth. Though this study offers insight to the physiological and taxonomic responses of bacteria to changes in pCO_2, predicting how elevated pCO_2 will affect carbon cycling in the ocean requires measurements of organic carbon removal and bacterial growth dynamics.

Here we present an analysis of the metabolic pathways encoded by marine bacterial communities during elevated pCO_2 conditions using metagenomic shotgun sequence libraries. Alterations in community structure and the overall functional potential, associated

with enhanced bacterial removal of organic carbon and decreased bacterial growth efficiency, provide new insight to physiological adaptations of marine bacteria to elevated pCO_2 conditions.

Methods

The seawater culture experiment was conducted using subsurface seawater (25 m) collected in July 2014 near French Polynesia in the South Pacific Subtropical Gyre (17˚ 26'S, 149˚ 43'W). A mixture of one-third whole surface seawater and two-thirds 0.2 µm- gravity filtered seawater (0.2 µm mixed cellulose ester filter, GSWP, Millipore, Billerica, MA) was combined to provide naturally occurring bacterial communities and dissolved organic carbon (DOC). Filtered and unfiltered seawater was combined and equally divided between two polycarbonate containers. In order to obtain the desired pCO_2 levels, water was bubbled at ~ 100 mL min^{-1} with CO_2-mixed air (Scott Marrin Inc.) to achieve low (250 ppm) or elevated (1000 ppm) levels. We were unable to measure pCO_2 at sea but applied the same flow rate and bubbling time that resulted in effective pCO_2 adjustment previously (James et al. 2017). pCO_2 adjusted seawater was then transferred into new polycarbonate carboys and a very small volume of *Emiliana huxleyi*-lysate (1.2 mL to 11.5 L of experimental seawater) was added to a final concentration of ~ 10 µmol C L^{-1}. Duplicate incubations were placed in a dark, temperature-controlled incubator at 22 ˚C. Culture experiments were sampled for total organic carbon (TOC), bacterial abundance, and bacterial DNA. Measured values of TOC include both DOC and particulate organic carbon as bacterial biomass. As such, the change in TOC between two time points is a measure of the amount of carbon lost to

bacterial respiration (James et al. 2017). Further methods describing the experimental design of the seawater culture experiment are reported in James et al. (2017).

Metagenomic samples were collected on day 0, 2 and 3 of the experiment. These time-points coincided with the start of the experiment, and the onset of, and just following, the development of stationary growth phase (Fig 1A). Samples were collected by filtering 300 mL of seawater through a 0.2 μm polyethersulfone filter (Supor-200, Pall, Port Washington, New York) under low vacuum pressure (≤ 10 mm Hg). Filters were loaded into sterile cryovials and stored frozen (-80 ˚C at sea, -40 ˚C onshore). Samples were lysed in sucrose lysis buffer (40 mmol L^{-1} EDTA, 50 mmol L^{-1} Tris-HCL, 750 mmol L^{-1} sucrose, 400 mmol L^{-1} NaCl, pH adjusted to 8.0) with 1% sodium dodecyl sulfate and 0.2 mg mL^{-1} proteinase-K at 55˚C for two hours. Genomic DNA was extracted using the MO BIO DNEasy PowerSoil Kit (QIAGEN, Carlsbad, California) and normalized to 0.2 ng μL^{-1}. Metagenomic libraries were prepared using Nextera XT (Illumina, San Diego, USA) and sequenced on the MiSeq2 Platform at San Diego State University using the 600 cycle PE sequencing reagent kit (Illumina, San Diego, USA). A total of 8,276,624 reads were obtained for samples collected on days 0, 2, and 3. The average length of pre-quality controlled forward sequence reads ranged from 200 ± 81 – 259 ± 62 base pairs, while reverse reads ranged from 203 ± 83 – 261 ± 62 base pairs.

Bacterial Community Structure & Metabolic Potential

Sequencing of community DNA obtained on days 2 and 3 of the seawater incubation experiments yielded between 259,418 and 452,287 quality controlled annotated sequence

counts per sample, resulting in 126,027 to 177,428 Identified Protein Features. The average length of quality controlled forward sequence reads ranged from 194 ± 78 – 245 ± 70 base pairs, while reverse reads were relatively shorter and ranged from 171 ± 69 – 214 ± 72 base pairs. We chose to analyze only forward reads as these were consistently longer in length. The criterion for low quality reads was those more than two standard deviations away from the mean read length. These and artificial duplicate reads were discarded. Metagenomic sequence reads were uploaded to the MG-Rast server (Meyer et al. 2008) and compared with the SEED protein database (Aziz et al. 2008). Taxonomic and functional annotations were analyzed using the default requirements in MG-Rast (i.e. e-value: 5, identity: 60 %, length: 15, and minimum abundance: 1). For taxonomic analysis, sequence counts were relativized to total sequence hits. For metabolic analysis, sequence counts were relativized to Identified Protein Features.

Average relative abundances of taxonomic and metabolic annotations were used to represent physiological state. As such, relative abundance of sequences at the start of the experiment (day 0) represent the average of duplicate samples (n = 2), while relative abundance during stationary growth phase represents the average of duplicate samples from days 2 and 3 (n = 4 per pCO_2 treatment). Statistical analysis of the community taxonomic and metabolic response to changes in pCO_2 was evaluated using analysis of similarity (ANOSIM) with 999 iterations. A randomized 1-way analysis of variance (ANOVA) with 999 iterations was performed to assess if significant differences existed in the response by individual bacterial groups to elevated pCO_2. ANOSIM and ANOVA statistical analyses were performed on arcsine (square root) transformed relative abundance data. Sequences from stationary growth

phase were combined to enhance statistical power and because the community taxonomic and metabolic responses did not differ between day 2 and 3 (p value ≥ 0.1, ANOSIM). Evaluation of significantly differentially abundant metabolic functions was conducted using EdgeR (Robinson et al. 2010, Jonsson et al. 2016). EdgeR applies a negative binomial distribution to sequence count data and identifies differential abundance using an exact test based on the quantile-adjusted conditional maximum likelihood method. These sequences are publicly available through the MG-Rast server under the project name OA8_OA11_2016_AJames (http://metagenomics.anl.gov/linkin.cgi?project=mgp19414).

Results

Growth patterns of the natural bacterial communities demonstrated typical seawater culture patterns of lag, exponential, and stationary growth (Fig 1A). Bacterial abundance yield through stationary growth phase showed no difference between pCO_2 treatments (0.97 ± 0.06 x10^6 cells mL^{-1} with elevated pCO_2, and 0.92 ± 0.07 x10^6 cells mL^{-1} with low pCO_2; Fig 1). In contrast, though non-significant (p value – 0.1, Alexander-Govern approximate test), the magnitude of cell–specific TOC removal through stationary growth phase was enhanced with elevated pCO_2 (127.7 ± 6.1 fg C L^{-1}), compared with low pCO_2 (103.4 ± 9.0 µmol C L^{-1}; Fig 1B). Cell-specific TOC removal was calculated as the change in TOC (ΔTOC) from the start of the experiment to stationary growth phase, divided by the concomitant change in cell abundance. Measured values of TOC include both DOC and the carbon associated with bacterial biomass. As such, ΔTOC represents the oxidation of organic carbon substrates and thus, bacterial respiration, indicating greater cell-specific bacterial respiration with elevated pCO_2 (James et al. 2017). Enhanced respiration and

similar bacterial abundance yield led to depressed bacterial growth efficiencies with elevated pCO_2 (7.3 ± 0.3 %), compared to (8.9 ± 0.7 %) with low pCO_2.

Bacterial Community Composition

Comparison of sequences to the SEED database indicates a significant shift in the bacterial community composition from the start of the experiment (T_0) to stationary growth phase (p value – 0.02, ANOSIM; Fig 2A). Higher relative abundance of Prochlorococcaceae (33.5 ± 0.7 %) and an unclassified-Rickettsiales (15.3 ± 0.9 %) at the beginning of the experiment was superseded by stationary growth phase, as Gammaproteobacterial groups, Pseudoalteromonadaceae (33.9 ± 6.7 %), Alteromonadaceae (24.3 ± 5.0 %), Shewanellaceae (6.6 ± 1.1 %), and Vibrionaceae (4.7 ± 0.8 %), obtained dominance (Fig 3, Table 1). Rhodobacteraceae remained among the most abundant groups over the course of the experiment, increasing from 6.6 ± 0.1 % at the beginning of the experiment to 10.8 ± 6.2 % by stationary growth phase (Fig 3, Table 1).

Changes in pCO_2 also led to significant shifts in the bacterial community composition by stationary growth phase (p value - 0.030, ANOSIM; Fig 2B). Higher relative abundance of Pseudoalteromonadaceae was obtained by stationary growth phase with elevated pCO_2 (39.42 ± 4.3 %), compared with low pCO_2 (28.4 ± 2.6 %), and lower abundance of Alteromonadaceae was observed over the same time frame in elevated pCO_2 treatments (20.3 ± 2.7 %), compared with low pCO_2 treatments (28.4 ± 2.6 %) (Fig 3, Table 1). Of the five most abundant taxa, three exhibited a significant response to pCO_2 (Table 1): Psuedoalteromonadaceae (p value – 0.004) and Shewanellaceae (p value – 0.005) were

significantly more abundant with elevated pCO_2, while abundance of Alteromonadacea was significantly reduced (p value – 0.005). In contrast, Rhodobacteraceae and Vibrionacea did not show a significant response to changes in pCO_2 (p values 0.7 and 0.1, respectively; Table 1). Four rare taxa (average relative abundance < 0.05 %) including Alcanivoracaceae, Ectothiorhodospiraceae, Methylococcaceae, and Desulfuromonadaceae, displayed a significant response to elevated pCO_2 (SI Table 1).

Bacterial Metabolic Potential

Comparison of sequences to the SEED database led to the identification of 4961 putative metabolic functions, and between 71,784 and 197,399 Identified Protein Features per sample. For the remainder of the paper, reference to metabolic functions refers to putative function assignments. The composition of community functions (i.e. Subsystem Level: Function) at the start of the experiment was significantly altered by stationary growth phase (p value - 0.027, ANOSIM; Fig 2C). In addition, the community functions (i.e. Subsystem Level: Function) encoded during stationary growth phase differed by pCO_2 level (p value - 0.03, ANOSIM; Fig 2D). Hierarchical grouping of genes into higher-order general metabolic functions (i.e. Subsystem Level 1) reveals significant shifts in 21 out of 28 functional categories from the start of the experiment to stationary growth phase (Fig 4, Table 2), indicating a pronounced effect of experimental time point on community metabolic potential. Comparing relative abundance of functions obtained during stationary growth phase, grouped by functional categories, also shows significant differences as a result of pCO_2 level (Fig 4, Table 2), indicating an effect of elevated pCO_2 on community metabolic potential.

Statistical analysis by EdgeR (Robinson et al. 2010) resulted in 415 (8.3 % of identified functions) functions that showed significant differential abundance as a function of pCO_2. Among these, 273 (65.8 %) were more abundant with elevated pCO_2, compared with 142 (34.2 %) with low pCO_2. To ensure biological relevance of the differences identified in EdgeR, we required average relative abundances in elevated pCO_2 treatments to be 1.5 times greater than the average relative abundances in low pCO_2 treatments, or vice versa. 341 of the 415 significantly differentially abundant functions exhibited a 1.5-fold difference in relative abundance (data not shown). The majority of these functions had greater abundance with elevated pCO_2 (233), compared to low (108) pCO_2 (Fig 5). The 233 functions that were significantly more abundant with elevated pCO_2 accounted for 10.9 ± 0.8 % of Identified Protein Features in elevated pCO_2 incubations. In contrast, the 108 genes that were significantly more abundant with low pCO_2 accounted for an average of 1.9 ± 0.2 % of Identified Protein Features in low pCO_2 incubations.

Functions with significantly higher relative abundance in elevated pCO_2 incubations corresponded to different functional categories than those with significantly higher relative abundance in elevated pCO_2 incubations (Fig 5). Elevated pCO_2 had a pronounced effect on metabolic functions related to carbohydrate metabolism (41 out of 233 functions that were significantly more abundant with elevated pCO_2), clustering-based subsystems (21), miscellaneous (20), fatty acids, lipids, and isoprenoids (17), membrane transport (16), and virulence, disease, and defense (15) (Fig 5). Significantly enriched genes related to carbohydrate metabolism were dominated by monosaccharide (37 %) and amino sugar (24

%) utilization (data not shown). 88 % of significantly enriched functions categorized as fatty acids, lipids, and isoprenoids were related to fatty acid and phospholipid biosynthesis, and nearly all (93 %) virulence, disease, and defense enriched functions aid in resistance to antibiotics and toxic compounds. 62 % (13 out of 21) of the significantly enriched functions identified in the clustering-based subsystems category were related to conjugative transfer. Additionally, 9 out of 16 (56.6 %) significantly enriched functions related to membrane transport were associated with conjugative transfer. Collectively, by stationary growth phase, 10 % of functions that were significantly more abundant with elevated pCO_2 were related to conjugative transfer. Though elevated pCO_2 did not have a pronounced effect on metabolic functions related to respiration (Fig 5), genes related to electron transport machinery (i.e. cytochromes) were significantly enriched with elevated pCO_2.

Discussion

The results indicate that elevated pCO_2 can directly influence bacterial community composition and metabolic potential. Elevated pCO_2 led to a shift in the taxonomic composition of natural bacterial communities (Fig 3), conferring dominance to Pseudoalteromonadaceae and Shewanellaceae, and reducing abundances of Alteromonadaceae. In addition, elevated pCO_2 had disproportionate effects on numerous functions, including those related to electron transport machinery, carbohydrate use, phospholipid and fatty acid biosynthesis, resistance to antibiotics and toxic compounds, and conjugative transfer (Fig 6). These results provide evidence to suggest that elevated organic carbon removal and enhanced bacterial respiration with elevated pCO_2 may have been

driven by shifts in the bacterial community and concomitant shifts in community metabolic potential.

Bacterial Community Composition

The bacterial community composition shifted from more oligotrophic bacterial clades such as Prochlorococcaceae and Rickettsiales at the start of the experiment to communities that were dominated by copiotrophic Gammaproteobacteria by stationary growth phase, with both low and elevated pCO_2 (Fig 3). Dominance by Gammaproteobacterial clades by stationary growth phase is not surprising, as groups such as Alteromonadaceae and Pseudoalteromonadacea have been shown to rapidly assimilate phytoplankton organic carbon (Nelson and Carlson 2012). In addition, these bacteria were observed to rapidly increase in abundance in response to recently produced organic material (Carlson et al. 2002, McCarren et al. 2010, Nelson and Carlson 2012, Sarmento and Gasol 2012). Thus, higher relative abundances of Gammproteobacteria obtained by stationary growth phase, with low and elevated pCO_2, likely resulted from the addition of labile compounds in the form of phytoplankton-derived organic carbon. Dominance by Gammaproteobacterial clades in a phytoplankton microcosm experiment was also observed by Bunse et al. (2016), with 30 – 50 % of annotated transcript reads being dominated by Gammaproteobacteria in both low and elevated pCO_2 treatments.

Despite the overwhelming dominance by traditionally copiotrophic Gammaproteobacteria clades (~ 70 % of total sequences) in low and elevated pCO_2 incubations, a significant shift in bacterial populations as a function of pCO_2 was still evident (Fig 3, Table 1). This result

provides evidence of a direct effect of elevated pCO_2 on bacterial populations. Further, bacterial community structure has been shown to influence the type and amount of organic carbon that is removed by heterotrophic bacteria (Cotrell and Kirchman 2000, Carlson et al. 2004, Nelson and Carlson 2012, Newbold et al. 2012, Nelson et al. 2013, Letscher et al. 2015, and Wear et al. 2015). In addition, estimates of marine bacterial growth efficiencies, which provide an estimate of how much consumed organic carbon is respired by bacteria, range from 0.05 to as high as 0.6 (delGiorgio and Cole 1998), and have been shown to vary based on bacterial community composition (Reinthaler et al. 2005, Nelson et al. 2013). Thus, the shift in bacterial community structure in our experiment provides a potential mechanism to explain the observation of enhanced organic carbon removal and bacterial respiration with elevated pCO_2. Why elevated pCO_2 confers advantage to Pseudoalteromonadaceae and Shewanellaceae in the presence of coccolithophore culture lysate remains unclear and requires further investigation to elucidate this result.

Bacterial Metabolic Potential

In addition to a shift in bacterial community structure, enhanced organic carbon removal by bacteria and increased bacterial respiration may be driven by a direct effect of pH on bacterial physiology. Bacteria rely on strategies for maintaining internal pH because proteins function within distinct pH ranges (Booth 1985 and citations therein). Authors of a recent phytoplankton microcosm study (Bunse et al. 2016) suggest that decreasing external pH causes protons to enter into bacterial cells and decrease intracellular pH. These researchers postulate that the observed up-regulation of respiratory and light-driven proton pumps resulted from a need to reestablish internal pH values through alkalization of the cytoplasm

(Bunse et al. 2016). Similarly, we also observed greater relative abundance of functions required to alkalize intracellular pH in elevated pCO_2 incubations. For example, two functions related to cytochrome c biogenesis were significantly enriched with elevated pCO_2 (relative abundance 1.8 to 4 times greater with elevated pCO_2). Cytochrome c is one of the main agents of the electron transport machinery within bacterial cells and aids in the removal of protons from the cytoplasm through active proton translocation across cellular membranes (Maurer et al. 2005, Slonczewski et al. 2009 and citations therein, Krulwich 2011, Bunse et al. 2016; Fig. 6). Further, cytochrome c biogenesis was shown to be one of the most responsive proteins to elevated pCO_2 for marine Rhodobacteriaceae bacteria (Bunse et al. 2016).

In addition to using proton pumps to alkalize the cytoplasm, several studies provide evidence to suggest that bacteria alter their catabolism of amino acids and carbohydrates in order to minimize intracellular acid production at low pH (Slonczewski and Foster 1996, Blankenhorn et al. 1999, Stancik et al. 2002, Foster 2004, Yohannes et al. 2004, Maurer et al. 2005, Hayes et al. 2006). Elevated pCO_2 incubations for our study were significantly enriched with metabolic functions related to the transport and subsequent decarboxylation of the amino acid arginine (Fig. 6). Arginine decarboxylase catalyzes the conversion of arginine to CO_2 and agamatine. This process contributes to the alkalization of the cytoplasm through the consumption of a proton and the production and subsequent diffusion of CO_2 from the cell, enabling bacteria to counteract the impact of invading protons that may result from low pH (Foster et al. 2004; Slonczewski et al. 2009 and citations therein). In addition, functions related to arabinose, fucose, and mannose metabolism were significantly enriched

with elevated pCO_2 (data not shown). A study of the metabolic response of *E.coli* to changes in pH revealed enhanced regulation of catabolic enzymes and transporters such as those for arabinose, fuculose, and gluconate in response to low pH (Hayes et al. 2006). The catabolism of these sugars and sugar derivatives produced fewer acids internally as compared to catabolism of glucose and maltose, which produce a burst of fermentation acids upon catabolism (Stancik et al. 2002, Hayes et al. 2006). Metabolic switching allows bacteria to adjust the concentration of protons across the cell membrane. Thus, greater abundance of metabolic functions related to the use of carbohydrates and amino acids indicates a potential of bacterial communities to alter their preference for various organic substrates in response to elevated pCO_2, possibly choosing to use substrates that produce more or fewer acids to counteract the consequences of elevated pCO_2 on intracellular pH.

Elevated pCO_2 will result in an influx of protons only if the pH of the external milieu drops below intracellular pH values. Studies of marine bacteria suggest that intracellular pH is maintained ~ 7.6 (Padan et al. 2005 and citations therein). Using ship-board measurements of total alkalinity (~2340 μmol kg^{-1}) and assuming successful alteration of pCO_2 to 1000 ppm enables estimation of pH in elevated pCO_2 incubations. This calculation indicates that at most, external pH values may have dropped from ~ 8.1 to ~7.7. If the natural bacteria collected for our study maintain an intracellular pH ~ 7.6, a decrease in external pH to 7.7 would not result in an influx of protons, as the external concentration of protons would remain lower than the concentration within bacterial cells. However, this change would diminish the transmembrane proton gradient, which is pivotal in establishing the proton motive force that drives cellular functions (Krulwich et al. 2011). Rather than expel protons

in response to declining external pH, bacteria may enhance proton uptake to reestablish the transmembrane proton gradient and thus the proton motive force. Elevated pCO_2 incubations were enriched with functions related to maltose utilization, metabolism of which produces a burst of fermentation acids internally (Stancik et al. 2002, Hayes et al. 2006). In addition, the Na^+/H^+ antiporter, which acidifies the cytoplasm through the exchange of Na^+ for H^+ (Kosono et al. 1999; Fig 6), was 1.6-fold more abundant with elevated pCO_2. Further, two functions related to cytochrome d-oxidase, which minimizes proton export, and was preferentially expressed by *E. coli* in response to external alkalization (Maurer et al. 2005), were significantly more abundant with elevated pCO_2 (Fig 6).

Though our analysis provides a conflicting illustration of cells metabolic potential to alkalize or acidify the cytoplasm in response to low pH, elevated pCO_2 had clear effects on functions related to carbohydrate metabolism, fatty acid and phospholipid biosynthesis, antibiotic and toxic compound resistance, and conjugative transfer. Functions related to carbohydrate metabolism were the most differentially abundant for our experiment, with the majority of these functions being more abundant in elevated, compared to low pCO_2 treatments (Fig 5). Nearly one third of the differentially abundant carbohydrate metabolism functions were related to bacterial use of chitin, N-acetyl-glucosamine (GlcNAc), and N-acetyl-galactosamine (GalNAc). Chitin is one of the most abundant polymers in the marine environment and potential sources include structural components of phytoplankton (Bassler et al. 1991, Riemann & Azam 2002), suggesting that the addition of phytoplankton-derived organic matter likely led to the availability of chitin in our experiment. GlcNAc is a monomeric unit of chitin and similar to GalNAc – both are major components of

peptidoglycan and capsular polysaccharides, as well as the outer membrane lipopolysaccharides of gram-negative bacteria (Brinkkotter et al. 2000, Leyn et al. 2012), suggesting that dying bacterial cells may have provided a source of carbon and nitrogen to surviving cells in elevated pCO_2 incubations. A recent mesocosm experiment conducted in the Ross Sea, Antarctica, investigating the effects of elevated pCO_2 on mixed-surface communities, found enhanced activities of chitinase, the enzyme involved in chitin utilization, in low pH mesocosms. This result is consistent with our finding that elevated pCO_2 increased the metabolic potential of bacterial communities for using chitin, and suggests that short-term exposure to elevated pCO_2 may lead to greater bacterial degradation of chitin and related amino sugars, such as GlcNAc and GalNAc, present in phytoplankton and bacterial cell walls.

Numerous studies point to bacterial modification of the phospholipid bilayer as a critical mechanism for enabling cells to cope with low pH stress (Brown et al. 1997, and reviews by Slonczewski et al. 2009, Zhang and Rock 2008, and Krulwich et al. 2011). For our experiment, 15 out of the 17 functions related to fatty acids, lipids, and isoprenoids that were enriched with elevated pCO_2, were related to phospholipid and fatty acid biosynthesis (Fig 6). Further, the average relative abundance of each of these functions with elevated pCO_2 was more than twice the average relative abundance in low pCO_2 incubations, and we found no differentially abundant functions related to phospholipid and fatty acid biosynthesis in low pCO_2 incubations (data not shown). Functions that were more abundant with elevated pCO_2 included multiple genes required for the elongation of fatty acid chains in bacteria, including enoyl-acyl carrier protein (ACP) reductase (FabI), 3-hydroxydecanoyl-ACP

dehydratase (FabA), and 3-oxoacyl-ACP synthase (FabB). FabI is required to complete the cycle of fatty acid elongation, while FabA and FabB work together to introduce double bonds into the growing acyl chain, resulting in the production of unsaturated fatty acids (Zhang & Rock 2008). Unsaturated fatty acids are more fluid than their saturated counterparts because the double carbon-carbon bonds incorporate kinks into the hydrocarbon chain that disable the lipids from packing tightly together. Multiple studies point to bacterial modification of the phospholipid bilayer to incorporate cyclopropane fatty acids, which mimic unsaturated fatty acids and increase the impermeability of the phospholipid bilayer to protons, as a critical mechanism for enabling cells to cope with low pH stress and proton flooding induced by low pH (Brown et al. 1997, Chang & Cronan 1999, and reviews by Slonczewski et al. 2009, Zhang and Rock 2008, and Krulwich et al. 2011). Exposure to low pH in our experiment may have conferred advantage to bacterial populations that contain greater abundance of genes enabling them to alter the permeability of their membrane in response to changing pH. This result provides further evidence to suggest that bacteria can alter the structure and composition of their cellular membranes as a mechanism for coping with low pH stress.

Elevated pCO_2 also had disproportionate effects on functions related to antibiotic and toxic compound resistance (Fig 6). Specifically, multiple functions regulating efflux of metal cations (50 % of the functions related to antibiotic and toxic compound resistance), and multidrug efflux pumps (43 %) were significantly more abundant in elevated pCO_2 incubations. Further, a copper chaperone that aids in copper homeostasis exhibited relative abundance 47.5 times greater with elevated pCO_2, as compared with low pCO_2. Copper

chaperones prevent cytoplasmic exposure to copper ions in transit (Harrison et al. 1999), and were shown to deliver copper to a membrane fusion protein for expulsion from bacterial cells (Franke et al. 2003). Hayes et al. (2006) observed a similar response by *E. coli* to low pH conditions – low pH led to upregulation of metal cation efflux proteins required to rid the cell of silver and copper. The researchers posit that the solubility of metals such as copper increased with decreasing pH. Other metals including zinc and iron were also shown to increase in solubility as a result of low pH (Millero et al. 2009), suggesting that bacteria induce metal efflux pumps to regulate the concentration of these potentially toxic metals in response to low pH. In addition to removing metal cations, greater abundance of multidrug efflux pumps suggest that bacteria require methods of removing other toxic compounds and antimicrobial agents from the cell (Anderson et al. 2015). Because efflux transporters require the import of a proton to drive the proton motive export of the toxic substrate, multidrug efflux pumps such as the Resistance-Nodulated-Division (RND) efflux system have been shown to aid in pH homeostasis and tolerance to alkali stress (Lewinson et al. 2004; Fig 6). As such, it is possible that bacteria in our experiments are using multidrug efflux pumps not only to remove potentially toxic compounds and metals, but also to reestablish the transmembrane pH gradient, and thus, the proton motive force.

Finally, functions related to conjugative transfer made-up ~ 10 % of the differentially abundant functions that were more abundant with elevated pCO_2 (Fig 6). Through direct transfer of single stranded DNA, conjugative transfer represents one of the dominant modes by which bacteria transfer genetic information between cells, and is an important mechanism for the spread of fitness-enhancing traits (Chen et al. 2005). As such, conjugative transfer

can contribute to the survival of bacteria in response to environmental stress (Burrus et al. 2004, Krause et al. 2000, Frost and Koraimann 2010 and citations therein). In addition to transferring beneficial DNA between cells, conjugative transfer was shown to enhance pathogenesis of a wide range of bacteria (Green and Mecsas 2016 and citations therein). Further, numerous food-safety studies report enhanced bacterial pathogenicity in response to low pH stress, and suggest that exposure to low pH through anti-bacterial sterilization methods leads to the exchange of stress-tolerant genes that enable pathogenic bacteria to survive exposure to low pH environments (Chung et al. 2006 and citations therein). Though bacteria in our experiments are not experiencing host induced low pH stress, these studies provide evidence that initial adaptation of bacteria to low pH environments may enable pathogenic groups to survive and persist at higher than normal relative abundances, conferring advantage to groups that would not be present in the absence of elevated pCO_2. The substantial number of functions related to conjugative transfer for our study suggests that a potential impact of elevated pCO_2 may be to enhance abundance of pathogenic bacteria through the direct transfer of genetic material that better enables these clades to cope with changes in environmental pCO_2.

Collectively, our sequencing results contribute to a growing understanding of the impacts of elevated pCO_2 on the metabolic potential of marine bacteria. Elevated pCO_2 had disproportionate effects on multiple functions related to previously described pH homeostasis mechanisms, including functions for proton pumps, carbohydrate and amino acid metabolism, modifications of the phospholipid bilayer, and resistance to toxic compounds (Fig 6). In addition, we provide evidence for the potential contribution of

functions related to conjugative transfer in response to elevated pCO_2 (Fig 6). The pronounced effect of elevated pCO_2 on metabolic functions related to bacterial use of carbohydrates provides a potential mechanism to explain why bacteria consumed greater amounts of organic carbon in response to elevated pCO_2– elevated pCO_2 may have caused bacteria to alter their preference for specific components of the organic carbon pool, enabling, or requiring them, to consume more to maintain pH homeostasis. Further, greater abundance of functions enabling bacteria to alter their membrane permeability and expel toxic metals and other compounds suggests that bacteria may divert energy from growth to counteract the effects of elevated pCO_2 on normal cellular functioning, thus decreasing their overall growth efficiency and likely increasing respiration.

Conclusions

In summary, the experimental metagenomics approach described here is contributing to our understanding of the effects of elevated pCO_2 on bacterial community composition and metabolic pathways. We show that short-term responses to a significant increase in pCO_2 altered natural bacterial communities and led to differential abundance of community functions. The shift in community structure and disproportionate effects of elevated pCO_2 on amino acid and carbohydrate metabolism provide a potential mechanism to explain why we observed enhanced organic carbon removal with elevated pCO_2 in this experiment. In addition, greater abundance of functions related to phospholipid and membrane maintenance, and toxin and antibiotic resistance, provide a potential mechanistic explanation for increased bacterial respiration with elevated pCO_2, as these mechanisms require energy that could otherwise be used for growth. Oceanic assemblages of bacteria in the South

Pacific Subtropical Gyre are likely to experience these changes in pCO_2 over long periods of time; however, our observations of enhanced metabolic potential for conjugative transfer indicate the potential for adaptation, suggesting that short-term responses may have long-term effects. Collectively, the combined effects of pCO_2 on bacterial community composition and metabolic functionality suggest that short-term increases in pCO_2 may alter bacterial ecological function, enhancing rates of bacteria-mediated removal of surface organic carbon and production of carbon dioxide in the surface ocean; however, further studies of the long-term effects of elevated pCO_2 are required to elucidate the long-term implications of these short-term impacts on bacteria-mediate carbon cycling in the marine system.

Figures for Chapter II

Figure 1. **Mean bacterial abundance and cell-specific TOC removal by natural bacterial communities in the South Pacific Subtropical Gyre**.

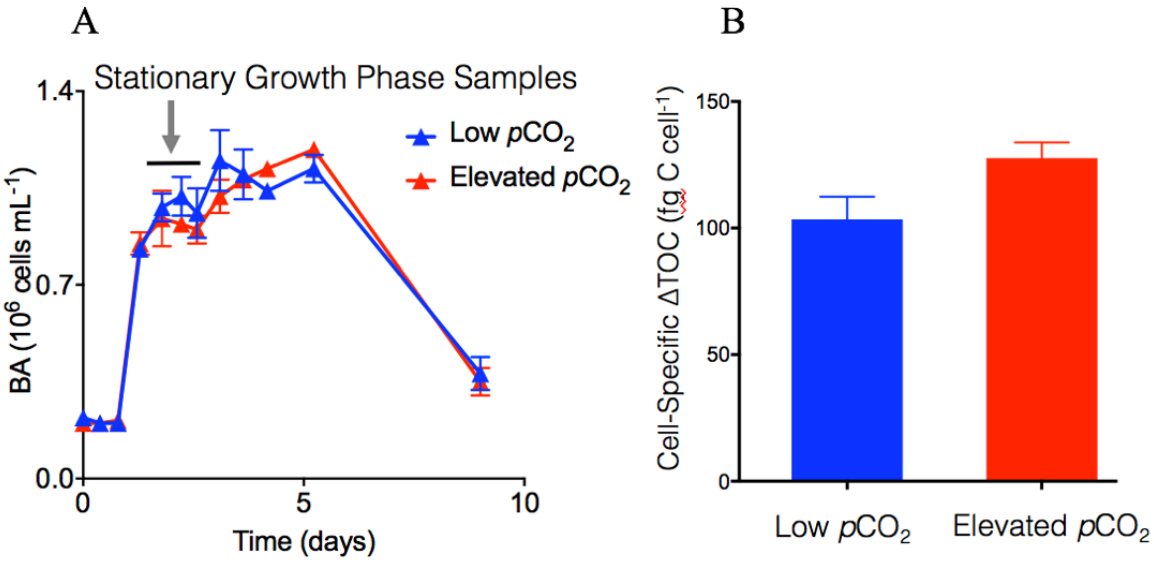

Mean bacterial abundance (BA; ± standard deviation) averaged across duplicate incubations and time as a function of pCO_2 for natural bacterial communities in the South Pacific Subtropical Gyre (A). Panel B shows mean cell-specific TOC removal by stationary growth phase as a function of pCO_2. Red denotes elevated (1000 ppm) pCO_2 while blue denotes low (250 ppm) pCO_2. Squares represent TOC (µmol C L^{-1}) while triangles denote BA (10^6 cells mL^{-1}) over the course of the incubation. Arrows indicate time points when stationary growth phase DNA samples were obtained. Data from James et al. 2017.

Figure 2. Nonmetric multidimensional scaling ordination plots of relative abundance of bacterial community composition.

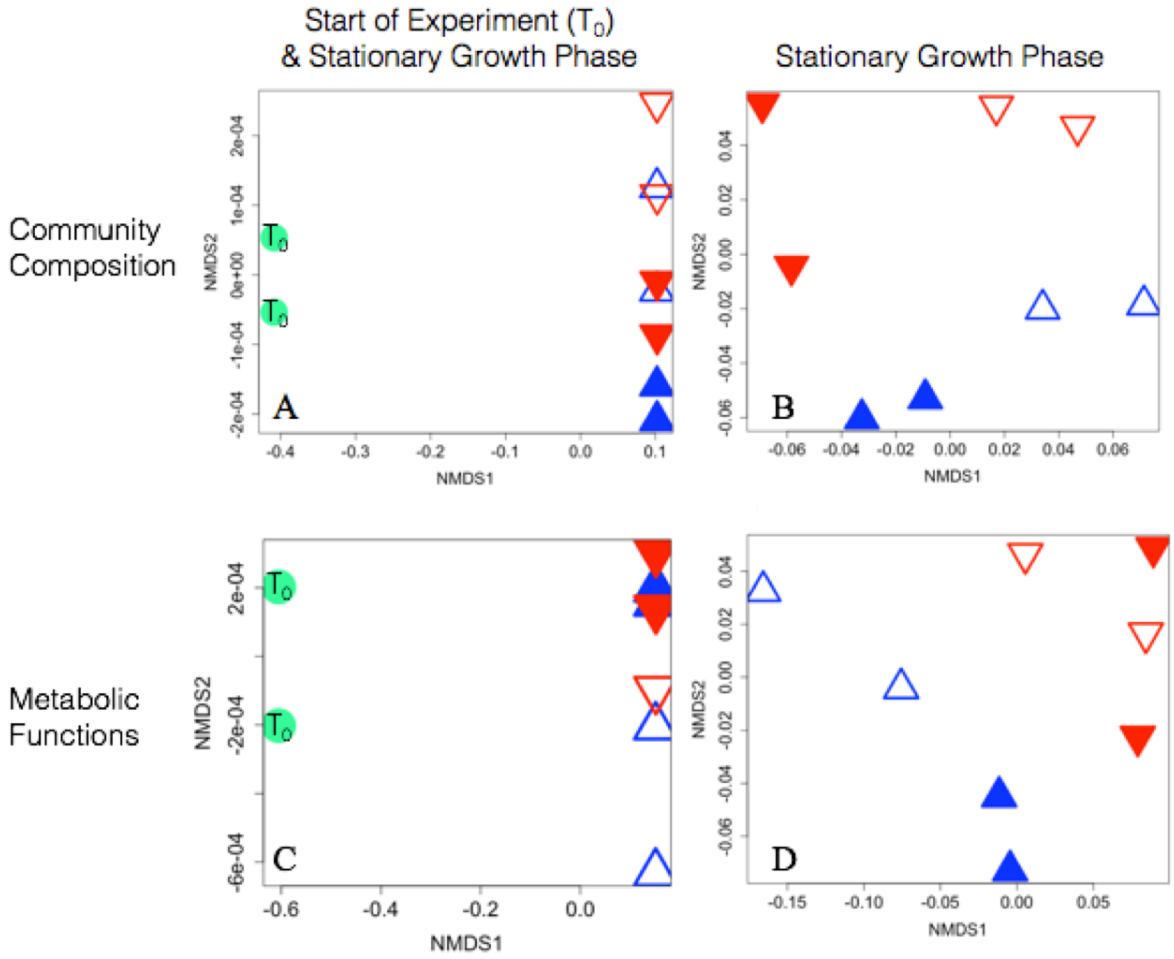

Nonmetric multidimensional scaling ordination plots of relative abundance of bacterial community composition (A & B), and bacterial metabolic functions (C & D) from DNA samples collected at the start of the experiment (T_0, green circles) and on day 2 (filled triangles), and day 3 (open triangles) of the experiment. Red denotes elevated (1000 ppm) pCO_2 while blue denotes low (250 ppm) pCO_2. The left panel includes samples from the start of the experiment and stationary growth phase (n = 10), while the right panel includes only samples from stationary growth phase (n = 8).

Figure 3. The average relative abundance of bacterial groups collected at the initiation of the experiment (T_0) and during stationary growth phase.

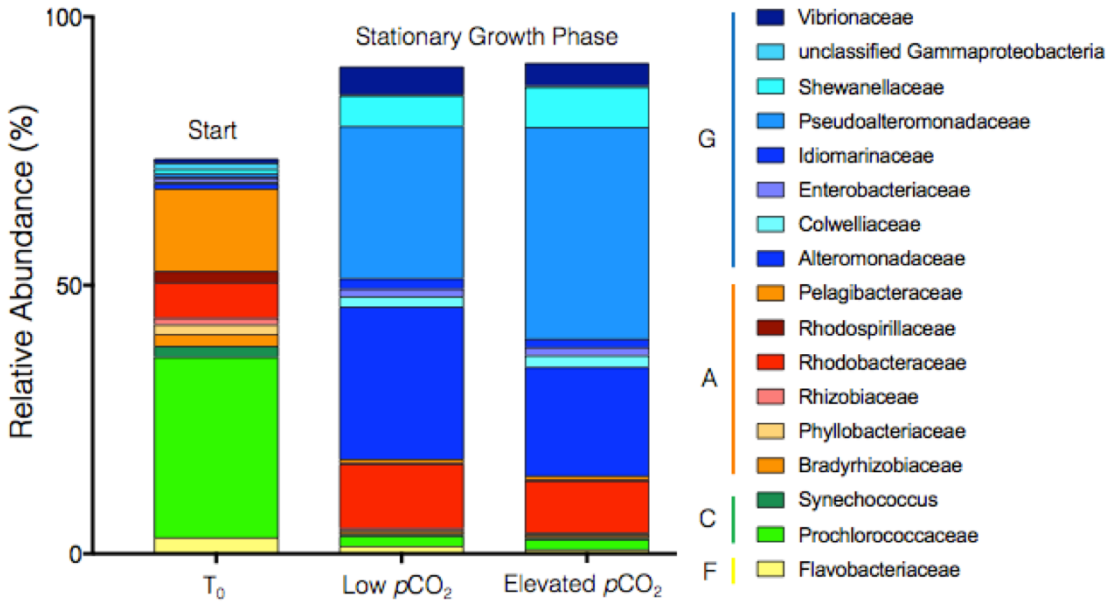

The average relative abundance of bacterial groups collected at the initiation of the experiment (T_0) and during stationary growth phase for low (250 ppm) and elevated (1000 ppm) pCO_2 treatments. Counts were normalized to total hits. Reads were taxonomically annotated by comparison with the SEED database. Coloration refers to bacterial clades – green hues correspond to Cyanobacteria (C), red and orange to Alphaproteobacteria (A), blues to Gammaproteobacterial (G) clades, and yellow represents to Flavobacteria (F).

Figure 4. The average relative abundance (± standard deviation) of metabolic functions.

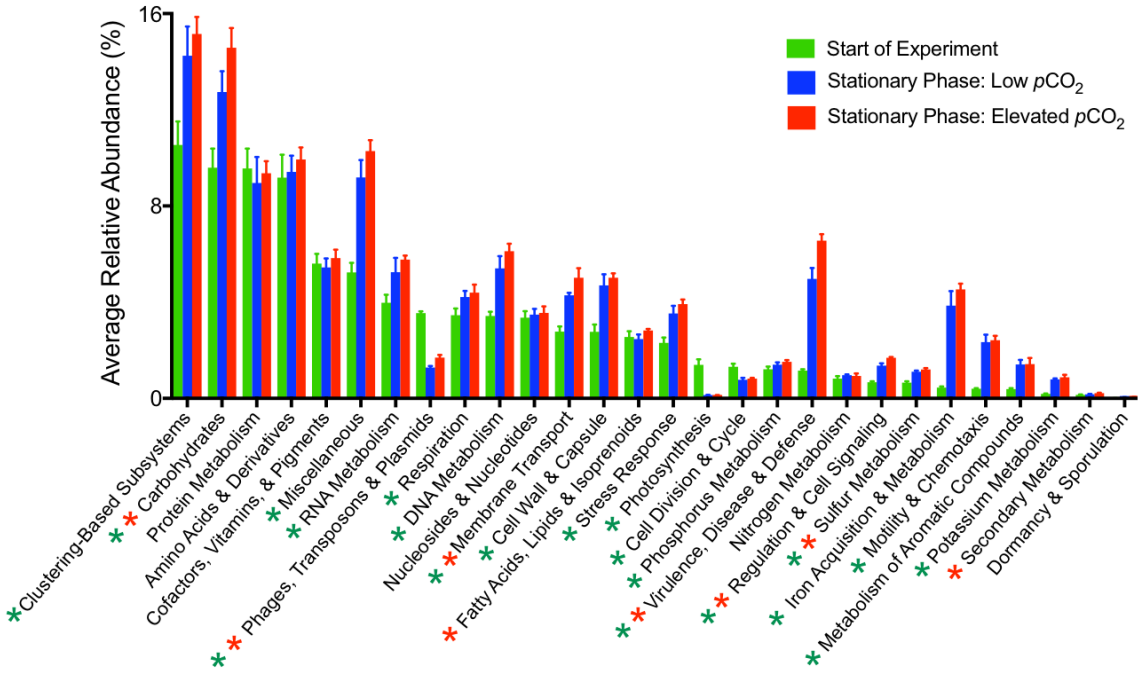

The average relative abundance (± standard deviation) of metabolic functions grouped by the broadest functional categories in the SEED database. For samples collected at the start of the experiment, green bars represent the average of duplicate samples. For samples collected during stationary growth phase, averages represent duplicate samples obtained on days 2 and 3 of the experiment (n = 4 per pCO_2 treatment), for low (blue; 250 ppm) and elevated (red; 1000 ppm) pCO_2 treatments. Counts were normalized to Identified Protein Features. Statistical analysis of the community metabolic response to changes in pCO_2 was evaluated using analysis of variance (ANOVA) – green asterisks denote significant difference in relative abundances between the start of the experiment and stationary growth phase. Red asterisks denote a significant difference in the relative abundance of functions obtained during stationary growth phase in response to elevated pCO_2.

Figure 5. Significantly differentially abundant metabolic functions encoded during stationary growth phase.

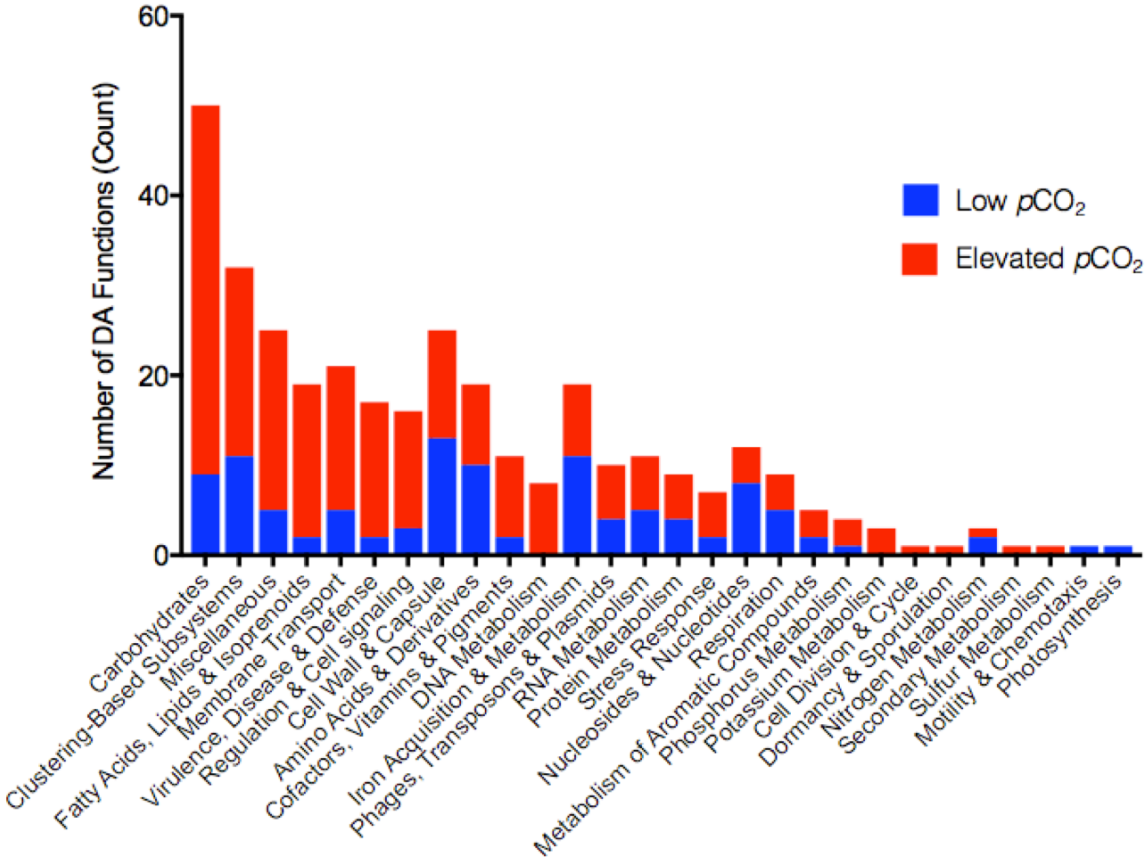

The number (count) of significantly differentially abundant (DA) metabolic functions encoded during stationary growth phase under low (blue) and elevated (red) pCO_2. Metabolic functions are grouped by the broadest functional categories in the SEED database (Subsystem Level 1). Statistical analyses were conducted using EdgeR and only the functions that exhibited a 1.5-fold change in relative abundance are reported.

Figure 6. Model of the potential physiological response of natural bacterial communities to elevated pCO_2.

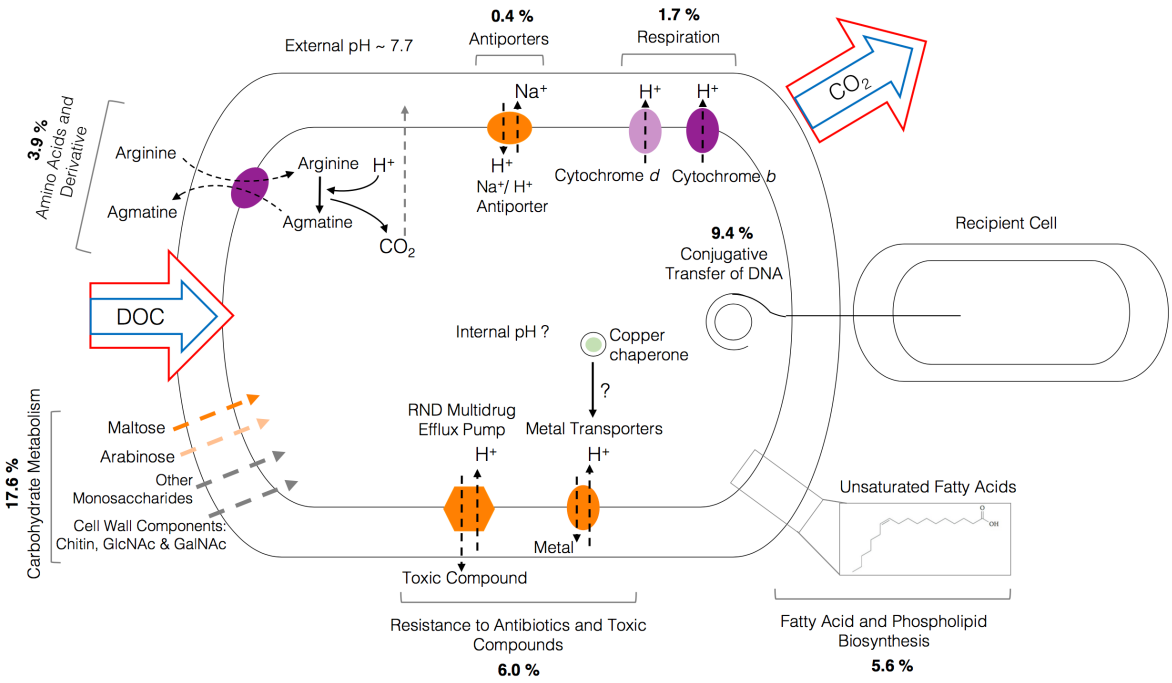

Model of the potential physiological response of natural bacterial communities to elevated pCO_2. Colors denote whether the cellular process results in the acidification (orange; i.e. importing protons) or alkalization (purple; i.e. expelling protons) of intracellular pH. Lighter colors indicate functions that result in less intracellular pH change, and have been implicated as mechanisms to cope with low pH (light orange) or base (light purple) stress. See text for citations. Grey arrows refer to more than one process and are not colored by their effects on intracellular pH. Bolded values represent the number of differentially abundant (DA) functions within each identified SEED category that were significantly more abundant with elevated pCO_2 – counts are normalized to total DA functions that were significantly more abundant in elevated pCO_2 incubations. Large arrows indicate the relative consumption of dissolved organic carbon (DOC) and production of CO_2 (i.e. respiration) by bacteria growing at low (blue) and elevated (red) pCO_2 levels. GlcNAc refers to N-acetyl-glucosamine, and GalNAc to N-acetyl-galactosamine. RND refers to Resistance-Nodulated-Division efflux pumps.

Tables for Chapter II
Table 1

Taxonomy			Average RA (%) ± SD			Statistical Analysis	
			Start of Experiment	Stationary Growth Phase		Community Response to pCO_2 During Stationary Growth Phase	
Phylum	Class	Family	T_0	Low pCO_2	Elevated pCO_2	P values	Storey q values
Bacteroidetes	Flavobacteria	Flavobacteriaceae	3.1 ± 0.03	1.5 ± 0.5	0.9 ± 0.2	0.06	0.15
Cyanobacteria	Cyanobacteria	Prochlorococcaceae	33.5 ± 0.7	1.9 ± 0.3	1.9 ± 0.4	0.94	0.43
Cyanobacteria	Cyanobacteria	Synechococcus	2.1 ± 0.1	0.2 ± 0.1	0.3 ± 0.1	0.69	0.38
Proteobacteria	Alphaproteobacteria	Bradyrhizobiaceae	2.2 ± 0.1	0.5 ± 0.2	0.4 ± 0.1	0.56	0.34
Proteobacteria	Alphaproteobacteria	Phyllobacteriaceae	1.8 ± 0.02	0.3 ± 0.1	0.2 ± 0.1	0.61	0.35
Proteobacteria	Alphaproteobacteria	Rhizobiaceae	1.2 ± 0.01	0.3 ± 0.1	0.3 ± 0.1	0.59	0.35
Proteobacteria	Alphaproteobacteria	Rhodobacteraceae	6.6 ± 0.1	12.0 ± 7.4	9.6 ± 5.7	0.66	0.37
Proteobacteria	Alphaproteobacteria	Rhodospirillaceae	2.1 ± 0.1	0.2 ± 0.1	0.2 ± 0.1	0.82	0.40
Proteobacteria	Alphaproteobacteria	Pelagibacteraceae	15.3 ± 0.9	0.7 ± 0.1	0.8 ± 0.1	0.51	0.34
Proteobacteria	Gammaproteobacteria	Alteromonadaceae	1.0 ± 0.04	28.4 ± 2.6	20.3 ± 2.7	0.005*	0.047
Proteobacteria	Gammaproteobacteria	Colwelliaceae	0.21 ± 0.01	1.9 ± 0.2	2.1 ± 0.2	0.18	0.21
Proteobacteria	Gammaproteobacteria	Enterobacteriaceae	0.7 ± 0.01	1.4 ± 0.1	1.5 ± 0.1	0.12	0.18
Proteobacteria	Gammaproteobacteria	Idiomarinaceae	0.3 ± 0.01	1.9 ± 0.2	1.6 ± 0.15	0.05	0.14
Proteobacteria	Gammaproteobacteria	Pseudoalteromonadaceae	0.6 ± 0.04	28.4 ± 2.6	39.4 ± 4.3	0.004*	0.047
Proteobacteria	Gammaproteobacteria	Pseudomonadaceae	2.0 ± 0.04	1.4 ± 0.1	1.4 ± 0.1	0.91	0.43
Proteobacteria	Gammaproteobacteria	Shewanellaceae	0.8 ± 0.04	5.7 ± 0.4	7.5 ± 0.7	0.005*	0.047
Proteobacteria	Gammaproteobacteria	unclassified (derived from Gammaproteobacteria)	1.1 ± 0.03	0.2 ± 0.1	0.3 ± 0.1	0.54	0.34
Proteobacteria	Gammaproteobacteria	Vibrionaceae	0.8 ± 0.04	5.1 ± 0.8	4.2 ± 0.4	0.09	0.16

Table 1. The average relative abundance (RA) (± standard deviation; SD) of Family level clades for bacterial communities sampled at the start of the experiment (T_0), and during stationary growth phase; considering only groups that exhibited > 1 % RA in T_0 samples or the samples collected during stationary growth phase. Statistical analysis was conducted using ANOVA and represents differences in the arc-sine transformed RA of bacterial groups collected during stationary growth phase, as a function of pCO_2 treatment. Asterisks indicate significant p values (< 0.05).

Table 2

Metabolic Functional Categories	Time Point	pCO_2
	T_0 Compared to SGP (p values)	Low pCO_2 Compared to Elevated pCO_2 During SGP (p values)
Amino Acids & Derivatives	0.38	0.27
Carbohydrates	<0.01*	0.02*
Cell Division & Cell Cycle	<0.01*	0.27
Cell Wall & Capsule	<0.01*	0.25
Clustering-Based Subsystems	<0.01*	0.25
Cofactors, Vitamins, & Pigments	0.93	0.18
DNA Metabolism	<0.01*	0.06
Dormancy & Sporulation	<0.01*	0.05
Fatty Acids, Lipids, & Isoprenoids	0.68	0.01*
Iron Acquisition & Metabolism	<0.01*	0.08
Membrane Transport	<0.01*	0.01*
Metabolism of Aromatic Compounds	<0.01*	0.92
Miscellaneous	<0.01*	0.04
Motility & Chemotaxis	<0.01*	0.64
Nitrogen Metabolism	0.08	0.60
Nucleosides & Nucleotides	0.45	0.71
Phages, Transposons, & Plasmids	<0.01*	<0.01*
Phosphorus Metabolism	0.01*	0.11
Photosynthesis	<0.01*	0.57
Potassium Metabolism	<0.01*	0.16
Protein Metabolism	0.55	0.51
Regulation & Cell Signaling	<0.01*	<0.01*
Respiration	<0.01*	0.42
RNA Metabolism	<0.01*	0.15
Secondary Metabolism	0.12	0.01*
Stress Response	<0.01*	0.08
Sulfur Metabolism	<0.01*	<0.01*
Virulence, Disease & Defense	<0.01*	<0.01*

Table 2. Significance values reported for the following comparisons: relative abundance of metabolic functions at the start of the experiment, compared to relative abundance of metabolic functions collected during stationary growth phase (column labeled Time Point). Effects of pCO_2 on the relative abundance of metabolic functions obtained during stationary growth phase are recorded in the column on the right (pCO_2). Metabolic functions were grouped by the broadest categories in the SEED database.

References

Allgaier, M., Riebesell, U., Vogt, M., Thyrhaug, R., and Grossart, H.-P. (2008). Coupling of heterotrophic bacteria to phytoplankton bloom development at different pCO2 levels: a mesocosm study. Biogeosciences 5, 1007–1022.

Andersen, J., He, G.-X., Kakarla, P., Kc, R., Kumar, S., Lakra, W., Mukherjee, M., Ranaweera, I., Shrestha, U., Tran, T., et al. (2015). Multidrug Efflux Pumps from Enterobacteriaceae, Vibrio cholerae and Staphylococcus aureus Bacterial Food Pathogens. International Journal of Environmental Research and Public Health 12, 1487–1547.

Arnosti, C., Grossart, H., Mühling, M., Joint, I., and Passow, U. (2011). Dynamics of extracellular enzyme activities in seawater under changed atmospheric pCO2: a mesocosm investigation. Aquatic Microbial Ecology 64, 285–298.

Azam, F., Fenchel, T., Field, J. G., Gray, J. S., Meyerreil, L. A., & Thingstad, F. (1983). The Ecological Role of Water-Column Microbes in the Sea. Marine Ecology Progress Series 10, 257-263. doi:DOI 10.3354/meps010257

Aziz, R.K., Bartels, D., Best, A.A., DeJongh, M., Disz, T., Edwards, R.A., Formsma, K., Gerdes, S., Glass, E.M., Kubal, M., et al. (2008). The RAST Server: Rapid Annotations using Subsystems Technology. BMC Genomics 9, 75.

Bassler, B.L., Yu, C., and Roseman S. (1991). Chitin utilization by marine bacteria. Degradation and catabolism of chitin oligosaccharides by Vibrio furnissii. J of Biological Chemistry 266, 24276-24286.

Blankenhorn, D.J., Phillips, J., and Slonczewski, J.L. (1999). Acid- and base-induced proteins during aerobic and anaerobic growth of Escherichia coli revealed by two-dimensional gel electrophoresis. J Bacteriol 181.

Booth, I.R. (1985). Regulation of cytoplasmic pH in bacteria. Microbial Reviews 49, 359-378.

Brinkkotter, A., Kloss, H., Alpert, C.-A., and Lengeler, J.W. (2000). Pathways for the utilization of N-acetyl-galactosamine and galactosamine in Escherichia coli. Molecular Microbiology 37, 125–135.

Brown, J.L., Ross, T., McMeekin, T.A., and Nichols, P.D. (1997). Acid habituation of Escherichia coli and the potential role of cyclopropane fatty acids in low pH tolerance. International Journal of Food Microbiology 37, 163–173.

Bunse, C., Lundin, D., Karlsson, C.M.G., Vila-Costa, M., Palovaara, J., Akram, N., Svensson, L., Holmfeldt, K., González, J.M., Calvo, E., et al. (2016). Response of marine bacterioplankton pH homeostasis gene expression to elevated CO2. Nature Climate Change.

Burrus, V., and Waldor, M.K. (2004). Shaping bacterial genomes with integrative and conjugative elements. Res. Microbiol. 155, 376–386.

Carlson, C., Giovannoni, S., Hansell, D., Goldberg, S., Parsons, R., Otero, M., Vergin, K., and Wheeler, B. (2002). Effect of nutrient amendments on bacterioplankton production, community structure, and DOC utilization in the northwestern Sargasso Sea. Aquatic Microbial Ecology 30, 19–36.

Chang, Y.-Y., and Cronan, J.E. (1999). Membrane cyclopropane fatty acid content is a major factor in acid resistance of Escherichia coli. Molecular Microbiology 33, 249–259.

Chen, I., Christie, P.J., and Dubnau, D. (2005). The Ins and Outs of DNA Transfer in Bacteria. Science 310, 1452–1456.

Endres, S., Galgani, L., Riebesell, U., Schulz, K.-G., and Engel, A. (2014). Stimulated Bacterial Growth under Elevated pCO2: Results from an Off-Shore Mesocosm Study. PLoS ONE 9, e99228.

Foster, J.W. (2004). Escherichia coli acid resistance: tales of an amateur acidophile. Nature Reviews Microbiology 2, 898–907.

Franke, S., Grass, G., Rensing, C., and Nies, D.H. (2003). Molecular Analysis of the Copper-Transporting Efflux System CusCFBA of Escherichia coli. Journal of Bacteriology 185, 3804–3812.

Frost, L.S., and Koraimann, G. (2010). Regulation of bacterial conjugation: balancing opportunity with adversity. Future Microbiology 5, 1057–1071.

Gehler, J., Cantz, M., O'Brien, J.F., Tolksdorf, M., and Spranger, J. (1975). Mannosidosis: clinical and biochemical findings. Birth Defects Orig. Artic. Ser. 11, 269–272.

del Giorgio, P.A., and Cole, J.J. (1998). BACTERIAL GROWTH EFFICIENCY IN NATURAL AQUATIC SYSTEMS. Annual Review of Ecology and Systematics 29, 503–541.

Green, E.R., and Mecsas, J. (2016). Bacterial Secretion Systems: An Overview. In Virulence Mechanisms of Bacterial Pathogens, Fifth Edition, I.T. Kudva, N.A. Cornick, P.J. Plummer, Q. Zhang, T.L. Nicholson, J.P. Bannantine, and B.H. Bellaire, eds. (American Society of Microbiology), pp. 215–239.

Grossart, H.-P., Allgaier, M., Passow, U., and Riebesell, U. (2006). Testing the effect of CO2 concentration on the dynamics of marine heterotrophic bacterioplankton. Limnol. Oceanogr. 51, 1–11.

Harrison, M.D., Jones, C.E., and Dameron, C.T. (1999). Copper chaperones: function, structure and copper-binding properties. JBIC Journal of Biological Inorganic Chemistry 4, 145–153.

Hayes, E.T., Wilks, J.C., Sanfilippo, P., Yohannes, E., Tate, D.P., Jones, B.D., Radmacher, M.D., BonDurant, S.S., and Slonczewski, J.L. (2006). Oxygen limitation modulates pH regulation of catabolism and hydrogenases, multidrug transporters, and envelope composition in Escherichia coli K-12. BMC Microbiology 6, 89.

Huertas, M., López-Maury, L., Giner-Lamia, J., Sánchez-Riego, A., and Florencio, F. (2014). Metals in Cyanobacteria: Analysis of the Copper, Nickel, Cobalt and Arsenic Homeostasis Mechanisms. Life 4, 865–886.

James, A.K., Passow, U., Brzezinski, M.A., Parsons, R.J., Trapani, J.N., and Carlson, C.A. (2017). Elevated pCO2 enhances bacterioplankton removal of organic carbon. PLOS ONE 12, e0173145.

Jonsson, V., Österlund, T., Nerman, O., and Kristiansson, E. (2016). Statistical evaluation of methods for identification of differentially abundant genes in comparative metagenomics. BMC Genomics 17.

Kelley, W.D., and Rodriguez-Kabana, R. (1976). Competition between Phytophthora cinnamomi and Trichoderma spp. in autoclaved soil. Can. J. Microbiol. 22, 1120–1127.

Kosono, S., Morotomi, S., Kitada, M., and Kudo, T. (1999). Analyses of a Bacillus subtilis homologue of the Na+/H+ antiporter gene which is important for pH homeostasis of alkaliphilic Bacillus sp. C-125. Biochimica et Biophysica Acta (BBA) - Bioenergetics 1409, 171–175.

Krause, E., Wichels, A., Giménez, L., Lunau, M., Schilhabel, M.B., and Gerdts, G. (2012). Small Changes in pH Have Direct Effects on Marine Bacterial Community Composition: A Microcosm Approach. PLoS ONE 7, e47035.

Krause, S., Pansegrau, W., Lurz, R., de la Cruz, F., and Lanka, E. (2000). Enzymology of type IV macromolecule secretion systems: the conjugative transfer regions of plasmids RP4 and R388 and the cag pathogenicity island of Helicobacter pylori encode structurally and functionally related nucleoside triphosphate hydrolases. J. Bacteriol. 182, 2761–2770.

Krulwich, T.A., Sachs, G., and Padan, E. (2011). Molecular aspects of bacterial pH sensing and homeostasis. Nature Reviews Microbiology 9, 330–343.

Letscher, R.T., Knapp, A.N., James, A.K., Carlson, C.A., Santoro, A.E., and Hansell, D.A. (2015). Microbial community composition and nitrogen availability influence DOC remineralization in the South Pacific Gyre. Marine Chemistry 177, 325–334.

Lewinson, O., Padan, E., and Bibi, E. (2004). Alkalitolerance: a biological function for a multidrug transporter in pH homeostasis. Proc Natl Acad Sci USA 101.

Leyn, S.A., Gao, F., Yang, C., and Rodionov, D.A. (2012). N -Acetylgalactosamine Utilization Pathway and Regulon in Proteobacteria: Genomic reconstruction and experimental characterization in Shewanella. Journal of Biological Chemistry 287, 28047–28056.

Maas, E., Law, C., Hall, J., Pickmere, S., Currie, K., Chang, F., Voyles, K., and Caird, D. (2013). Effect of ocean acidification on bacterial abundance, activity and diversity in the Ross Sea, Antarctica. Aquatic Microbial Ecology 70, 1–15.

Maurer, L.M., Yohannes, E., Bondurant, S.S., Radmacher, M., and Slonczewski, J.L. (2005). pH Regulates Genes for Flagellar Motility, Catabolism, and Oxidative Stress in Escherichia coli K-12. Journal of Bacteriology 187, 304–319.

McCarren, J., Becker, J.W., Repeta, D.J., Shi, Y., Young, C.R., Malmstrom, R.R., Chisholm, S.W., and DeLong, E.F. (2010). Microbial community transcriptomes reveal microbes and metabolic pathways associated with dissolved organic matter turnover in the sea. Proceedings of the National Academy of Sciences 107, 16420–16427.

Meyer, F., Paarmann, D., D'Souza, M., Olson, R., Glass, E., Kubal, M., Paczian, T., Rodriguez, A., Stevens, R., Wilke, A., et al. (2008). The metagenomics RAST server – a public resource for the automatic phylogenetic and functional analysis of metagenomes. BMC Bioinformatics 9, 386.

Millero, F., Woosley, R., DiTrolio, B., and Waters, J. (2009). Effect of Ocean Acidification on the Speciation of Metals in Seawater. Oceanography 22, 72–85.

Nelson, C.E., Alldredge, A.L., McCliment, E.A., Amaral-Zettler, L.A., and Carlson, C.A. (2011). Depleted dissolved organic carbon and distinct bacterial communities in the water column of a rapid-flushing coral reef ecosystem. The ISME Journal 5, 1374–1387.

Nelson, C.E., and Carlson, C.A. (2012). Tracking differential incorporation of dissolved organic carbon types among diverse lineages of Sargasso Sea bacterioplankton: DOC incorporation by Sargasso Sea bacterioplankton. Environmental Microbiology 14, 1500–1516.

Nelson, C.E., Carlson, C.A., Ewart, C.S., and Halewood, E.R. (2014). Community differentiation and population enrichment of Sargasso Sea bacterioplankton in the euphotic

zone of a mesoscale mode-water eddy: Bacterioplankton in a Sargasso Sea mode-water eddy. Environmental Microbiology 16, 871–887.

Nelson, C.E., Goldberg, S.J., Wegley Kelly, L., Haas, A.F., Smith, J.E., Rohwer, F., and Carlson, C.A. (2013). Coral and macroalgal exudates vary in neutral sugar composition and differentially enrich reef bacterioplankton lineages. The ISME Journal 7, 962–979.

Newbold, L.K., Oliver, A.E., Booth, T., Tiwari, B., DeSantis, T., Maguire, M., Andersen, G., van der Gast, C.J., and Whiteley, A.S. (2012). The response of marine picoplankton to ocean acidification: Response of picoplankton to ocean acidification. Environmental Microbiology 14, 2293–2307.

Padan, E., Bibi, E., Ito, M., and Krulwich, T.A. (2005). Alkaline pH homeostasis in bacteria: New insights. Biochimica et Biophysica Acta (BBA) - Biomembranes 1717, 67–88.

Passow, U., and Carlson, C. (2012). The biological pump in a high CO<sub>2 world. Marine Ecology Progress Series 470, 249–271.

Piontek, J., Lunau, M., Händel, N., Borchard, C., Wurst, M., and Engel, A. (2010). Acidification increases microbial polysaccharide degradation in the ocean. Biogeosciences 7, 1615–1624.

Piontek, J., Borchard, C., Sperling, M., Schulz, K.G., Riebesell, U., and Engel, A. (2013). Response of bacterioplankton activity in an Arctic fjord system to elevated pCO2: results from a mesocosm perturbation study. Biogeosciences 10, 297–314.

Reinthaler, T., Winter, C., and Herndl, G.J. (2005). Relationship between Bacterioplankton Richness, Respiration, and Production in the Southern North Sea. Applied and Environmental Microbiology 71, 2260–2266.

Rensing, C., and Mitra, B. (2007). Zinc, Cadmium, and Lead Resistance and Homeostasis. In Molecular Microbiology of Heavy Metals, D.H. Nies, and S. Silver, eds. (Berlin, Heidelberg: Springer Berlin Heidelberg), pp. 321–341.

Riemann, L., and Azam, F. (2002). Widespread N-Acetyl-D-Glucosamine Uptake among Pelagic Marine Bacteria and Its Ecological Implications. Applied and Environmental Microbiology 68, 5554–5562.

Robinson, M.D., McCarthy, D.J., and Smyth, G.K. (2010). edgeR: a Bioconductor package for differential expression analysis of digital gene expression data. Bioinformatics 26, 139–140.

Roy, A.-S., Gibbons, S.M., Schunck, H., Owens, S., Caporaso, J.G., Sperling, M., Nissimov, J.I., Romac, S., Bittner, L., Mühling, M., et al. (2013). Ocean acidification shows negligible impacts on high-latitude bacterial community structure in coastal pelagic mesocosms. Biogeosciences 10, 555–566.

Sarmento, H., and Gasol, J.M. (2012). Use of phytoplankton-derived dissolved organic carbon by different types of bacterioplankton: Use of phytoplankton-derived DOC by bacterioplankton. Environmental Microbiology 14, 2348–2360.

Schmoldt, A., Benthe, H.F., and Haberland, G. (1975). Digitoxin metabolism by rat liver microsomes. Biochem. Pharmacol. 24, 1639–1641.

Siu, N., Apple, J.K., and Moyer, C.L. (2014). The Effects of Ocean Acidity and Elevated Temperature on Bacterioplankton Community Structure and Metabolism. Open Journal of Ecology 04, 434–455.

Slonczewski, J.L., and Foster, J.W. (1996). pH-regulated genes and survival at extreme pH. In Escherichia Coli and Salmonella: Cellular and Molecular Biology, Neidhardt, C. F, III,

J.L. Ingraham, E.C.C. Lin, K.B. Low, B. Magasanik, W.S. Reznikoff, M. Riley, M. Schaechter, et al., eds. (Washington, DC: ASM Press), p.

Slonczewski, J.L., Fujisawa, M., Dopson, M., and Krulwich, T.A. (2009). Cytoplasmic pH Measurement and Homeostasis in Bacteria and Archaea. In Advances in Microbial Physiology, (Elsevier), pp. 1–317.

Sperling, M., Piontek, J., Gerdts, G., Wichels, A., Schunck, H., Roy, A.-S., La Roche, J., Gilbert, J., Nissimov, J.I., Bittner, L., et al. (2013). Effect of elevated CO2 on the dynamics of particle-attached and free-living bacterioplankton communities in an Arctic fjord. Biogeosciences 10, 181–191.

Stancik, L.M., Stancik, D.M., Schmidt, B., Barnhart, D.M., Yoncheva, Y.N., and Slonczewski, J.L. (2002). pH-Dependent Expression of Periplasmic Proteins and Amino Acid Catabolism in Escherichia coli. Journal of Bacteriology 184, 4246–4258.

Wear, E.K., Carlson, C.A., James, A.K., Brzezinski, M.A., Windecker, L.A., and Nelson, C.E. (2015). Synchronous shifts in dissolved organic carbon bioavailability and bacterial community responses over the course of an upwelling-driven phytoplankton bloom: Bloom-induced shifts in DOC availability. Limnology and Oceanography 60, 657–677.

Wiesmann, U.N., DiDonato, S., and Herschkowitz, N.N. (1975). Effect of chloroquine on cultured fibroblasts: release of lysosomal hydrolases and inhibition of their uptake. Biochem. Biophys. Res. Commun. 66, 1338–1343.=

Yamada, N., and Suzumura, M. (2010). Effects of seawater acidification on hydrolytic enzyme activities. Journal of Oceanography 66, 233–241.

Yohannes, E., Barnhart, D.M., and Slonczewski, J.L. (2004). pH-Dependent Catabolic Protein Expression during Anaerobic Growth of Escherichia coli K-12. Journal of Bacteriology 186, 192–199.

Zeebe, R.E., and Wolf-Gladrow, D.A. (2001). CO_2 in seawater: equilibrium, kinetics, isotopes (Amsterdam ; New York: Elsevier).

Zhang, Y.-M., and Rock, C.O. (2008). Membrane lipid homeostasis in bacteria. Nature Reviews Microbiology 6, 222–233.

Zhang, R., Xia, X., Lau, S.C.K., Motegi, C., Weinbauer, M.G., and Jiao, N. (2013). Response of bacterioplankton community structure to an artificial gradient of pCO2 in the Arctic Ocean. Biogeosciences 10, 3679–3689.

IV. CHAPTER III

Physical Processes and Biogeochemical Patterns Near Moorea, French Polynesia

Anna K James[1], Craig A Carlson[1], Chris Gotschalk[1], and Libe Washburn[1]

[1] Marine Science Institute, Department of Ecology, Evolution, and Marine Biology, University of California, Santa Barbara, CA, United States of America

Abstract

Oceanographic variables were sampled during a 3-week research cruise from July 19 to August 8, 2014 in French Polynesia as part of the Moorea Coral Reef Long Term Ecological Research effort to map key biogeochemical constituents in the waters around the islands of Moorea and Tahiti. High-resolution sampling in a rectangular grid around the islands revealed vertical patterns in hydrographic conditions, inorganic nutrients, rates of productivity, and concentrations of organic matter that are characteristic of oligotrophic gyre ecosystems. Levels of net primary productivity (NPP), chlorophyll a (Chl), bacterioplankton productivity (BP), and particulate organic carbon (POC) exhibited concurrent enhancement at stations located near Moorea, and between Tahiti and Moorea, within the upper euphotic zone (0 – 75 m). Shipboard current profiling revealed a counterclockwise flow around Moorea within the upper 75 m of the water column, suggesting that retention of inorganic nutrients and organic matter near Moorea may have contributed to the patterns in PP, Chl, BP, and POC. This observation may also represent a wake effect from islands with implications for the transport and retention of key biochemical constituents near Moorea and Tahiti. In addition to patchiness in the surface layer, significant variability in the

concentrations of particulate and dissolved organic carbon (DOC) was observed beneath the thermocline (100 – 300 m), with a number of stations exhibiting elevated concentrations of DOC and POC throughout the mesopelagic between 100 – 300 m depths. These elevated concentrations extended through isopycnal surfaces and thus likely occurred in the absence of deep mixing events.

Introduction

The reefs around Moorea, French Polynesia, rely on the transport and retention of key biogeochemical constituents to support the high biomass and productivity present on the reef (Odum and Odum 1955, Johannes et al. 1972, Leichter et al. 2013). Located in the westward flowing South Equatorial Current, Moorea is surrounded by nutrient-depleted waters that form the northern portion of the South Pacific Subtropical Gyre (Rougerie and Rancher, 1994). Highly stratified, the South Pacific Subtropical Gyre contains some of the least biologically productive waters in the ocean (Longhurst et al. 1995). However, the waters near Moorea are distinct from offshore waters (Nelson et al. 2011, Leichter et al. 2013), indicating a potential of islands to alter water in their vicinity on timescales of water residence times. As such, retention of nutrients and organic material that are ephemerally transported to the island through physical processes, as well as accumulation of material that is locally produced, is critical to support coral reef communities (Odum and Odum 1955, Johannes et al. 1972, Leichter et al. 2013).

One mechanism by which Moorea may retain material that was locally produced and/or transported to the island is through the presence of island wake effects (Rissik et al 1997).

Numerous studies of island wake effects provide evidence to suggest that wind and current-induced island wakes are capable of significantly altering the biogeochemical characteristics of otherwise stable environments (e.g. Takahashi et al., 1981, Hamner and Hauri 1981, Hernandez-Leon 1991, Barton et al., 2000, Xie et al. 2001, Martinez and Maamaatuaiahutapu 2004, Hasegawa et al. 2004, Dong et al. 2005, Caldeira et al. 2005). Current wakes are formed through the deflection of incoming ocean currents by island bathymetry, which may form eddies and induce upwelling of cool deep water associated with higher productivity. These wakes were also shown to influence particle accumulation through partial trapping of water near islands (Rissik et al. 1997). Thus, an island wake effect induced by movement of the South Equatorial Current around Tahiti and Moorea may have implications for the retention and accumulation of organic material near the islands.

Evidence of distinct current patterns along Moorea's 15 m isobath, in contrast to the westward flowing South Equatorial Current, were identified by Leichter et al. (2013) through observations of the presence of a persistent counterclockwise flow around the island. Leichter et al. (2013) posit that the movement of the South Equatorial Current around Tahiti influences the production of the counterclockwise flow around Moorea, indicating a wake effect between islands. Our observations provide further evidence of a counterclockwise flow around Moorea, and measurements of key biogeochemical constituents between Moorea and Tahiti support the presence of a wake effect between islands.

Methods

Site Description

Oceanographic variables were sampled during a 3-week research cruise from July 19 – August 8, 2014 aboard the *R/V Kilo Moana* in the waters surrounding the island of Moorea, French Polynesia, in the South Pacific Subtropical Gyre (17° 36'S, 149° 43'W). Over 1.5 million years old, Moorea is part of a volcanic chain formed by the northwestward movement of the Pacific Plate over a fixed hotspot (Neall and Trewick 2008). The island is surrounded by a barrier reef which crests within 0.5 - 1 km of shore. Bordering the island is a fringing reef (~10 – 12 m deep) that is separated from the barrier reef crest by shallow lagoons (< 3 m). The lagoons are connected to the open ocean by reef pass channels that are present around the island, and occur approximately every 5 – 10 km. The offshore reef slopes steeply to > 500 m within 1 – 2 km of the reef.

Local flow-dynamics near Moorea are dominated by the South Equatorial Current, which flows west and constitutes the northern portion of the counterclockwise flowing South Pacific Subtropical Gyre (Rougerie and Rancher 1994, Leicther et al. 2013). Net alongshore surface flow to the west on the north shore, to the southeast on the southwest shore, and to the northeast on the southeast shore, is characterized as a low-frequency counterclockwise flow around the island (Leichter et al. 2013). Water residence times are estimated on the order of hours to days on Moorea's reefs (Delasalle and Sournia 1992, Hench et al. 2008).

Sampling Scheme

High resolution hydrographic and biogeochemical sampling was conducted in a rectangular grid around the island of Moorea that extended from -17.36˚S to -17.82˚S, and -150.12˚W to -149.58˚W (Fig 1). To characterize the water column, vertical profiles of water samples to measure biogeochemical variables including inorganic nutrients (nitrogen and phosphorous), net primary production (NPP), chlorophyll a (Chl), bacterial productivity (BP), bacterial abundance (BA), dissolved organic carbon (DOC), and particulate organic carbon (POC) were collected via Niskin bottles attached to a SBRE 9 conductivity, temperature, depth (CTD) rosette. CTD profiles were conducted at every station to systematically determine the hydrographic and biogeochemical properties of the water column. Samples were collected from ten depths between 0 – 500 m (nominally 10, 25, 50, 75, 100, 150, 200, 250, 300, and 500 m), with the 100 m sample shifted to correspond to the deep chlorophyll fluorescence maximum. Water samples were processed as described below. In addition to the suite of standard CTD variables, oxygen, photosynthetically available radiation (PAR), beam transmission, and chlorophyll a fluorescence profiles were also measured. Two shipboard Acoustic Doppler Current Profilers (ADCP) sampled continuously during the cruise. A WH300 sampled near surface waters from 11 to 75 m and an OS38BB sampled between the depths of 36 and 1400 m. CDT data were calibrated and output for further analysis using the SeaBird data processing software.

Sample Processing

Inorganic nutrients – Seawater for inorganic nutrient analysis was filtered through 0.6 μm polycarbonate filters (Nuclepore, Whatman), stored frozen, and analyzed using flow injection analysis on a QuickChem 8000 (Lachat Instruments, Loveland, CO) by the

University of California, Santa Barbara Marine Science Institute Analytical Laboratory (detection limits: $NO_2^- + NO_3^-$, 0.2 μmol L^{-1}; PO_4^{3-}, 0.1 μmol L^{-1}).

Net Primary productivity measurements – Seawater was collected from six depths between 10 – 150 m (nominally, 10, 25, 50, 75, and 150) into 500 mL acid-washed polycarbonate bottles in triplicate, spiked with $NaH^{14}CO_3$, and incubated on-depth over the full daylight period according to Letellier et al. 1996. At the end of the incubation, ^{14}C assimilation was quantified by filtering seawater onto 25 mm Whatman GF/F filters placed into scintillation vials. These were acidified with 1 mL of 2 M HCL and allowed to sit for 24 h to remove inorganic ^{14}C. 10 mL of scintillation cocktail (UltimaGold LLT, PerkinElmer) was then added to each vial and the radioactivity was counted on a Packard TriCarb Liquid Scintillation Counter.

Chlorophyll measurements – Chlorophyll *a* (Chl) was collected on 0.45 μm mixed cellulose ester filters (HAWP, Millipore), extracted in acetone, and quantified by fluorescence with acidification as in Anderson et al. (2006).

Bacterioplankton productivity measurements – Samples for bacterioplankton production were analyzed via ^3H-leucine incorporation (14 –19 nmol L^{-1} H-leucine; specific activity 54.1 Ci/mmol; PerkinElmer, Boston, MA), using a modified microcentrifuge method (Halewood et al. 2012, Wear et al. 2015). All samples were processed at sea. Radioactivity was analyzed by a Packard TriCarb Liquid Scintillation Counter and corrected with external standard and quench curve. Leucine incorporation was converted to bacterial carbon

production by applying a carbon conversion factor of 1.5 kg C mol Leu^{-1} (Simon and Azam 1989).

Bacterioplankton abundance measurement – Samples for bacterioplankton abundance were analyzed by Flow Cytometry (FCM) on BD Bioscience LSR II with SYBR Green I according to sample preparation and instrument settings described in Nelson et al. (2011). FCM analysis enumerates total prokaryotic abundance thus we were not able to differentiate between bacterial and archaeal domains and refer to the combined cell densities as bacterioplankton abundance (Glockner et al. 1999).

DOC measurements – DOC samples were filtered through combusted glass fiber filters (GF/F) placed in polycarbonate cartridges and attached directly to the Niskin bottle via silicone tubing. Samples were collected into 60 mL high-density polyethylene bottles and frozen at -20 °C until analysis on shore at UC Santa Barbara. Samples were analyzed via high temperature combustion method on a modified Shimadzu TOC-V or Shimadzu TOC-L using the standardization and referencing approaches described in Carlson et al. (2010).

POC measurements – Positive pressure displacement was used to concentrate POC from 4 L of seawater onto pre-combusted glass fiber filters (25 mm; GF/F filter) placed in high density polyethylene filter holders. Sample bottles were pressurized at low pressure (~ 10 PSI). Immediately following filtration, filters were placed into pre-combusted glass scintillation vials and stored at -20 ˚C until prepped for analysis at UC Santa Barbara. To prepare samples for analysis, glass vials containing filters were removed from -20 ˚C storage

and placed in an acid fumer (deep covered Pyrex dish containing a 25 mL beaker of concentrated hydrochloric acid in center) and allowed to sit overnight. The following day, vials were loosely capped and placed in a 65 ˚C drying oven for 48 hours. When dry, the vials were removed from the oven, capped tightly, and submitted to the Marine Science Institute analytics laboratory for analysis. POC was quantified by combustion elemental analysis on a CE440 Elemental Analyzer (Exeter Analytical Inc., North Chelmsford, MA).

Current measurements

Horizontal current components u and v (u positive northward, v positive eastward) were measured using two shipboard ADCPs, one operating at 300 kHz and the other at 38 kHz. Data from the 300 kHz ADCP were averaged vertically over 2 m depth bins and the shallowest bin that was consistently measured was 11 m. Low concentrations of scattering particles limited the range of this ADCP to about 75 m depth. Velocity components from the 38 kHz ADCP were averaged over 12 m depth bins and current data extended from 37 m to about 1100 m.

To better visualize current patterns and to facilitate flow calculations, ADCP data were interpolated on to a regular grid with a spacing of 4 km using optimal interpolation (e.g. Thompson and Emery, 2014). In the optimal interpolation procedure, a spatial autocorrelation function was calculated from the data and fitted to a Gaussian curve with a standard deviation of 15 km.

Geostrophic currents were calculated from the interpolated CTD and ADCP data using the method described by Rudnick (1996). A stream function was determined over the interval 17-500 m (assuming 1 dbar corresponds to 1 m depth) to estimate a barotropic velocity field. To this was added a depth varying velocity component consistent with the thermal wind equation.

CTD measurements

CTD data were processed using standard SeaBird software. Data were averaged into 1-m depth bins to form water property profiles that extended from the surface to about 500 m at all stations. Data were optimally interpolated onto the same grid as the ADCP data. Dynamic height was computed at various levels with respect to a reference level of 500 dbar. Mixed layer depth was calculated as the depth where density increased by 0.02 kg m^{-3} from the near-surface value.

Data and Statistical Analyses

Statistical analysis of the difference in biogeochemical rates and concentrations as a function of station location were evaluated using a randomized 1-way analysis of variance (ANOVA) with 999 iterations (Sheffé 1959). Post-hoc Tukey Honest Significance Differences (Tukey HSD) tests were conducted to assess variance among groups. All statistical analyses were conducted in JMP, Version *Pro 13* (SAS Institute Inc., Cary, NC, 1989 – 2007). Graphical presentations were created using Ocean Data View 4.7.10 (Schlitzer R, Ocean Data View, odv.awi,de, 2017).

Results and Discussion

Vertical Variability

Vertical variability in hydrographic conditions and biogeochemical variables were evaluated by comparing direct measurements of temperature and salinity, as well as rates of productivity and concentrations of inorganic nutrients and organic matter, across the upper 300 m of the water column. Vertical patterns were evaluated within distinct depth layers including the *upper euphotic* zone (0 – 75 m), the *lower euphotic* zone which contained the deep chlorophyll maximum (75 – 150 m) and the *upper mesopelagic* (150 – 300 m). In addition, to assess vertical variability across all stations sampled during the cruise, we present vertical contour plots with station number (#) on the X-axis. Station number corresponds to Figure 1 and viewing the data in this manner enabled us to evaluate vertical variability in the context of station proximity to Moorea (see station location above contour plots).

Hydrographic conditions

High-resolution sampling near the islands of Moorea and Tahiti during austral winter 2014 revealed expected characteristics of hydrographic conditions in the upper 300 m of the water column of Pacific subtropical gyre ecosystems (Karl and Church 2014, Wilson et al. 2015, Karl and Church 2017; Fig 2A & B). Relatively warm surface temperatures (mean, 26.8 ± 0.2 ˚C, range: 25.9 – 27.2 ˚C) and low salinity (mean: 35.7 ± 0.1 PSU, range: 35.6 – 36.1 PSU) resulted in a low-density layer of water that extended from the surface to approximately 75 m that isolated the upper euphotic zone from the remainder of the water column throughout the sampling period (Fig 2A & B). In the lower euphotic zone, between

the depths of 75 – 150 m (approximately 0.1 % light level), mean temperatures decreased to 25.1 ± 1 ˚C and mean salinity increased to a maximum of 36.0 ± 0.2 PSU, leading to maximum density stratification between approximately 75 – 150 m. These observations of stratification are similar to those previously observed within 1 km of Moorea during the austral winter (Leicther et al. 2012).

The mixed layer depth (MLD) was determined to be the depth where potential density anomaly exceeded the surface value by 0.02 kg m^{-3}. Mean MLD was 53.8 ± 24 m but was highly variable across stations, spanning 93.9 m and ranging from 5.0 – 98.9 m (Fig 2A & B). The MLD was consistently shallower than the upper portion of the nutricline (approximately 100 – 150 m; Fig 3A & B), and the depth of the deep chlorophyll maximum (DCM; Fig 4B). In contrast, the MLD was consistently deeper than the depth of maximum rates of net primary productivity (NPP; Fig 4A). These observations indicate that the MLD vertically separated maximum rates of NPP from the upper portion of the nutricline, as well from the DCM, throughout the sampling period (see below for further discussion of these observations).

Inorganic nutrients

Inorganic nutrients exhibited typical patterns for Pacific subtropical gyre environments (Church et al. 2013, Karl and Church 2014), with consistently low concentrations in the upper water column that increased with depth (Fig 3A & B). Concentrations of inorganic nitrogen (DIN; $NO_2^- + NO_3^-$) and inorganic phosphorous (DIP; PO_4^{3-}) were consistently low or below limits of detection in the upper euphotic zone and increased in the lower euphotic

zone and mesopelagic, indicating that the nutricline was persistently deeper than MLD (Fig 3A & B). This observed separation between the upper portion of the nutricline and the MLD is consistent with previous studies within 1 km of Moorea during the austral winter (Leichter et al. 2012) and indicates that vertical mixing at the time of sampling was not sufficiently deep enough to entrain nutrients from depth into the upper euphotic zone.

Dissolved oxygen

Concentrations of dissolved oxygen (O_2) were highest, and supersaturated within much of the upper and lower euphotic zones (Fig 3C). Concentrations decreased in the upper mesopelagic and ranged from 164.1 – 191.7 μmol L^{-1} (Fig 3C). Interestingly, there was substantial variability in O_2 concentrations within the upper mesopelagic during our sampling period. Some of the variability was consistent with isopycnal displacement both to deeper or shallower depths (e.g. potential density anomaly 25 km m^{-3}); however, some stations exhibited elevated concentrations of O_2 that crossed isopycnal layers in the upper mesopelagic (e.g. station # 16 – 18, 20 – 24). Integrated (150 – 300 m) and depth-normalized concentrations of O_2 in the upper mesopelagic were strongly correlated with integrated and depth-normalized concentrations of inorganic nitrogen (p value < 0.0001, R^2 adjusted 0.5, ANOVA) and DOC (p value < 0.0001, R^2 adjusted 0.4, ANOVA), and to a much lesser degree, concentrations of POC (p value < 0.006, R^2 adjusted 0.2, ANOVA). Concentrations of O_2 were also correlated to integrated and depth-normalized measurements of temperature (p value 0.0001, R^2 adjusted 0.3, ANOVA). Collectively, these observations suggest that a relatively warm water mass, with low concentrations of inorganic nutrients and high concentrations of O_2 and organic carbon, was present within the upper mesopelagic

during our study period. These are characteristics of surface water and may be indicative of horizontal advection of a physically and biogeochemically distinct water mass to our study site after it was mixed or subducted to depth at some distant location. Alternatively, previous vertical subduction of water from the lower euphotic zone into the upper mesopelagic may have contributed to the introduction of low-nutrient, high O_2, and warm water into the upper mesopelagic. Interestingly, this "surface-like" water mass was more frequently present at stations near Moorea and between islands, compared with stations west of Moorea (see station location above contour plots in Fig 3C, Fig 4E & F), and may have resulted from altered physical flow-dynamics near the islands; however, the lack of temporal resolution precludes us from evaluating these potential mechanisms.

Net primary productivity and chlorophyll a

Rates of net primary productivity (NPP) were highest and most variable in the upper 25 m of the water column, ranging from 0.2 – 1.5 μmol C L^{-1} d^{-1} with a mean value of 0.5 ± 0.3 μmol C L^{-1} d^{-1} (Fig 4A). The depth of maximum NPP was consistently shallower than the depth of the upper portion of the nutricline (Fig 3A & B), and was approximately 65 – 90 m shallower than the DCM (compare Fig 4A & B). This observation is consistent with oligotrophic gyre ecosystems in the North Pacific and North Atlantic Subtropical Gyres, where the DCM is generally deeper in the water column than maximum rates of NPP due to photoadaptation of phytoplankton cells over depth (Steinberg et al. 2001, Karl and Church 2014, Cullen 2015).

Rates of NPP decreased by an order of magnitude in the lower euphotic zone and were below limits of detection by approximately 120 m for all stations (Fig 4A). In the upper euphotic zone, 17 out of 38 (44 %) stations demonstrated above mean rates of NPP, and the majority of these stations were located near Moorea and between islands, with fewer stations exhibiting elevated rates of NPP at stations west of Moorea (see station location above contour plot; Fig 4A). 64 % of the stations demonstrating above mean rates of NPP were coincident with MLDs shallower than 54 m (Fig 4A). Statistical analysis revealed a negative correlation between integrated and depth-normalized rates of NPP and MLDs, in the upper euphotic zone (p value < 0.0001, R^2 0.36, ANOVA). This observation indicates that there was continuous vertical separation between the depth of mixing and the upper portion of the nutricline during the sampling period (Fig 3A & B), suggesting that processes other than vertical entrainment of nutrients from depth into the upper euphotic zone enhanced NPP near Moorea and Tahiti. An alternative mechanism may have included lateral transport of nutrients. The introduction of inorganic nutrients to the surface ocean near Moorea and Tahiti via processes such as runoff, or atmospheric deposition, and the subsequent transport of these nutrients to offshore stations, may have enhanced the role of lateral transport in stimulating rates of NPP in the upper water column near these islands. This would also explain greater enhancement of NPP at stations near Moorea and between islands, compared with stations west of Moorea; however, further studies are required to elucidate this compelling observation.

Mean concentrations of Chl were approximately 35 % lower in the upper euphotic zone (0.11 ± 0.06 µg Chl L^{-1}), compared with the lower euphotic zone (0.18 ± 0.09 µg Chl L^{-1};

Fig. 4B). The DCM was consistently present in the lower euphotic zone between the 23.5 – 24.5 kg m^{-3} potential density isoclines, and was bound by sampling depths of approximately 75 – 150 m (Fig 4B). The depth of maximum concentrations of Chl varied by station, ranging from 73.5 – 149.4 m, with a mean depth of 107.4 ± 17.5 m. Two of the stations exhibiting relatively shallow depths (< 75 m) of maximum Chl concentrations were characterized by above-mean concentrations of Chl throughout the upper 75 m of the water column (stations # 16 & 33; Fig 4B). Three other stations also demonstrated above-mean concentrations of Chl throughout the upper 75 m of the water column (stations # 21, 36, & 40); though, the depth of maximum concentrations of Chl at these stations was closer to 110 m. All five of these stations exhibited MLDs that were substantially shallower (< 52 m; Fig 4B) than the depth of maximum Chl concentration, and the upper portion of the DCM, indicating that vertical mixing at the time of sampling was not sufficiently deep enough to entrain high concentrations of Chl from the DCM into the upper euphotic zone. Rather than mixing elevated concentrations of Chl from the DCM into the upper euphotic zone, local NPP may have contributed to the production and accumulation of Chl in the upper 75 m of the water column. Though the source of nutrients to support the elevated NPP are unknown, all five of the stations exhibiting elevated concentrations of Chl throughout the upper 75 m of the water column are present at stations near Moorea and between islands, indicating that, similar to NPP, lateral transport of nutrients introduced to the surface ocean near Moorea and Tahiti may have enhanced NPP, and thus Chl, at these stations.

Bacterioplankton dynamics

Rates of bacterioplankton production (BP) and concentrations of bacterioplankton abundance (BA) decreased over the upper 300 m of the water column and ranged from 0 – 0.1 μmol C L^{-1} d^{-1}, and 0.6 – 8.5 x10^5 cells mL^{-1}, respectively. To evaluate the contribution of bacterioplankton biomass to carbon dynamics, we converted BA to bacterioplankton carbon (BC) using a carbon conversion factor of 10 fg C $cell^{-1}$ to reflect small cells in oligotrophic regions (Gundersen et al. 2002; Fukuda et al. 1998, Caron et al. 1995). Concentrations of BC, and rates of BP, were elevated in the upper and lower euphotic zones and substantially decreased in the mesopelagic (Fig 5C & D). Though weak, rates of BP were significantly correlated to rates of NPP in the upper 25 m (p value < 0.0001, R^2 adjusted 0.24, ANOVA), and may indicate a rapid response of bacterioplankton to freshly produced organic matter from enhanced rates of NPP. However, this observation may also be indicative of a contemporaneous response by bacterioplankton and phytoplankton to a direct input of inorganic nutrients (Cotner et al. 1997, Rivkin and Anderson 1997).

Rates of BP were substantially reduced and demonstrated low variability in the upper mesopelagic (Fig 4D). In contrast, concentrations of BC were variable and exhibited elevated concentrations that extended throughout the upper mesopelagic at stations west of Moorea (# 7 – 10), near Moorea (# 16 – 19), and between islands (# 30, 31, and 34 – 36), among others (e.g. 23 – 26, 29; Fig 4C). These elevated concentrations of BC in the upper mesopelagic may have been indicative of recent vertical export of organic material and subsequent utilization of this material by extant bacterioplankton communities (Doval and Hansell 2000, Hansell and Carlson 2001, Carlson et al. 2004, Carlson et al. 2010, Letscher et al. 2013, Letscher et al. 2015). Statistical comparisons of concentrations of DOC versus BC

(p value < 0.0001, R^2 adjusted 0.4, ANOVA) indicated that for at least some of the stations, elevated concentrations of BC were coincident with elevated concentrations of dissolved organic matter; however, further observations of the temporal development of BC in response to dissolved organic matter production with the upper mesopelagic are required to understand the processes leading to enhanced BC within the mesopelagic.

Organic carbon

Concentrations of particulate and dissolved organic carbon were highest in the upper and lower euphotic zones and decreased in the mesopelagic (Fig 4E & F). Concentrations of POC in the upper euphotic zone were low (< 3 μmol C L^{-1}), and similar in amount to those observed in the oligotrophic waters of the North Pacific (Karl and Church 2014, Wilson et al. 2015) and North Atlantic Subtropical Gyres (Lomas et al. 2013). In contrast, concentrations of DOC in the upper euphotic zone were elevated, ranging from 62.2 – 76.3 μmol C L^{-1}, and reflected the accumulation of DOC within surface waters of subtropical gyres (Hansell et al. 2009). Concentrations of both POC and DOC decreased in the lower euphotic zone and upper mesopelagic.

Despite lower concentrations of POC and DOC in the upper mesopelagic, several stations exhibited elevated concentrations of POC (e.g. stations # 22, 34, 36, 38, and 39; Fig 4E) and DOC (e.g. # 16, 17, 19, 20, 21 – 23, 30, 34, 36, 39, and 40; Fig 4F), similar to those observed for concentrations of BC (Fig 4C). In contrast to concentrations of BC, elevated concentrations of POC and DOC were more abundant at stations near Moorea and between islands, compared with stations west of Moorea (see station location along the top of contour

plots). These elevated concentrations of POC and DOC extended through isopycnal surfaces and thus likely occurred in the absence of deep mixing. Statistical analysis revealed a strong correlation between concentrations of POC and DOC in the upper mesopelagic (p value <0.0001, R^2 adjusted 0.68, ANOVA), indicating coincident enhancement of particulate and dissolved organic carbon within this depth layer. Though we lack measurements of the amount of POC exported from the upper and lower euphotic zone, as well as sinking rates into the upper mesopelagic, solubilization of POC to DOC (Smith et al. 1992) may have partially contributed to contemporaneous enhancement of organic carbon in the upper mesopelagic. Solubilization can occur in the absence of mixing and may help to explain elevated concentrations of organic matter in the mesopelagic in the absence of deep mixing; however, further estimates of the POC flux rate, solubilization rates, and persistence of DOC produced by solubilization are required to elucidate dynamics of organic carbon solubilization in the upper mesopelagic near Moorea. Lateral advection of warm, high O_2, high organic carbon may also have contributed to anomalously elevated concentrations of POC and DOC in the upper mesopelagic (see discussion of *dissolved oxygen*, above).

Contribution of DOC removal to AOU in the mesopelagic

Estimates of apparent oxygen utilization (AOU) in the upper mesopelagic reflect remineralization of organic carbon and the removal of O_2 by respiration (Doval and Hansell 2000, Carlson et al. 2010). AOU was converted to carbon equivalents (AOU-C_{eq}) using a molar ratio of -ΔC: ΔO_2 of 0.72 (Anderson 1995) in order to directly assess the contribution of DOC to changes in AOU-C_{eq} (Doval and Hansell 2000, Carlson et al. 2010). Using the slope of the Model II regression of DOC concentration versus AOU-C_{eq}, we estimated that

DOC remineralization accounted for approximately 35 % of AOU-C_{eq} within the upper mesopelagic. This observation is consistent with previous reports of the contribution of DOC oxidation to AOU-C_{eq} in the upper mesopelagic of subtropical gyre ecosystems (Abell et al. 2000, Doval and Hansell 2000, Santinelli et al. 2010, Pan et al. 2014). The remaining AOU signal is likely due to remineralization of sinking particle flux over an unknown period of time.

Overall, high-resolution sampling in the upper 300 m of the waters surrounding the islands of Moorea and Tahiti revealed vertical variability in hydrographic conditions, rates of productivity, and concentrations of inorganic nutrients and organic matter (Fig 2 - 4). The production of low-density surface water effectively isolated the upper euphotic zone from the remainder of the water column throughout our sampling period (Fig 2A). Concentrations of Chl (Fig 4B) and inorganic nutrients (Fig 3A & B) were low in this surface layer, while rates of NPP, likely driven by the availability of excess solar radiation, were elevated (Fig 4A). However, continuous isolation of the euphotic zone from the upper portion of the nutricline, suggests that vertical mixing was not sufficiently deep enough to entrain nutrients from depth to support elevated NPP in this sun-lit zone. Thus, an alternative mode of nutrient transport must have supported elevated NPP at stations near Moorea and between islands, and may have included lateral transport of nutrients from near the islands to offshore via physical flow dynamics.

In contrast to surface waters, the upper mesopelagic was characterized by higher concentrations of inorganic nutrients (Fig 3A & B), but limited solar energy likely led to

reduced rates of NPP (Fig 4A), low concentrations of Chl (Fig 4B), and low biomass of bacterioplankton (Fig 4C). Particulate and dissolved organic carbon concentrations also decreased with depth (Fig 4E & F). Overall, our observations of hydrographic conditions and concentrations of inorganic nutrients and organic carbon, as well as rates of productivity, provide insight to vertical variability in key physical and biogeochemical constituents near the islands of Moorea and Tahiti.

Horizontal variability in the upper euphotic zone (0 – 75 m)

In addition to vertical variability, we observed horizontal gradients in biogeochemical variables within the upper euphotic zone (0 – 75 m). To evaluate horizontal gradients, we present integrated and depth-normalized rates of productivity, and concentrations of inorganic nutrients and organic matter, in the upper euphotic zone. Reference to mean concentrations and rates in this section refer to integrated and depth-normalized values. In addition, to assess evidence for the presence of a wake effect between islands, mean concentrations and rates were grouped by relative proximity to Moorea as described in Figure 1 and included stations west of Moorea (# 1 – 12), near Moorea (# 16 – 22), and between islands (# 30 – 38; Fig 1). The number of stations within each location differed, with 12 stations west of Moorea, 8 stations near Moorea, and 9 stations between islands; these stations totaled 29 of the 40 stations sampled. Statistical analyses were performed to evaluate differences in concentrations and rates as a function of station proximity to Moorea.

In the upper euphotic zone, grouping stations by proximity to Moorea (Fig 1) revealed coincident horizontal variability in DIP, NPP, Chl, BP, and POC (0 – 75 m; Fig 5B, Fig 6A

– C, and E; Table 1). Stations near Moorea and between islands exhibited significantly elevated concentrations of Chl and POC (p value ≤ 0.01, ANOVA), as well as higher mean rates of NPP and BP, compared with stations west of Moorea (Fig 6; Table 1). Only concentrations of DIP varied significantly between stations near Moorea and between islands (Fig 5B; Table 1); however, measurements of DIP were low or below limits of detection in the upper euphotic zone and likely reflected analytical variability in sample analysis rather than actual differences between stations. These observations in the upper euphotic zone indicated that key biogeochemical constituents were more similar between stations near Moorea and between islands, compared with stations west of Moorea, during our sampling period. Greater similarity between stations near the islands, compared with west of Moorea, may be indicative of a wake effect that resulted in distinct biogeochemical characteristics near the islands (Takahashi et al., 1981, Hamner and Hauri 1981, Hernandez-Leon 1991, Barton et al., 2000, Xie et al. 2001, Martinez and Maamaatuaiahutapu 2004, Hasegawa et al. 2004, Dong et al. 2005, Caldeira et al. 2005).

In addition to altering the biogeochemical characteristics near islands, a wake effect between islands may have contributed to elevated rates of productivity (both NPP and BP), as well as concentrations POC and Chl, through the introduction of limiting nutrients to stations between islands and near Moorea, thus stimulating productivity and production of organic matter. However, in contrast to previous observations of upwelling induced by island-wakes near deep-sea islands (Heywood et al. 1990, Furuya et al. 1986, Hasegawa et al. 2004), our observations of MLDs (see *hydrographic conditions*) suggest that vertical mixing was not sufficiently deep enough to entrain nutrients from the upper portion of the nutricline into the

upper euphotic zone during our sampling period (Fig 3A & B). In addition, satellite altimetry data (http://marine.copernicus.eu/) during the sampling period revealed generally positive sea surface height anomalies at large scales around Moorea and Tahiti, indicating the predominance of anticyclonic (counter-clockwise) flow in the region (Fig. 7A). A somewhat smaller number of areas of cyclonic flow were also observed. Anticyclonic flow at mesoscales results in elevated sea surface height and downward displacement of the pycnocline, depressing the nutricline and reducing nutrient supply to the upper euphotic zone (McGilicuddy et al. 2007, Ewart et al. 2008).

The dynamic height (DH) pattern on smaller scales around Moorea was consistent with larger scale anticyclonic patterns in the region. A continuous pattern of elevated DH (10/500 dbar) with values exceeding 1.4 m was observed around and west of Moorea and to the northwest of Tahiti (Fig 7B). Values less than 1.4 m were observed to the north, southeast, and southwest of Moorea. Overall DH ranged from 1.364-1.466 over the survey region. This DH pattern is consistent with the anticyclonic flow at larger scales (Fig 7A) and with the pattern of counterclockwise, near-shore currents recorded by three oceanographic moorings in 15 m depth (Leicther et al. 2013).

Despite the presence of anticyclonic flow across a range of spatial scales, productivity and production of organic matter was enhanced at stations near Moorea and between islands in the upper euphotic zone (Fig 6). We suggest that lateral transport of inorganic nutrients, rather than vertical transport via mixing, may have played a critical role in stimulating productivity at these stations. In addition to stimulating productivity, lateral transport of

inorganic nutrients to stations near the islands may have reduced variability between these stations, relative to stations west of Moorea. Our observations of offshore flow along western Tahiti, as well as counterclockwise flow around Moorea (Fig 7B), during the sampling period may have led to the introduction of nutrients near Tahiti and Moorea via runoff, atmospheric deposition, or previous upwelling induced by a wake effect (Heywood et al. 1990, Furuya et al. 1986, Hasegawa et al. 2004). Lateral transport of limiting nutrients from near the islands to "offshore" locations may have stimulated productivity at stations between islands and near Moorea. Further, entrainment of inorganic nutrients and organic matter in the counterclockwise flow around Moorea could lead to retention of material near the island. Transport of nutrients and organic matter from nearshore to offshore stations near Tahiti and Moorea, may explain greater similarities between stations near Moorea and between islands, compared with stations west of Moorea.

Summary

Overall, our observations of physical and biogeochemical variables in the upper 300 m of the water column suggest that physical connectivity between nearshore and offshore sites, as well as enhanced retention at stations near Moorea, may have reduced variability between stations near Moorea and between islands, compared with stations west of Moorea. Further, the production of distinct physical dynamics and biogeochemical characteristics at stations near Moorea and Tahiti may provide evidence of a wake effect between islands. Ultimately, the presence of an island wake effect may enhance the role of lateral transport of inorganic nutrients and organic matter in supporting the high biomass and productivity on Moorea's coral reefs.

Figures for Chapter III

Figure 1. Map of rectangular sampling grid.

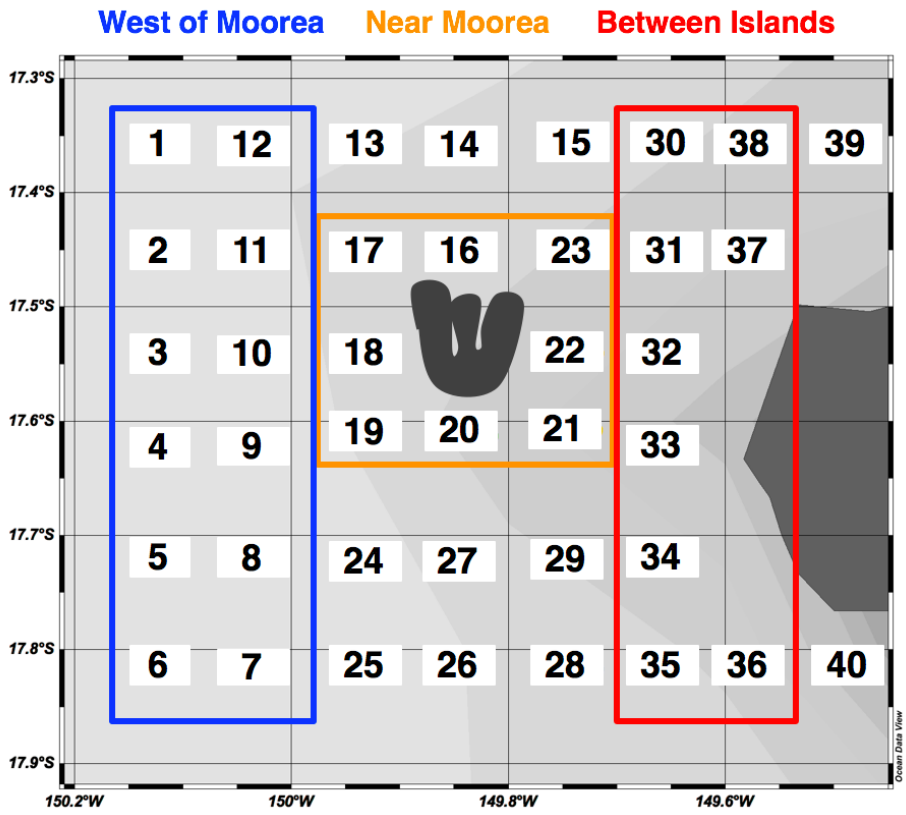

Map of rectangular sampling grid conducted as part of the Moorea Coral Reef Long Term Ecological Research cruise in 2014. Labels indicate station number and blue (west of Moorea), orange (near Moorea), and red (between islands) boxes indicate station proximity to Moorea.

Figure 2. Contour plots of temperature and salinity in the upper 300 m of the water column.

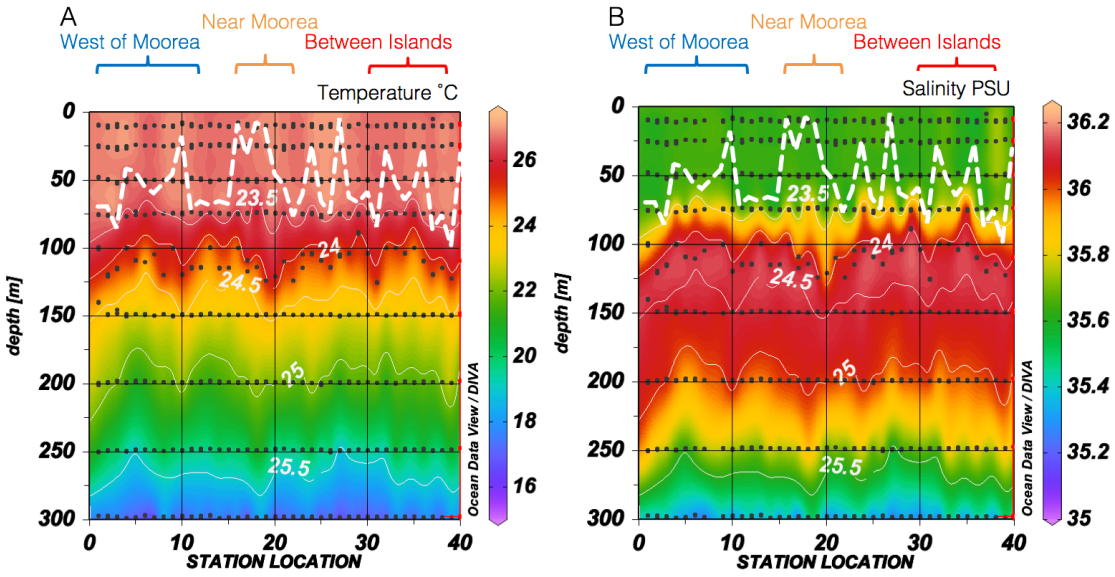

Contour plots of temperature (A), and salinity (B) in the upper 300 m of the water column. Black dots indicate sites of seawater collection and blue (west of Moorea), orange (near Moorea), and red (between islands) bars indicate station proximity to Moorea. The dashed white line represents mixed layer depth at each station. Contours representing potential density anomaly (kg m^{-3}) are overlaid on biogeochemical measurements.

Figure 3. Contour plots of concentrations of inorganic nutrients and dissolved oxygen in the upper 300 m of the water column.

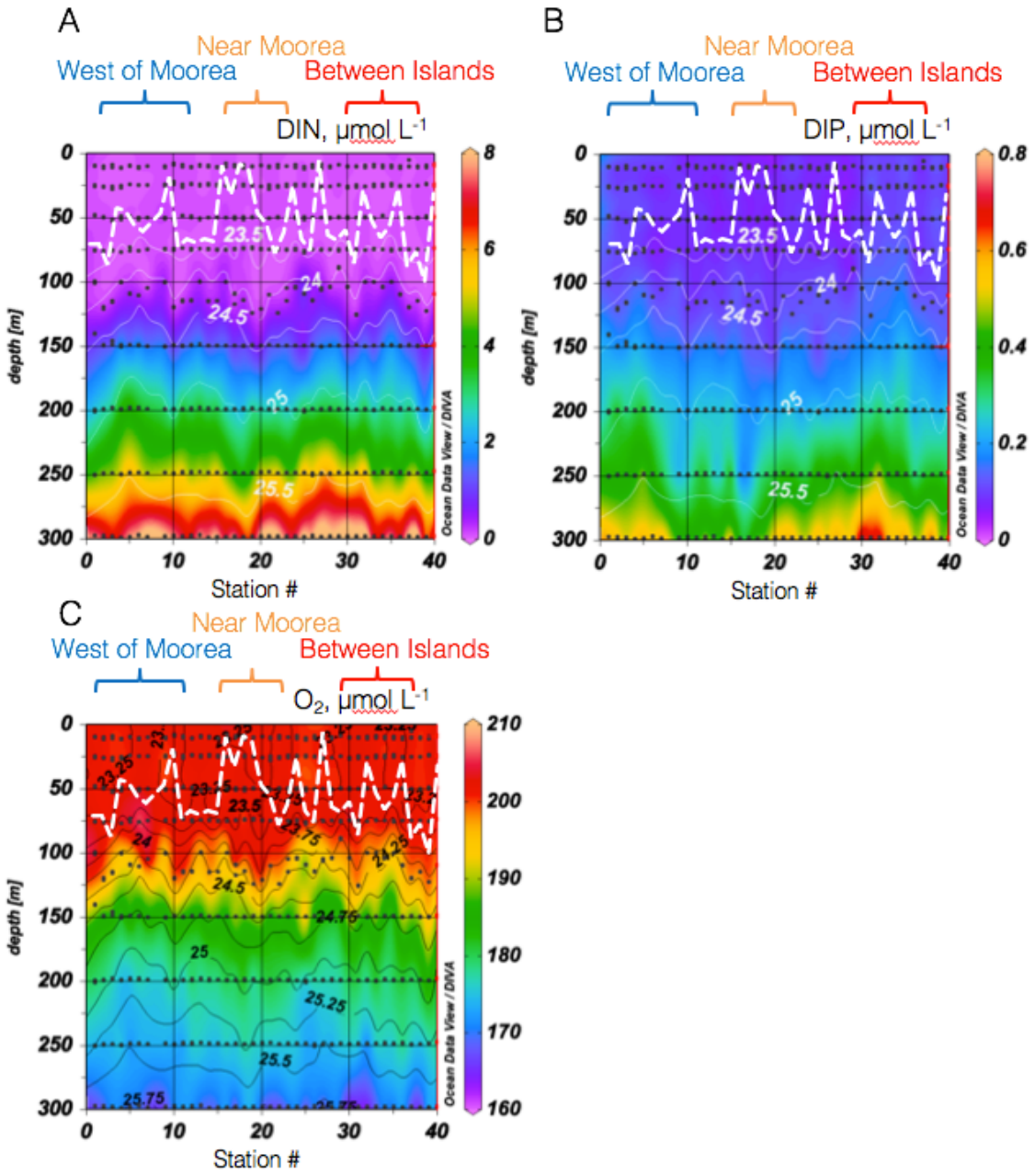

Contour plots of concentrations of inorganic $NO_2^- + NO_3^-$ (DIN; A), inorganic PO_4^{3-} (DIP; B), and oxygen (O_2; C) in the upper 300 m of the water column. The dashed white line represents mixed layer depth at each station. Black dots indicate sites of seawater collection and blue (west of Moorea), orange (near Moorea), and red (between islands) bars indicate

station proximity to Moorea. Contours representing potential density anomaly (kg m^{-3}) are overlaid on biogeochemical measurements.

Figure 4. Contour plots of biogeochemical variables over the upper 300 m of the water column.

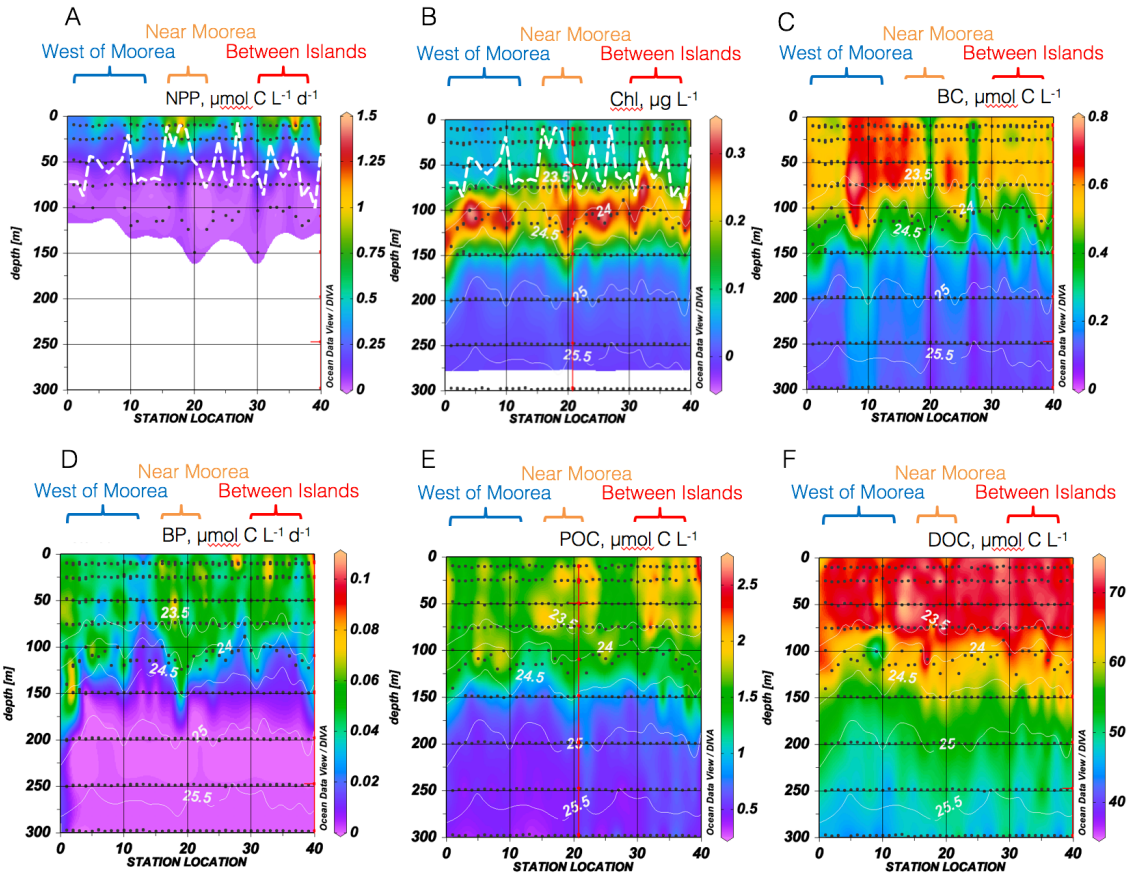

Fig 4. Contour plots of net primary productivity (NPP; A), chlorophyll a (Chl; B), bacterioplankton carbon (BC; C), bacterioplankton productivity (BP; D), particulate organic carbon (POC; E), and dissolved organic carbon (DOC; F) in the upper 300 m of the water column. Black dots indicate sites of seawater collection and blue (west of Moorea), orange (near Moorea), and red (between islands) bars indicate station proximity to Moorea. Contours representing potential density anomaly (kg m^{-3}) are overlaid on biogeochemical measurements. The dashed white line overlaid on NPP and Chl represents the mixed layer depth at each station.

Figure 5. Contour plots of integrated and depth-normalized inorganic nutrients and dissolved oxygen in the upper euphotic zone (0 – 75 m).

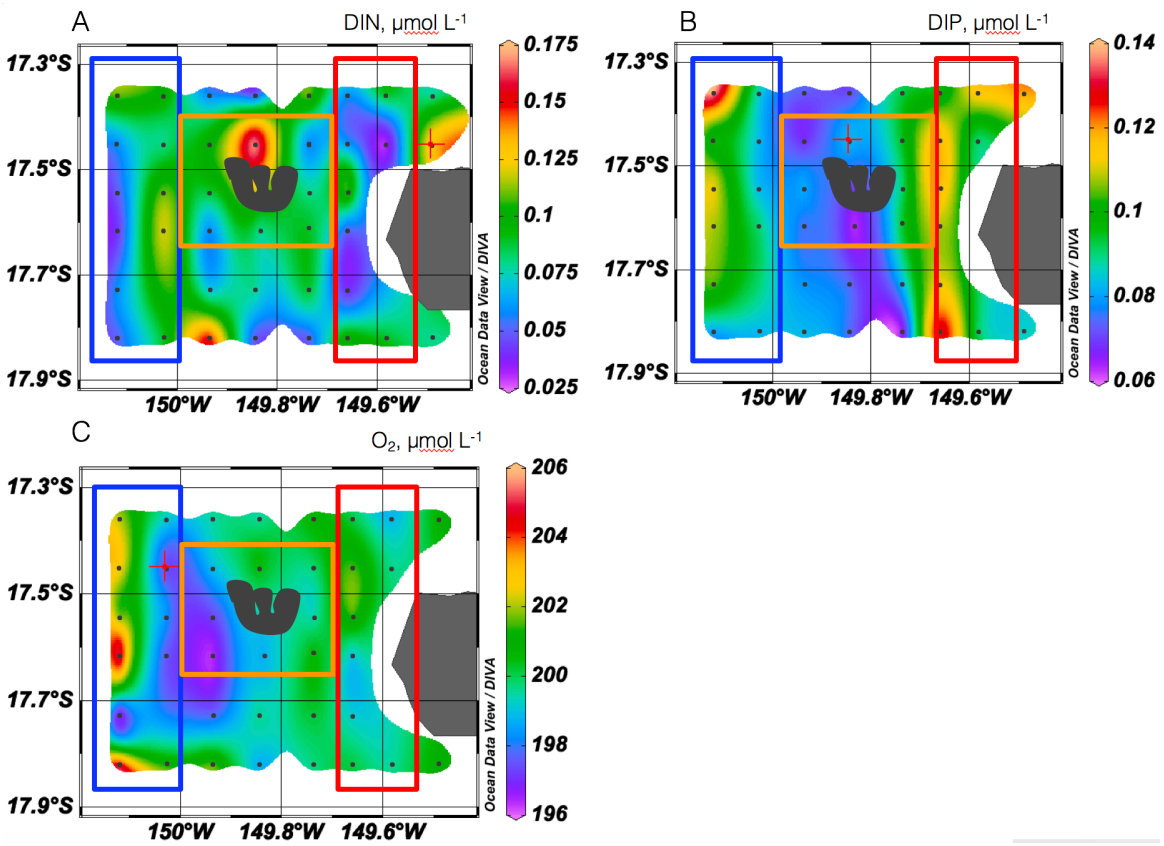

Contour plots of integrated and depth-normalized upper euphotic zone (0 – 75 m) values of concentrations of inorganic nitrogen (NO_2^- + NO_3^-; A), dissolved inorganic phosphorous (PO_4^{3-}; B), and oxygen (O_2; C). Black dots indicate stations and blue (west of Moorea), orange (near Moorea), and red (between islands) boxes indicate station proximity to Moorea.

Figure 6. Contour plots of integrated and depth-normalized biogeochemical variables in the upper euphotic zone (0 – 75 m).

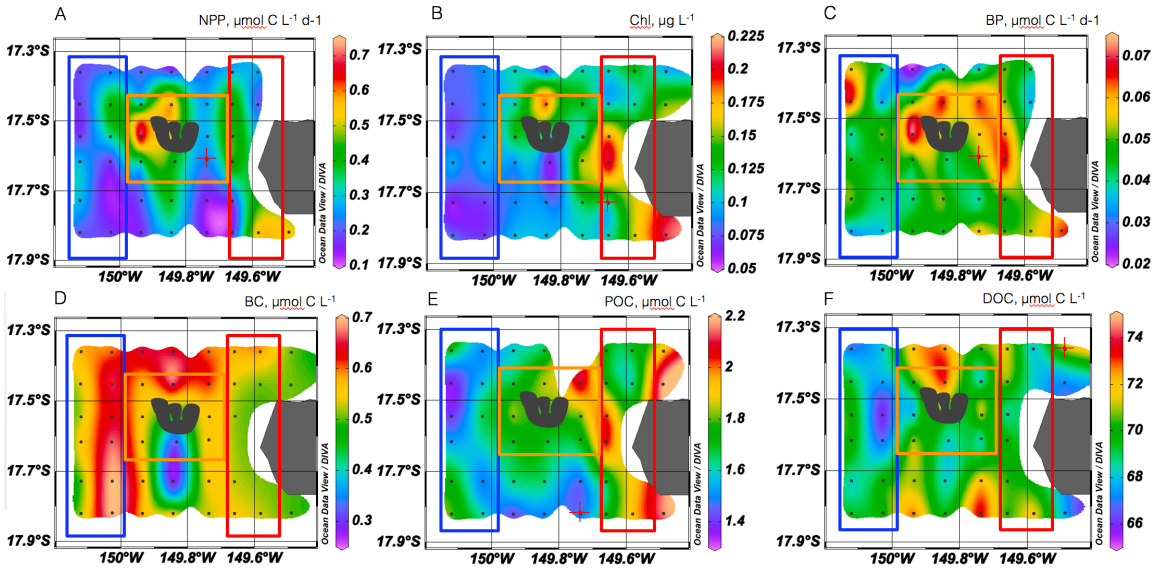

Contour plots of upper water column (0 – 75 m) depth-normalized and integrated values of primary productivity (PP; A), chlorophyll a (Chl; B), bacterioplankotn carbon (BC; C), bacterioplankton productivity (BP; D), particulate organic carbon (POC; E), and dissolved organic carbon (DOC; F). Black dots indicate sites of seawater collection and blue (west of Moorea), orange (near Moorea), and red (between islands) boxes indicate station location relative to Moorea.

Figure 7. Current patterns near Moorea and Tahiti.

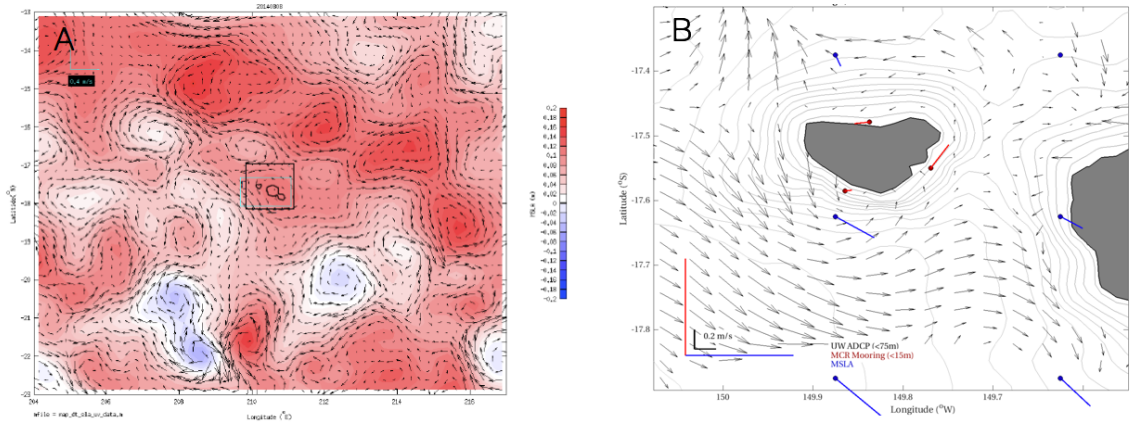

Current patterns around the islands of Moorea and Tahiti (A) and within the sampling grid (B). Large-scale current patterns were evaluated using satellite radar altimetry (http://marine.copernicus.edu/). Within-grid current patterns were obtained via optimal interpolation of ADCP data on to a regular grid with a spacing of 4 km.

Tables for Chapter III

Table I

	WEST	SD	NEAR	SD	BETWEEN	SD	ANOVA	W v N	N v B	W V B
Upper Euphotic (0 - 75 m)										
[Z] N+N 0-75 [µM]	0.08	0.03	0.09	0.03	0.07	0.03	0.37	ns	ns	ns
DIP [µM]	0.10	0.02	0.08	0.01	0.11	0.01	< 0.01	0.07	< 0.01	0.22
Oxygen [µM]	200.62	3.00	198.97	1.49	199.98	1.00	0.27	ns	ns	ns
[Z] PP 0-75 [µM C/d]	0.24	0.08	0.40	0.17	0.33	0.14	0.05	ns	ns	ns
[Z] Chl 0-75 [µg Chl L-1]	0.08	0.01	0.12	0.04	0.14	0.04	< 0.01	0.02	0.68	< 0.01
[Z] BP 0-75 [µM C/day]	0.05	0.01	0.06	0.01	0.05	0.01	0.09	ns	ns	ns
[Z] BC 0-75 [µM C]	0.60	0.07	0.55	0.10	0.54	0.03	0.21	ns	ns	ns
[Z] POC 0-75 [µM C]	1.58	0.14	1.80	0.14	1.80	0.17	< 0.01	0.01	0.99	0.01
[Z] DOC 0-75 [µM C]	68.56	1.47	69.84	2.01	70.93	2.59	0.04	ns	ns	ns
Lower Euphotic (75 - 150 m)										
[Z] NN 75-150	0.50	0.19	0.45	0.17	0.47	0.23	0.85	ns	ns	ns
[Z] DIP [µM]	0.13	0.02	0.11	0.02	0.15	0.02	< 0.01	0.07	< 0.01	0.14
[Z] Oxygen [µM]	192.57	4.42	193.73	1.69	193.43	2.08	0.71	ns	ns	ns
[Z] PP 75-150 [µM C/d]	0.01	0.01	0.02	0.02	0.02	0.01	0.98	ns	ns	ns
[Z] Chl 0-75 [µg Chl L-1]	0.19	0.02	0.20	0.03	0.18	0.02	0.46	ns	ns	ns
[Z] BP 75-150 [µM C/ d]	0.04	0.02	0.04	0.01	0.03	0.01	0.22	ns	ns	ns
[Z] BC 75-150 [µM C]	0.48	0.08	0.40	0.07	0.39	0.07	0.02	0.06	0.98	0.04
[Z] POC 75-150	1.37	0.17	1.39	0.15	1.38	0.15	0.65	ns	ns	ns
[Z] DOC 75-150	59.94	3.49	64.86	3.56	64.07	3.07	< 0.01	0.01	0.88	0.03
Upper Mesopelagic (150 - 300 m)										
[Z] NN 75-150	4.13	0.42	3.80	0.34	3.99	0.40	0.20	ns	ns	ns
[Z] DIP [µM]	0.32	0.05	0.27	0.04	0.35	0.04	< 0.01	0.05	< 0.01	0.42
[Z] Oxygen [µM]	173.52	0.95	175.87	0.90	175.22	1.60	< 0.001	< 0.01	0.50	0.01
[Z] PP 75-150 [µM C/d]	0.01	0.00	0.01	0.01	0.01	0.01	0.93	ns	ns	ns
[Z] Chl 0-75 [µg Chl L-1]	0.07	0.03	0.07	0.02	0.05	0.01	0.22	ns	ns	ns
[Z] BP 75-150 [µM C/ d]	0.01	0.01	0.00	0.00	0.00	0.00	0.60	ns	ns	ns
[Z] BC 75-150 [µM C]	0.19	0.04	0.16	0.04	0.14	0.02	0.06	ns	ns	ns
[Z] POC 75-150	0.56	0.06	0.61	0.10	0.69	0.09	0.01	0.33	0.16	< 0.01
[Z] DOC 75-150	49.21	1.14	52.50	0.85	51.33	2.08	< 0.001	< 0.001	0.24	< 0.01

Mean (± standard deviation; SD) integrated and depth-normalized values of rates of productivity and concentrations of inorganic nutrients and organic matter. Concentrations and rates are integrated and depth-normalized within the upper euphotic zone (0 – 75 m), lower euphotic zone (75 – 150 m), and upper mesopelagic zone (150 – 300 m). Concentrations and rates were averaged across stations west of Moorea (W; total of 12 stations), near Moorea (N; total of 8 stations), and between islands (B; total of 9 stations). Statistical analysis of the difference in biogeochemical rates and concentrations as a function of station location were evaluated using a randomized 1-way analysis of variance (ANOVA) with 999 iterations. Post-hoc Tukey Honest Significance Differences tests were conducted to assess variance among group.

References

Abell, J., Emerson, S., and Renaud, P. (2000). Distributions of TOP, TON and TOC in the North Pacific subtropical gyre: Implications for nutrient supply in the surface ocean and remineralization in the upper thermocline. Journal of Marine Research 58, 203–222.

Anderson, L.A. (1995). On the hydrogen and oxygen content of marine phytoplankon. Deep Sea Research Part I: Oceanographic Research Papers 42, 1675–1680.

Anderson, C.R., Brzezinski, M.A., Washburn, L., and Kudela, R. (2006). Circulation and environmental conditions during a toxigenic Pseudo-nitzschia australis bloom in the Santa Barbara Channel, California. Marine Ecology Progress Series 327, 119–133.

Barton, E.D., Basterretxea, G., Flament, P., Mitchelson-Jacob, E.G., Jones, B., Aristegui, J., and Herrera, F. (2000). Lee region of Gran Canaria. Journal of Geophysical Research 105, 17,173-17,193.

Caldeira, R.M.A., Marchesiello, P., Nezlin, N.P., DiGiacomo, P.M., and McWilliams, J.C. (2005). Island wakes in the Southern California Bight. Journal of Geophysical Research 110.

Carlson, C.A., Ducklow, H.W., and Sleeter, T.D. (1996). Stocks and dynamics of bacterioplankton in the northwestern Sargasso Sea. Deep Sea Research Part II: Topical Studies in Oceanography 43, 491–515.

Carlson, C.A., Giovannoni, S.J., Hansell, D.A., Goldberg, S.J., Parsons, R., and Vergin, K. (2004). Interactions among dissolved organic carbon, microbial processes, and community structure in the mesopelagic zone of the northwestern Sargasso Sea. Limnology and Oceanography 49, 1073–1083.

Carlson, C.A., Hansell, D.A., Nelson, N.B., Siegel, D.A., Smethie, W.M., Khatiwala, S., Meyers, M.M., and Halewood, E. (2010). Dissolved organic carbon export and subsequent

remineralization in the mesopelagic and bathypelagic realms of the North Atlantic basin. Deep Sea Research Part II: Topical Studies in Oceanography 57, 1433–1445.

Caron, D.A., Dam, H.G., Kremer, P., Lessard, E.J., Madin, L.P., Malone, T.C., Napp, J.M., Peele, E.R., Roman, M.R., and Youngbluth, M.J. (1995). The contribution of microorganisms to particulate carbon and nitrogen in surface waters of the Sargasso Sea near Bermuda. Deep Sea Research Part I: Oceanographic Research Papers 42, 943–972.

Church, M.J., Lomas, M.W., and Muller-Karger, F. (2013). Sea change: Charting the course for biogeochemical ocean time-series research in a new millennium. Deep Sea Research Part II: Topical Studies in Oceanography 93, 2–15.

Cotner, J.B., Ammerman, J.W., Peele, E.R., and Bentzen, E. (1997). Phosphorus-limited bacterioplankton growth in the Sargasso Sea. Aquatic Microbial Ecology 13, 141–149.

Cullen, J.J. (2015). Subsurface Chlorophyll Maximum Layers: Enduring Enigma or Mystery Solved? Annual Review of Marine Science 7, 207–239.

Delesalle, B., and Sournia, A. (1992). Residence time of water and phytoplankton biomass in coral reef lagoons. Continental Shelf Research 12, 939–949.

Dong, C., McWilliams, J.C., and Shchepetkin, A.F. (2007). Island Wakes in Deep Water. Journal of Physical Oceanography 37, 962–981.

Doval, M.D., and Hansell, D.A. (2000). Organic carbon and apparent oxygen utilization in the western South Pacific and the central Indian Oceans. Marine Chemistry 68, 249–264.

Ewart, C.S., Meyers, M.K., Wallner, E.R., McGillicuddy, D.J., and Carlson, C.A. (2008). Microbial dynamics in cyclonic and anticyclonic mode-water eddies in the northwestern Sargasso Sea. Deep Sea Research Part II: Topical Studies in Oceanography 55, 1334–1347.

Fukuda, R., Ogawa, H., Nagata, T., and Koike, I. (1998). Direct determination of carbon and nitrogen contents of natural bacterial assemblages in marine environments. Applied and Environmental Microbiology 64, 3352–3358.

Furuya, K., Takahashi, M., and Nemoto, T. (1986). Summer phytoplankton community structure and growth in a regional upwelling area off Hachijo Island, Japan. Journal of Experimental Marine Biology and Ecology 96, 43–55.

Glöckner, F.O., Fuchs, B.M., and Amann, R. (1999). Bacterioplankton compositions of lakes and oceans: a first comparison based on fluorescence in situ hybridization. Applied and Environmental Microbiology 65, 3721–3726.

Gundersen, K., Heldal, M., Norland, S., Purdie, D.A., and Knap, A.H. (2002). Elemental C, N, and P cell content of individual bacteria collected at the Bermuda Atlantic Time-series Study (BATS) site. Limnology and Oceanography 47, 1525–1530.

Halewood, E., Carlson, C., Brzezinski, M., Reed, D., and Goodman, J. (2012). Annual cycle of organic matter partitioning and its availability to bacteria across the Santa Barbara Channel continental shelf. Aquatic Microbial Ecology 67, 189–209.

Hamner, W.M., and Hauri, I.R. (1981). Effects of island mass: water flow and plankton pattern around a reef in the Great Barrier Reef lagoon, Australia. Limnology and Oceanography 26, 1084–1102.

HanseH, D.A., and Carlson, C.A. (2001). Marine Dissolved Organic Carbon and the Carbon Cycle. Oceanography 14, 41.

Hansell, D.A., and Carlson, C.A. (1998). Deep-ocean gradients in the concentraion of dissolved organic carbon. Nature 395, 263–266.

Hansell, D.A., Carlson, C.A., Repeta, D.J., and Schlitzer, R. (2009). Dissolved organic matter in the ocean: A controversy stimulates new insights. Oceanography 22, 202–211.

Hasegawa, D. (2004). How islands stir and fertilize the upper ocean. Geophysical Research Letters 31.

Hench, J.L., Leichter, J.J., and Monismith, S.G. (2008). Episodic circulation and exchange in a wave-driven coral reef and lagoon system. Limnology and Oceanography 53, 2681–2694.

Hernández-León, S. (1988). Gradients of mesozooplankton biomass and ETS activity in the wind-shear area as evidence of an island mass effect in the Canary Island waters. Journal of Plankton Research 10, 1141–1154.

Heywood, K.J., Barton, E.D., and Simpson, J.H. (1990). The effects of flow disturbance by an oceanic island. Journal of Marine Research 48, 55–73.

Johannes, R.E., Alberts, J., D'Elia, C., Kinzie, R.A., Pomeroy, L.R., Sottile, W., Wiebe, W., Marsh, J.A., Helfrich, P., Maragos, J., et al. (1972). The Metabolism of Some Coral Reef Communities: A Team Study of Nutrient and Energy Flux at Eniwetok. BioScience 22, 541–543.

Johnson, K.S., Riser, S.C., and Karl, D.M. (2010). Nitrate supply from deep to near-surface waters of the North Pacific subtropical gyre. Nature 465, 1062–1065.

Karl, D.M., and Church, M.J. (2014). Microbial oceanography and the Hawaii Ocean Time-series programme. Nature Reviews Microbiology 12, 699–713.

Karl, D.M., and Church, M.J. (2017). Ecosystem Structure and Dynamics in the North Pacific Subtropical Gyre: New Views of an Old Ocean. Ecosystems 20, 433–457.

Leichter, J., Alldredge, A., Bernardi, G., Brooks, A., Carlson, C., Carpenter, R., Edmunds, P., Fewings, M., Hanson, K., Hench, J., et al. (2013). Biological and Physical Interactions on a Tropical Island Coral Reef: Transport and Retention Processes on Moorea, French Polynesia. Oceanography 26, 52–63.

Leichter, J.J., Stokes, M.D., Hench, J.L., Witting, J., and Washburn, L. (2012). The island-scale internal wave climate of Moorea, French Polynesia: Internal waves on Moorea. Journal of Geophysical Research: Oceans 117.

Letelier, R.M., Dore, J.E., Winn, C.D., and Karl, D.M. (1996). Seasonal and interannual variations in photosynthetic carbon assimilation at Station ALOHA. Deep Sea Research Part II: Topical Studies in Oceanography 43, 467–490.

Letscher, R.T., Knapp, A.N., James, A.K., Carlson, C.A., Santoro, A.E., and Hansell, D.A. (2015). Microbial community composition and nitrogen availability influence DOC remineralization in the South Pacific Gyre. Marine Chemistry 177, Part 2, 325–334.

Lomas, M., Bates, N., Johnson, R., Knap, A., K. Steinberg, D., and Carlson, C. (2014). Lomas et al., 2013.

Longhurst, A., Sathyendranath, S., Platt, T., and Caverhill, C. (1995). An estimate of global primary production in the ocean from satellite radiometer data. Journal of Plankton Research 17, 1245–1271.

Martinez, E., and Maamaatuaiahutapu, K. (2004). Island mass effect in the Marquesas Islands: Time variation. Geophysical Research Letters 31.

McGillicuddy, D.J., Anderson, L.A., Bates, N.R., Bibby, T., Buesseler, K.O., Carlson, C.A., Davis, C.S., Ewart, C., Falkowski, P.G., Goldthwait, S.A., et al. (2007). Eddy/Wind Interactions Stimulate Extraordinary Mid-Ocean Plankton Blooms. Science 316, 1021–1026.

Michaels, A.F., and Knap, A.H. (1996). Overview of the U.S. JGOFS Bermuda Atlantic Time-series Study and the Hydrostation S program. Deep Sea Research Part II: Topical Studies in Oceanography 43, 157–198.

Neall, V.E., and Trewick, S.A. (2008). The age and origin of the Pacific islands: a geological overview. Philos Trans R Soc Lond B Biol Sci 363, 3293–3308.

Nelson, C.E., Alldredge, A.L., McCliment, E.A., Amaral-Zettler, L.A., and Carlson, C.A. (2011). Depleted dissolved organic carbon and distinct bacterial communities in the water column of a rapid-flushing coral reef ecosystem. The ISME Journal 5, 1374.

Odum, H.T., and Odum, E.P. (1955). Trophic Structure and Productivity of a Windward Coral Reef Community on Eniwetok Atoll. Ecological Monographs 25, 291–320.

Pan, X., Achterberg, E.P., Sanders, R., Poulton, A.J., Oliver, K.I.C., and Robinson, C. (2014). Dissolved organic carbon and apparent oxygen utilization in the Atlantic Ocean. Deep Sea Research Part I: Oceanographic Research Papers 85, 80–87.

Rissik, D., Suthers, I.M., and Taggart, C.T. (1997). Enhanced zooplankton abundance in the lee of an isolated reef in the south Coral Sea: the role of flow disturbance. Journal of Plankton Research 19, 1347–1368.

Rivkin, R.B., and Anderson, M.R. (1997). Inorganic nutrient limitation of oceanic bacterioplankton. Limnology and Oceanography 42, 730–740.

Rougerie, F., and Rancher, J. (1994). The Polynesian south ocean: features and circulation. Marine Pollution Bulletin 29, 14–25.

Rudnick, D.L. (1996). Intensive surveys of the Azores Front: 2. Inferring the geostrophic and vertical velocity fields. Journal of Geophysical Research 101, 16291–16303.

Santinelli, C., Nannicini, L., and Seritti, A. (2010). DOC dynamics in the meso and bathypelagic layers of the Mediterranean Sea. Deep Sea Research Part II: Topical Studies in Oceanography 57, 1446–1459.

Scheffé, Henry (1959). The Analysis of Variance. New York: Wiley.

Simon, M., and Azam, F. (1989). Protein content and protein synthesis rates of planktonic marine bacteria. Marine Ecology Progress Series 201–213.

Smith, D.C., Simon, M., Alldredge, A.L., and Azam, F. (1992). Intense hydrolytic enzyme activity on marine aggregates and implications for rapid particle dissolution. Nature 359, 139–142.

Steinberg, D.K., Carlson, C.A., Bates, N.R., Johnson, R.J., Michaels, A.F., and Knap, A.H. (2001). Overview of the US JGOFS Bermuda Atlantic Time-series Study (BATS): a decade-scale look at ocean biology and biogeochemistry. Deep Sea Research Part II: Topical Studies in Oceanography 48, 1405–1447.

Takahashi, M., Yasuoka, Y., Watanabe, M., Miyazaki, T., and Ichimura, S. (1981). Local upwelling associated with vortex motion off Oshima Island, Japan. Coastal Upwelling 119–124.

Thomson, R.E. and W.J. Emery, "Data analysis methods in physical oceanography", 3rd Ed., Elsevier, 2014, p. 716, Waltham, MA, USA

Wear, E.K., Carlson, C.A., James, A.K., Brzezinski, M.A., Windecker, L.A., and Nelson, C.E. (2015). Synchronous shifts in dissolved organic carbon bioavailability and bacterial community responses over the course of an upwelling-driven phytoplankton bloom: Bloom-induced shifts in DOC availability. Limnology and Oceanography 60, 657–677.

Wilson, S.T., Barone, B., Ascani, F., Bidigare, R.R., Church, M.J., del Valle, D.A., Dyhrman, S.T., Ferrón, S., Fitzsimmons, J.N., Juranek, L.W., et al. (2015). Short-term variability in euphotic zone biogeochemistry and primary productivity at Station ALOHA: A case study of summer 2012: BIOGEOCHEMICAL CYCLING AT STATION ALOHA. Global Biogeochemical Cycles 29, 1145–1164.

Xie, S.-P., Liu, W.T., Liu, Q., and Nonaka, M. (2001). Far-reaching effects of the Hawaiian Islands on the Pacific ocean-atmosphere system. Science 292, 2057–2060.

IV. Conclusions and Future Directions

The results described in this dissertation contribute to a growing understanding of the effects of short-term increases in pCO_2 on bacterioplankton-mediated carbon cycling. Chapter I reveals a direct impact of pCO_2 on bacterioplankton removal of organic carbon in seawater culture experiments. All experiments for which TOC removal was measurable resulted in systematically greater cell-specific respiration in elevated pCO_2 treatments; even in cases where bacterioplankton abundance yield was greater under elevated pCO_2. These experiments indicate that abrupt exposure to elevated pCO_2 can lead to decreased bacterioplankton growth efficiencies, and increase the ability of bacterioplankton to consume DOC. The cumulative effect of enhanced rates of consumption and respiration under elevated pCO_2 could decrease the rate of DOC accumulation in the surface ocean, ultimately reducing the export potential of DOC in the biological carbon pump. Incorporation of these results into numerical models will enable more accurate understanding of the impact of increases in pCO_2 in surface waters on biogeochemical cycles. However, our results pertain to the short-term impacts of elevated pCO_2. Long-term experiments mimicking gradual increases in surface ocean pCO_2 are required to evaluate the long-term impacts of rising atmospheric CO_2 on bacterioplankton-mediated carbon cycling in the surface ocean.

The experimental metagenomics approach described in Chapter II contributes to a growing understanding of the effects of elevated pCO_2 on bacterioplankton community composition and metabolic pathways. In this Chapter, I show that elevated pCO_2 can alter natural

bacterioplankton communities and the relative abundance of metabolic functions. The observed shift in community taxonomic composition, as well as the disproportionate effects of elevated pCO_2 on amino acid and carbohydrate metabolism, provide a potential mechanism by which natural bacterioplankton communities were able to remove organic carbon at a faster rate when exposed to pulses of elevated pCO_2. In addition, a greater abundance of functions related to phospholipid and membrane maintenance, and toxin and antibiotic resistance, provide a potential mechanistic explanation for increased bacterial respiration with elevated pCO_2, as these maintenance functions require energy that could otherwise be used for growth. Collectively, the combined effects of pCO_2 on bacterioplankton community composition and metabolic functionality suggest that elevated pCO_2 can alter bacterioplankton ecological function, enhancing rates of bacterioplankton-mediated removal of surface organic carbon through enhanced rates of respiration. Comparing our results to similar studies at contrasting ocean regions would provide insight as to whether our observed response in community taxonomic composition and metabolic potential is conserved across natural bacterioplankton communities. In addition, understanding the long-term effects of elevated pCO_2 on bacterioplankton community composition and metabolic potential is imperative to understanding how future bacterioplankton communities will impact marine carbon cycle.

Finally, high resolution sampling in the upper 300 m of the waters surrounding the islands of Moorea and Tahiti for Chapter III provides the first survey of these highly oligotrophic waters. Spatial variability in hydrographic, biogeochemical, and physical dynamics near the islands provides a baseline for understanding future variation in local dynamics. In addition,

our measurements provide further evidence to support a previously hypothesized island wake effect, which may have profound implications for our understanding of the physical and biogeochemical processes that enable high productivity and biomass to thrive on coral reefs in the subtropical oligotrophic gyre ecosystems. Future assessment of these dynamics may provide insight to the effects of long-term climate variability on local marine dynamics and the resulting implications for coral reefs.

The experimental and observational studies constructed for and described in this dissertation provide new insight to the effects of pCO_2 on natural bacterioplankton communities in the surface ocean. These studies elucidate the short-term effects of pCO_2 on bacterioplankton-mediated carbon cycling from individual genes to mesoscale biogeochemical patterns. Directly linking measurements of bacterioplankton-mediated carbon cycling to changes in taxonomic composition and metabolic potential provide a unique evaluation of the effects of elevated pCO_2 on the ecological function of natural bacterioplankton. Further, linking the results revealed by experimental work to observations of large-scale biogeochemical dynamics provides the environmental context required to understand how short-term perturbations of elevated pCO_2 may alter carbon cycling in the surface ocean.